TRANSPORT PHENOMENA IN INORGANIC PRECIPITATED MEMBRANES

ABSTRACT

OF THE

THESIS

SUBMITTED FOR THE AWARD OF THE DEGREE OF

Doctor of Philosophy

IN

CHEMISTRY

BY

TANVIR ARFIN

Under the Supervision of

DR. RAFIUDDIN

DEPARTMENT OF CHEMISTRY
ALIGARH MUSLIM UNIVERSITY
ALIGARH (INDIA)

2009

ABSTRACT

A membrane can be defined as a thin and selective barrier which enables the transport or the retention of compounds between two media. Membranes can be classified in different ways depending on what criteria one chooses to use. Membranes can be divided into living and non-living membranes, the first category is essential to all life, whereas non living membranes are synthetic membranes, which have enormous applications in industries. On the basis of structure, membranes can be further divided into symmetric and asymmetric; the symmetric membranes consist of only one layer, whereas the asymmetric membranes consist of a dense toplayer having a porous support. An important class of the asymmetric membranes is the composite membranes, where the toplayer and support are made of different polymer materials. The dense skin layer is responsible for the selectivity, whereas all layers contribute to the flow resistance. The symmetric and asymmetric membranes can be further divided into porous and nonporous membranes.

Membrane filtration has emerged as a technology of choice in the water industry. It has numerous advantages over conventional treatment technology. These include small footprint, low or almost zero chemical consumption, capability to upscale and retrofit to existing facility with the ease or to combine with other treatment processes to maximize efficiency, and above all, and superior product water quality. Over time, problematic technical and economical drawbacks associated with membrane technology such as membrane fouling, energy consumption, and limited membrane lifetime have been progressively

addressed. Consequently, numbers of membrane filtration applications in the water industry have sky-rocketed over the last few years.

Microfiltration, ultrafiltration, nanofiltration and reverse osmosis are all pressure driven membrane processes which differ in membrane pore size. The pore diameter in microfiltration membranes are in the range of 100-1000 nm, in ultrafiltration membranes range is 5-100 nm, in nanofiltration membranes it is 1-100 nm whereas in reverse osmosis membranes are below 1nm.

Membrane transport models have been derived from two independent approaches. The first category of models assumes a separation or transport mechanism and calculates the fluxes according to these mechanisms. The second category of transport models is based on the theory of irreversible thermodynamics, also referred to as non-equilibrium thermodynamics.

In this thesis, preparation and transport properties of number of inorganic precipitated membranes are presented and in order to simplify, the contents of the thesis are divided into four parts.

Chapter I gives general introduction regarding inorganic precipitated membranes.

Chapter II describes transport phenomena in polystyrene based nickel arsenate membrane The membrane potentials of nickel arsenate membrane were measured with uni-univalent electrolytes solution using saturated calomel electrodes. Theories for the salt concentration dependence of uni-univalent potentials proposed by Teorell-Meyer-Siever and Kobatake methods and have been

compared in order to obtain a relationship for the theoretical values of uni-univalent potentials. The order of fixed charge density for electrolytes used was found to be KCl >NaCl> LiCl. The conductance values were found to increase with the increase in concentration as well as with temperature. The specific conductance values of electrolytes follow the sequence for the cations: K^+> Na^+ > Li^+. The membrane pores reduce the conductance of small ions, which are much hydrated. An increase in conductance with increase in temperature may have been due to the state of hydration, which implies that the energy of activation for the ionic transport across the membrane follows the sequence of crystallographic radii of ions accordingly. Negative ΔS^* values indicate the formation of a covalent bond between the permeating species and the membrane material The structure of the membrane was observed with the aid of a scanning electron microscope. Membrane had random non-preferential orientation with no visible cracks and appeared to be composed of dense and loose aggregation of small particles.

Chapter III describes transport phenomena in polystyrene based titanium arsenate membrane. Membrane potential is a measurable and reliable parameter to characterize the charge property of membrane. Membrane potentials have been measured across polystyrene based titanium arsenate membrane separating various 1:1 electrolytes at different concentrations. Membrane potential data have been used to calculate transference number of ions, mobility, distribution coefficient, charge effectiveness, permselectivity and also to derive the thermodynamically fixed charge density which is an important characteristic governing the membrane

phenomena by utilizing the generally accepted theories for the salt concentration dependence of uni-univalent potentials proposed by Teorell-Meyer-Sievers and Kobatake methods and these are compared in order to obtain a relationship for the theoretical data of uni-univalent potentials. The good agreement between the theoretical and the experimental data of uni-univalent potentials prove the applicability of the relationship derived to the membrane system. Kobatake's equation was used under two limiting conditions, namely in the concentration range and in the dilute range. The two limiting forms of Kobatake's equation gave identical values of θ for the membrane taken in this investigation. Membrane is negatively charged (cation selective) and the selectivity increases with dilution. The structure of the membrane was observed with the aid of a scanning electron microscope. The order of fixed charge density for electrolytes used was found to be KCl> NaCl> LiCl.

The ionic conductance across titanium arsenate membrane has been recorded. Aqueous solutions of LiCl, NaCl and KCl were used. The conductance values have been found to increase with increase in concentration. The slope of the plots of specific conductance versus concentration exhibits a decrease in its values at relatively higher concentrations compared to those in extremely dilute solutions. The specific conductance values of electrolytes follow the sequence for the cations: $K^+ > Na^+ > Li^+$. Specific conductance increases with increase in temperature, due to the state of hydration which implies that the activation energy decreases. The activation energy decreases with the increase in the concentration

of the electrolyte solution and the sequence for energy of activation is $K^+ > Na^+ > Li^+$. Negative ΔS^* values indicate the formation of a covalent bond between the permeating species and the membrane material

Chapter IV describes transport phenomena in polystyrene based cobalt arsenate membrane. Aqueous solutions of LiCl, NaCl and KCl were used. Membrane potential data have been used to calculate transference number of ions, mobility, distribution coefficient, charge effectiveness, permselectivity and also to derive the thermodynamically fixed charge density which is an important characteristic governing the membrane phenomena by utilizing the generally accepted theories for the salt concentration dependence of uni-univalent potentials, proposed by Teorell-Meyer-Sievers and Kobatake methods and have been compared in order to obtain a relationship for the theoretical data of uni-univalent potentials. The good agreement between the theoretical and the experimental data of uni-univalent potentials prove the applicability of the relationship derived to the membrane system. The conductance values have been found to increase with increase in concentration as well as with temperature. The slope of the plots of specific conductance versus concentration exhibits a decrease in its values at relatively higher concentrations compared to those in extremely dilute solutions. The specific conductance values of electrolytes follow the sequence for the cations: $K^+ > Na^+ > Li^+$ An increase in the conductance with the increase in temperature may have been due to the state of hydration, which implies that the energy of activation for the ionic transport across the membrane follows the

sequence of crystallographic radii of ions. Negative ΔS^* values indicate the formation of a covalent bond between the permeating species and the membrane material. The structure of the membrane was observed with the aid of a scanning electron microscope.

TRANSPORT PHENOMENA IN INORGANIC PRECIPITATED MEMBRANES

THESIS

SUBMITTED FOR THE AWARD OF THE DEGREE OF

Doctor of Philosophy

IN

CHEMISTRY

BY

TANVIR ARFIN

Under the Supervision of

DR. RAFIUDDIN

DEPARTMENT OF CHEMISTRY
ALIGARH MUSLIM UNIVERSITY
ALIGARH (INDIA)

2009


Maulana Azad Library
T. 7378
Aligarh Muslim University, Aligarh

Dr. Rafiuddin
Reader

Department of Chemistry
Aligarh Muslim University
Aligarh 202002 (U.P) India
Phone No: +0571-2508686

Dated..22.May.2009..

CERTIFICATE

This is to certify that the work presented in this thesis entitled **"transport phenomena in inorganic precipitated membranes,"** is original work carried out by Mr. **Tanvir Arfin**, under my supervision and is suitable for submission for the award of Ph.D. degree in chemistry of this University.

(Dr. Rafiuddin)

.....Dedicated to

My family members whose support and contribution has been something, words cannot express

&

above all ALLAH for showing us the right path

Table of Contents

Acknowledgments

"In the name of ALLAH the most beneficent and merciful"

I fell immense pleasure in expressing my regards, deep sense of gratitude, heartful devotion and sincere thanks to my respected royal teacher and supervisor, ***Dr.Rafiuddin****, Reader, Department of Chemistry, A.M.U., Aligarh, who despite of his busy schedule, provided me excellent guidance, motivation, constant help and took keen interest in my thesis, without whose untiring efforts and able guidance this work would have never taken the present shape. It was a great opportunity to work under his supervision.*

I pay my thanks to the chairman, Department of Chemistry, Prof. Arunima Lal for providing necessary facilities.

I would like to express our respect and gratitude to our Alma mater "Raza High School", Patna for the foundation they helped to lay in shaping our respective careers.

I also wish to express my sincere thanks to my respected teachers, Dr. Md. Israrul Haque (Reader, Department of Business Administration, A.M.U.), Dr. Gulfishan Khan (Reader, Department of History, A.M.U.) and Dr. Shabbir Ashraf (Reader, Department of Plant Protection, A.M.U.), for their moral encouragement, invaluable advice and affection they gave to me.

I am equally thankful to the staff of Seminar Library of the Department, especially Mr. Yusuf Jamal (Incharge, Seminar Library), Mrs. Tasneem Jahan, and Mr. Hashmat Ali, who has rendered great assistance to me in the collection of materials. My thanks are also due to the office staff for their help during the session.

I thank my Lord for giving me nice parents ***Mr. Ghyasul Arfin*** *and* ***Mrs. Moina Khatoon*** *whose, care, sacrifice and sustained efforts enable me to acquire knowledge. Whatever, I am today is because of*

their prayer, love and care. Heartily thanks to my younger sister ***Ms. Zeba Rukhsar*** *and brothers* ***Mr. Rameez Arfin*** *and* ***Mr. Zeeshan Arfin*** *for their encouragement and moral support.*

Expressions & emotions fail to find words to highlight the role of our sisters & brothers, who are always there as pillars of support, whernever we need them. ***Hira, Zareen, Insa, Zoya, Nadeem, Daniyal, Farzan, Laraeb, Wakas, Adnan, Daeyan*** *and* ***Muzammil.***

I am very thankful to my labmates Ms. Fakhra Jabeen, Ms. Zoya Zaheer, and Ms. Saima Sultana for their valuable suggestions and support during my research work.

My special thanks goes to Dr. Mohammed Hassan Ali Saleh who always been a source of strength, inspiration and encouragement to me throughout the work and prayed for my success.

I have no words to express my extreme thanks to my special friends Azmat, Bushra, Dr. Abdus, Jamal and Shakeel, who always stood by me through thick and thin and for their care, co-operation, inspiring and moral support.

I must acknowledge my sincere appreciation to all my friends Alka, Arif, Azmat, Dr. Imran, Dr. Saba, Dr. Sarwander, Er. Irshat, Er. Saiful, Farah, Inam, Ishaat, Masood, Mumtaz, Mujahid, Nazia, Neeti, Nusrat, Saba, Sadaf, Dr. Salma, Shahid, Shakeel, Shazia, Tabrez, and Zain, who directly and indirectly provided a stimulus, creative and conducive atmosphere in the successful completion of my thesis.

The financial assistance provided by University Grant Commission (U.G.C), Govt. of India, New Delhi is gratefully acknowledged.

I am thankful to the Indian institute of Technology (IIT), Roorkee for providing SEM micrographs.

Last but not the least; I would like to pay my sincere thanks to non-teaching staff of the department.

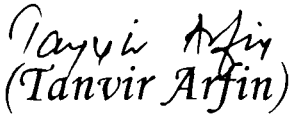
(Tanvir Arfin)

List of Conferences

1. *Tanvir Arfin,* National Conference on Advances in Petroleum Refining & Petrochemical Technologies, 21st March, 2009, Department of Petroleum Studies, Z.H. College of Engg. & Tech. A.M.U., Aligarh
2. *Tanvir Arfin,* Satellite Meeting 2009 of Society for Free Radical Research-India, 17th – 18th March, 2009, Department of Biochemistry, Faculty of Life Sciences, A.M.U., Aligarh
3. *Tanvir Arfin* and Rafiuddin, *Thermodynamic Properties of Inorganic Precipitate Membrane,* National Conference on Chemistry of Materials [NCCM 2009], 20th - 21st February, 2009, University of Mumbai, Mumbai.
4. *Tanvir Arfin* and Rafiuddin, *Effect of Inorganic Electrolytes on thermodynamics of Inorganic Precipitate Membrane,* 11th CRSI National Symposium in Chemistry 6th - 8th February,2009, National Chemical Laboratory, Pune.
5. *Tanvir Arfin,* 3rd CRSI-RSC Symposium on Chemical Sciences, 5th February, 2009, National Chemical Laboratory, Pune.
6. *Tanvir Arfin* and Rafiuddin, *Ion Transport Through Inorganic Precipitate Membrane By The Teorell-Meyer-Sievers Method And The*

Comparison With Kobatake Method, NCETCR-2008, 17th-18th October, 2008 Annamalai University, Annamalainagar.

7. *Tanvir Arfin* and Rafiuddin, *Studies on Ionic Transport of Inorganic Precipitate Membrane in Aqueous Solution,* Presented in National Conference on Advanced Materials, 8th -9th March, 2008, Udai Pratap Autonomous College, Varanasi.

List of Publications

This thesis contains the following papers:

1. *Tanvir Arfin* and Rafiuddin, Transport studies of Nickel Arsenate Membrane, communicated to *Journal of Electroanalytical Chemistry* (Elsevier).
2. *Tanvir Arfin* and Rafiuddin, Electrochemical Properties of Titanium Arsenate Membrane, communicated to *Journal of Electrochimica Acta* (Elsevier).
3. *Tanvir Arfin* and Rafiuddin, Effect of entropy of activation across Titanium Arsenate Membrane, communicated to *Journal of Sol-Gel Science and Technology* (Springer).
4. *Tanvir Arfin* and Rafiuddin, Study on Electrochemical characterization of Cobalt Arsenate Membrane, communicated to *Journal of Applied Electrochemistry* (Springer).

List of Abbreviations

AR	analytical reagent
C_1, C_2	concentration of electrolyte solution either side of the membrane (mol/l)
$\overline{C}_{1+}$	cation concentration in membrane phase 1 (mol/l)
$\overline{C}_{2+}$	cation concentration in membrane phase 2 (mol/l)
C_i	i^{th} ion concentration of external solution (mol/l)
$\overline{C}_i$	i^{th} ion concentration in membrane phase (mol/l)
$K_{\pm}$	distribution coefficient of ions
$K''_{\pm}$	distribution coefficient of ions (electrolyte solution C_2)
q	charge effectiveness of membrane phase 1
q''	charge effectiveness of membrane phase 2
SCE	saturated calomel electrode
SEM	scanning electron microscopy
TMS	Teorell, Meyer and Sievers
W_w	weight of the soaked/wet membrane (g)
W_d	weight of the dry membrane (g)
A	area of the membrane (cm^2)
L	thickness of the membrane (cm)
ρ_w	density of water (g/cm^3)
$\overline{D}$	charge density in membrane (eq/l)
$\overline{U}$	$\left(\frac{\bar{u}-\bar{v}}{\bar{u}+\bar{v}}\right)$
$\bar{u}$	mobility of cations in the membrane phase ($m^2/v/s$)
$\bar{v}$	mobility of anions in the membrane phase ($m^2/v/s$)
R	gas constant (J/K/mol)
T	absolute temperature (K)

F	Faraday constant (C/mol)
P_s	permselectivity of the membrane-electrolyte system
t_+	transport number of cations
t_-	transport number of anion
$\overline{t_+}$	transport number in membrane
V_k	valency of cation
V_x	valency of fixed charge group
$\gamma'_{\pm}, \gamma''_{\pm}$	mean ionic activity coefficients
$\overline{\omega}$	mobility ratio (TMS extension theory)
$\Delta\phi$	membrane potential (mV) (TMS theory)
$\Delta\phi_m$	membrane potential (mV) (TMS extension theory)
$\Delta\phi_{Don}$	donnan potential (mV)
$\Delta\phi_{diff}$	diffusion potential (mV)
Λ	specific conductance ($m\Omega^{-1}cm^{-1)}$
h	Planck's Constant (Js)
N	Avogadro number
ΔG^*	free energy of activation (KJ/mole)
ΔH^*	enthalpy of activation (KJ/mole)
E_a	activation energy (KJ/mole)
ΔS^*	entropy of activation ($JK^{-1}mol^{-1}$)

Preface:-

"Success begins with the fellows will, its all in the state of mind, life's battles don't always go to the stronger or faster man, but sooner or later the man who wins is the man who thinks he can".

The aim of this work is to prepare inorganic precipitate membranes based on sol gel method. Membranes may be solid, liquid or gas and the outer phases are usually liquid or solid. Membranes are usually thin in one dimension relative to the other two dimensions. This property is only functional or operational.

This thesis has been divided into four chapters. The first chapter contains general introduction regarding inorganic precipitated membranes. The second, third and forth chapters report preparation and transport properties of number of inorganic precipitated membranes.

Membrane potential and conductance are a measurable and reliable parameter to characterize the charge property of membrane. Membrane potentials have been measured across polystyrene based arsenate membranes separating various 1:1 electrolytes at different concentrations. Membrane potentials data have been used to calculate transference number of ions, permselectivity and also to derive the thermodynamically fixed charge density which is an important characteristic governing the membrane phenomena. In addition to evaluation of distribution coefficient, mobility, charge effectiveness and other related parameters were calculated for the characterizing the prepared membranes.

At the same time experimentally observed membrane conductance values at different temperatures have been used to compute various thermodynamic parameters.

CHAPTER 1

General Introduction

The study of transport phenomena in inorganic precipitate membrane is one of the major problems in which the chemists and biologists are equally interested. Tremendous progress has been made during the last decade pertaining to membrane diffusion and transport problems in various fields of research [1-8]. The literature on the subject, both theoretical and experimental has reached impressive proportions. Chemists and chemical engineers would like to understand the mechanism of transport and with the knowledge gained they would be able to fabricate membranes of desired properties [9,10]. Biologists, on the other hand, would like to use them as simple models for the physiological membranes in order to understand, in terms of established physical chemical principles, the behavior of complex cell membranes [11,12]. Pharmacologists, however, would use the knowledge to understand the controlled delivery of drugs to their respective targets in the human body [13,14]. Physists and mathematicians have also tried and introduced theories to know the transport mechanisms [15,16]. The recent progress of the physico-chemical [17] aspect of membrane is entirely due to the applications of the thermodynamics [18].

It is very difficult to give a precise and complete definition of the word "membrane" because any definition given to cover all the facets of membrane behavior will be simply incomplete. According to Sollner [19,20] "A membrane is a phase or structure interposed between two phases or compartments, which obstructs or completely prevents gross movement between the latter, but permits passage, with various degree of restriction, of one or several species of particles

from the one to the other or between the two adjacent phases or compartments and thereby, acting as a physico-chemical machine. Lakshminarayanaiah [21] has given a simple definition and described the membrane as a phase, usually heterogeneous, acting as a barrier to the flow of molecular and ionic species present in the liquid and/or vapor contacting the two surfaces. The term heterogeneous has been used to indicate the internal physical structure and external physico-chemical performance [22,23].

The current theories [24] on the transport of charged or uncharged particles across membranes can be roughly divided into the following three groups:

One school of thought considers the membrane as a surface of discontinuity separating the two adjacent phases and setting up different resistances to the passage of various molecular and/or ionic species. Second school of thought considers the membrane as a quasi homogeneous intermediate phase of finite thickness while the third one considers the membrane as a series of potential energy barriers. This grouping attempts to classify the various mathematical approaches according to the ideal models on which they are based. Many of the theories based on the Nernst Planck flux equations are placed in the first group whereas those dealing with the principles of irreversible thermodynamics and the theory of rate processes are placed in the second and third groups respectively. According to Lakshminarayanaiah the theories of group one are based on the ideas of classical thermodynamics or quasi thermodynamics which are restricted to isothermal systems. The theories of group two, apart from being more rigorous

and realistic, allow a better understanding of transport phenomena in membranes and are useful in dealing with non isothermal systems. The theories of group three contain parameters which are still unknown and hence have restricted applicability.

A membrane is an interphase between two adjacent phases acting as a selective barrier, regulating the transport of substances between the two compartments. According to Lonsdale's viewpoint [25] a membrane is not just an object that obstructs but its definition must embody its function. A membrane is a thin wall made of materials that provide an unequal resistance to the transport of different molecules. The molecules are driven across the membrane by forces arising from imposed chemical or electrochemical potential gradients. Such potential gradients may be induced within the film by inserting the membrane between two media differing in pressure, temperature, composition and electric potential. Membranes are a part and parcel of biological systems and are believed to be involved in innumerable fundamental life processes such as ion accumulation, conduction of nerve impulses, protein synthesis, energy transduction, immunological reactions, phagocytosis and pinocytosis, etc. vital for sustaining life on this planet.

A membrane can be homogeneous or heterogeneous, symmetric or asymmetric in structure, solid or liquid can carry a positive or negative charge or be neutral or bipolar. Membranes may be natural or artificial, carry ionizable

groups either fixed to the three dimensional membrane matrixes or adsorbed as found in some colloidal systems.

1. Type of Membranes

1.1. Ion- Exchange Membranes

Ion-exchange membranes carry the fixed positive or negative charges (called anion exchange membranes, AFM or cation exchange membranes, CEM, respectively). Ion-exchange membranes are one of the most advanced separation membranes. The basic applications of the ion exchange membrane processes are based on the Donnan membrane equilibrium principle. They are generally used in the treatment of ionic aqueous solutions, e.g. electrodialytic concentration of seawater, desalination of saline water, demineralization process, acid and alkali recovery and other [26-30]. Ion-exchange charged membranes, which are now extensively utilized in industries, have attracted considerable attentions due to their extraordinary properties and practical demands and thus a large number of researchers have concentrated on these investigations for many years [31]. With the rapid development of industry and population explosion throughout the world, the demand for fresh water has become increasingly urgent due to the scarcity of drinking water resource and the contamination of environment due to industrial wastes. Hence the treatment of industrial wastewater is becoming imperative; while innovative technologies, which are used to prepare fresh water such as the desalination of brackish water and treatment of the industrial refuses, have

attracted numerous researches. Among these novel methods, ion-exchange membrane based technologies have been regarded as both effective and economical due to its lower operational expense and secure processes etc. [32,33]. Ion-exchange membranes discriminate cation and anions, thus they should have a high transport number for counter-ions.

For these wide applications, the most desired properties required for successful ion-exchange membranes are:

- High perm selectivity — an ion-exchange membrane should be highly permeable to counter-ion, but should be impermeable to co-ions.
- Low electrical resistance — an ion-exchange membrane should have low electrical resistance and thus there will be less potential drop during electro-membrane processes.
- Good mechanical stability — the membrane should be mechanically strong and should have a low degree of swelling or shrinking in transition from dilute to concentrated ionic solutions.
- High chemical stability—the membrane should be stable over a pH-range of 0 to 14 in the presence of oxidizing agents.

Most of the commercial ion-exchange membranes can be divided into two major categories. On the basis of their structure and preparation procedure: most of the commercial ion-exchange membranes can be divided into two homogeneous and heterogeneous. According to Molau [34], depending on the degree of heterogeneity, ion-exchange membranes can be divided into the following types:

(a) homogeneous ion-exchange membranes, (b) interpolymer membranes, (c) micro-heterogeneous graft- and block-polymer membranes, (d) snake-in-the-cage ion-exchange membranes, (e) heterogeneous ion-exchange membranes [35].

All the intermediate forms are considered as the polymer blends from the viewpoint of macromolecular chemistry. On one hand, a phase separation of the different polymers is obtained, while on the other hand, a specific aggregation of the hydrophilic and hydrophobic properties of the electrolyte is obtained. A classification of the membrane morphology is then possible, depending on the type and size of the micro phase. The membranes are translucent, an indication that inhomogeneities, if any, are smaller than the wavelength of visible light (400 nm). Thus, these membranes are called interpolymer or micro-heterogeneous membranes.

1.1.1. Homogeneous Ion-Exchange Membranes

The method used for the preparation of homogeneous ion exchange membranes can be summarized in three different categories:

1. Polymerization or polycondensation of monomers; at least one of them must contain a moiety that either is or can be made anionic or cationic, respectively
2. Introduction of anionic or cationic moieties into a preformed solid film

3. Introduction of anionic or cationic moieties into a polymer, such as polysulfone, followed by the dissolution of the polymer and casting it into a film.

Examples:--

- Fluorinated ionomer membranes
- Styrene–divinylbenzene based membranes
- Partially fluorinated ionomer membranes
- Polysulfone based ion-exchange membranes
- Partially sulphonated poly(ether ether ketone) (PEEK) membranes
- Polybenzimidazole based ion-exchange membranes
- Polyimide based ion-exchange membrane
- Polyphosphazene ion-exchange membranes
- Styrene/ethylene-butadiene/styrene triblock copolymers
- Ion-exchange membranes by the sol–gel method

Homogeneous membranes having good electrochemical properties lack in their mechanical strength, whereas heterogeneous membranes having very good mechanical strength are comparatively poor in their electrochemical performance [36].

1.1.2. Heterogeneous Ion-Exchange membranes

Heterogeneous membranes, which consist of neutral polymer matrix, such as polyethylene are randomly filled with micron-sized ion-exchange particles. Both

membrane types are often reinforced with a net of polymeric material, such as polyamide or polyester. A heterogeneous membrane becomes an ion-conductive permselective membrane when the so-called percolation concentration [37] of the ion-exchange particles is surpassed. The concentration of ion-exchange particles in the matrix required for reasonable ion transport through the membrane is 50–70 wt. % [38]. At such concentrations, the specific conductivity of commercial membranes lies in the range 4–12 $mScm^{-1}$. The above-mentioned concentrations of ion-exchange particles are, in fact, the maximum possible concentrations for electrodialysis applications: any attempt to obtain higher conductivity by increasing the concentration of ion exchanger beyond this range results in a loss of membrane strength and in reduced shape stability due to increased swelling upon exposure of the membranes to aqueous salt solutions. These properties are important for membranes used in electrodialysis stacks, since they limit the range of conditions under which electrodialysis may be applied.

In power sources, particularly fuel cells, the Nafion^{TM} membrane is widely used because of its remarkable proton conduction (0.15 S cm^{-1}) and its stability to oxidation [39]. However, new generations of fuel cell require both higher proton conductivity and lower permeability to the fuel (for example, hydrogen or methanol). Inorganic or hybrid inorganic–organic composite membranes (both of the heterogeneous type) are currently under intensive development for such applications [40-43]. One of the problems encountered in the development of such

membranes is that as the proton conductivity or the ionic conductivity in general increases, permeability to the fuel also increases [44].

1.2. Liquid Membranes

In recent years, the liquid membrane has been widely used to study ion transport against a concentration gradient [45,46]. Ion transport through the liquid membrane plays an important role in simulating biological membrane functions and separation technologies because of the high transport efficiency, excellent selectivity and economic advantages of the liquid membrane. A number of successful studies involving the transport of metal ions [47-50], rare earth elements [51,52], drugs [53], phenols [54], fructose [55] and the treatment of seawater and wastewater [56-58] through the liquid membrane have been carried out. Selective transport of transition metal ions through liquid membranes has become increasingly noteworthy. A number of carriers for heavy metal ions and in particular Cu(II), which is both vital and toxic to many biological systems, have been reported [59,60]. Two configurations of liquid membrane are currently being used: emulsion liquid membrane [ELM] and supported liquid membrane [SLM] [61,62].

1.3. Bipolar Membranes

Bipolar membranes are known since the 1950s and have aroused a renewed interest for their ability to generate hydrogen ions (H^+) and hydroxyl ions (OH^-) by water dissociation via electrodialysis during the last decade [63,64]. BM is

generally composed of a layered polymer structure composed of a juxtaposed cation selective exchange region (CM) joined to an anion selective region (AM), and the electro-dissociation of water is achieved. BM and its related technology have found many applications in industries and in daily life, such as chemical production and separation and environmental conservation, etc.

Bipolar membranes have recently gained attention as efficient tool for the production of acids and bases from their corresponding salts by electrically enforced accelerated water dissociation. Bipolar membranes can be prepared by simply laminating conventional cation- and anion-exchange membranes. The total potential drops depend on the applied current density, the resistance of the two membranes and solution resistance. Since the specific resistance of deionized water is very high, the distance between the membranes of opposite polarity should be as low as possible.

1.4. Inorganic Membranes

The inorganic membrane was first developed and used in large scale in gas separation processes in 1940. New processes and techniques in inorganic membrane technology have been revolutionizing the chemical industry in recent year and acting as substitute of polymeric membranes [65]. Inorganic membranes exhibit unique physical and chemical properties compared to the other membranes. These can significantly be used at higher temperatures with structural stability without swelling or compaction and can withstand harsh chemical

environment without undergoing microbiological attack. They posses very high resistance towards acid and has remarkably high selectivity [66]. There are extensively used in separation processes. Their high electrical conductivity and better current efficiency have been used in desalting of brackish water [67], fuel cell and electrical storage batteries [68]. The inorganic ion-exchange membranes are useful in a variety of selective separation processes such as water purification, catalyst recovery, solvent cleanup, food and beverage processing. However, they have made little headway as a model for biological membranes in spite of the fact that comparatively simpler inorganic systems made up of amino, imido and phosphate groups comparable to phospholipids can be investigated and subsequently synthesized.

Two types of inorganic membranes are generally known viz., (i) crystalline and (ii) amorphous. Heteropolysalts such as phosphomolybdates, aminosilicates, etc., belong to the former category, and simple and mixed hydrous oxides of group IV, V and VI to the latter category. Ceramic membrane is the another recent development of inorganic membrane system and probably the most attractive system for gas separation processes [69] due to its high molecular sieve like selectivity and high stability at enhanced temperature (300-1000°C) and are chemically quite stable. Ceramic membrane is used in membrane reactor. It uses catalytically active or passive membrane and is proved to be very promising. Amorphous type inorganic membranes have not been used extensively in practical and industrial purposes. In order to obtain both categories of membranes as sheets

of sufficient mechanical strength, they are amalgamated with polystyrene [70].The parchment supported membranes have also been employed for this study [71]. Inorganic membranes are versatile; they can operate at elevated temperatures, with metal membranes stable at temperature ranging from 500-800 °C and with various ceramic membranes usable over 1000 °C. They are also much more resistant to chemical attack. A variety of materials has been used in the fabrication of inorganic membranes and manipulates their features according to necessity that is resistance to corrosive liquids and gases, mechanical and thermal stability, etc. Inorganic membranes compete with organic membranes for the commercial use and in many of the harsh operational environment organic membranes do not perform well or remain stable.

1.5. Non Porous and Porous Membranes

Membranes are considered to be nonporous or porous depending upon the extent of solvent penetration [72]. At the nonporous extreme, membranes that are nonionic and contain negligible transportable species at equilibrium, e.g., ceramic, quartz, antharacene crystal and teflon film, are examples of solid membranes. Organic liquid film such as hydrocarbon and fluorocarbon are examples of liquid membranes. At the porous extreme, the membranes can be solvated and contain components from the outer phases. Inorganic gels are loosely compressed powder in contact with aqueous solution. These materials absorb solvent from the surrounding media and may also interact with other neutral molecules and ionic

salts. More widely studied membranes are polyelectrolyte (solid ion-exchanger), aqueous immiscible organic liquid electrolytes (liquid ion-exchanger), various parchment supported inorganic precipitate [73], solid ion conducting electrolytes including silver halide, rare earth fluoride, alkali silicates and alumino silicate glasses. All these material contain ionic or ionizable groups within the membranes, which are capable of transport under diffusive or electric field forces and these material possess the properties of porosity. Polyelectrolytes tend to swell rapidly by osmotic pressure and uptake of the solvent. Liquid ion-exchangers are surprisingly slow to take up of water, while the inorganic salt have no tendency to hydrate, glass membrane are complicated by simultaneous hydrolysis of the polyelectrolyte during uptake of water [74].

1.6. Polymeric Membranes

Polymeric membranes are well known for their uniformity, chemical stability and controlled ion-exchange properties. These membranes have significant advantages over conventional membranes, owing to their electrical nature, adhesive property, thermal conductivity, chemical resistivity and biochemical properties. Polymeric membranes are important separation device extensively used as biomedical membranes in applications such as heamodialysis, heamofiltration, reverse osmosis, blood purification, and control drug delivery, etc. [75]. In the natural kidney, ultrafiltration of the blood occurs through the capillaries leading to the removal of waste product and purification of blood. In an artificial unit, a

membrane dependent ultrafiltration achieved essentially the same results. Membranes in the form of either flat sheets or hollow fibers are employed. A synthetic polymer substitute is being experimented with a polyethylene glycol, a block copolymer membrane which can filter selectively [76]. A modified polymeric unit has been used as membrane in which oxygenated blood is allowed to flow through membrane barrier which have very high permeablities to both oxygen and carbon dioxide. The flow of oxygen, which is maintained at high partial pressure, displaces carbon dioxide and thus this unit is accounted for effective purification. Silicon is the best membrane material available and extensive used as a polymeric membrane. It has a high permeability to gases and low permeability to water and can also be autoclaved [77]. Synthetic polymeric membranes are the crucial compounds of controlled drug delivery system [78]. The advantage of drug delivery in this fashion is that the drug can be maintained at optimum therapeutic concentration in the body over long period of time. Besides silicon membranes, ethylenevinlylacetate copolymers, polyglycollic acid, lactic acid, block copolymer and certain verities of hydrogel have drawn attention. A hydro gel system is based on butylmethacrylate, which has been tested for antitumor drug delivery. Polymeric membrane bearing ion-exchange property has the distinction of being the most widely studied systems [79].

1.7. Lipid Membranes

Tethered bilayer lipid membrane (tBLM) systems, which have been developed for biological membranes [80], have been used in the investigation of membrane proteins to study processes such as redox activity and ion transport across the membrane [81-83]. The general concept of tBLMs is to prepare a SAM on a metal surface using thiol-lipids that consist of a lipid tail and a hydrophilic spacer attached to the thiol. In a second step, the other leaflet of the lipid bilayer is formed by fusion of phospholipids vesicles, sometimes supplemented with sterols. The thiol-lipids can also be 'diluted' on the surface by mixing them with smaller thiol compounds [84-86].

An important issue is whether the hydrophilic region of a tBLM (the sublayer) is able to accept and store ions [86-89]. This is especially important when studying membrane proteins that are active in charge transport, such as ion channels and active transporters. Becucci et al. have performed a thorough and detailed analysis of a tBLM on mercury which shows that ions are indeed able to penetrate in the sublayer, albeit with high resistance values up to 0.2 $M\Omega\ cm^2$ [87-89]. However, it is not known whether similar properties are exhibited by tBLMs prepared on solid metals like gold. Using mixed SAMs might further change the properties of the sublayer and therefore the ability of the tBLM to store ions [86]. In a recent neutron reflectivity study it was shown that water is present in the sublayer when mixed SAMs are used [90].

1.8. Charged and Uncharged Membranes

The term charged and uncharged in the membrane literature is usually unsound electrostatically, but does provide an intuitive chemical description. A charged membrane refers to an electrolyte membrane viz., solid or liquid ion-exchangers, where the fixed and mobile sites are having the charges. Actually these membranes are quasi electroneutral in their bulk when the thickness is large compared with the Debye thickness at each interface. Quasi-electroneutrality means that any volume element is larger compared with the distance between ions and the sum of ionic charges. In the literature uncharged membranes are those, like cellophanes, with no fixed charges. This frequently used literature definition provide no place for liquid layer membranes. These are electrostatically neutral only in the absence of charge carriers and bathing solutions whose salts possess preferential solubility of anion over cation or vice-versa but are usually electrostatically charged by an amount of ion of same sign in normal operation. Thick hydrocarbon membranes, membrane of diphenyl ether, phthalate and sebacate esters are generally neutral in the presence of most bathing electrolyte. The may be charged electrostatically, depending on the thickness, in the presence of neutral carrier species that preferentially solubalize ions of one sign. The use of term charged and uncharged is described electrolyte and non electrolyte membranes have been discussed unless the precise electrostatic interaction is involved [91].

1.9. Fixed Site and Mobile Site Membranes

The electrolyte membranes are characterized by the presence of charged sites. The sites are partially or completely ionized depending on the dielectric constant and solvent penetration [92]. If ionic groups for example $-SO_3^{2-}$, $-COO^{2-}$, $-PO_4^{2-}$ are fixed in the membrane, attached to cation-exchangers, the membrane is considered to posses fixed sites even though protons or metal ions are covalently bonded to the sites. In glass membrane, the fixed sites are SiO^- and AlO^- groups, while in anion exchangers these are $-N^+$ and $-NH_4^+$. The membranes having same fixed charged groups exclude co-ions by electrostatic repulsion. The extent of exclusion is governed by the concentration of external electrolyte and the magnitude of the charge fixed to the membrane matrix. On the other hand, liquid ion-exchangers that are water immiscible, such as diesters of phosphoric acid, can be viewed as a mobile site membrane. The acid is trapped in the organic phase, while the proton and other cations can move in and out of the membrane frame work.

1.10. Organic-Inorganic Hybrid Membranes

The nanostructure organic-inorganic hybrid materials are currently the subject of intensive research, because they combine in a single solid both, the attractive properties of a mechanically and thermally stable inorganic backbone and the specific chemical reactivity and flexibility of the organo-functional group. These combined properties of the hybrid nanostructure materials with diverse

applications have attracted attention in the fields of material science [93-96], heterogeneous catalysis [97], separation science, and fuel cells [98,99]. Most of the properties of these new materials are dependent on their structural and chemical composition as well as on the dynamic properties inside the hybrid. To develop functionalized materials/membranes, several investigators worked on the organic-inorganic hybrid materials, in which functional groups were covalently attached to the organic part of the hybrid [100-102] (such as sulfonated polysulfones, sulfonated polyetherketones, and polybenzeneimidazole). The problem with the hybrid material is that if the organic chains in these hybrids bear functional groups such as sulfonic or sulfonamide, usually they are soluble in water [103]. To decrease solubility and increase plasticity and mechanical strength, in most cases, the hybrids were cross-linked. However, very little work has been done for the applications of these materials as ion-exchange membranes, in which a functional group is attached to the inorganic part of the hybrid materials. Another choice is to disperse hybrid ion-exchangers into inorganic substrates to form supported membranes.

2. Membrane Separation Technology

A membrane separation system separates an effluent stream into two sub-streams known as permeate and concentrate. The permeate is the portion of the fluid that has passed through the semi-permeable membrane, whereas the

concentrate stream contains the constituents that have been rejected by the membrane.

Passive transport through membranes occurs as consequence of a driving force, i.e. a difference in chemical potential by a gradient across the membrane in, e.g. concentration or pressure, or by an electrical field [104]. The barrier structure of membranes can be classified according to their porous character (Table 1).

Active development is also concerned with the combination of nonporous or porous membranes with additional separation mechanisms, and the most important ones are electrochemical potentials and affinity interactions.

For non-porous membranes, the interactions between permeate and membrane material dominate transport rate and selectivity; the transport mechanism can be described by the solution/diffusion model [105,106].

The separation selectivity between two compounds can be determined by the solution selectivity or by the diffusion selectivity. However, even for systems without changes of the membrane by the contact with the permeand—as it is the case for permanent gases with dense glassy polymers—a dual-mode transport model is the most appropriate description of fluxes and selectivities [107]. This model takes into account that two different regions in a polymer, the free volume and more densely packed domains, will contribute differently to the overall barrier properties.

For porous membranes, transport rate and selectivity are mainly influenced by viscous flow and sieving or size exclusion [108]. Nevertheless, interactions of

Table 1 Classification of membranes and membrane processes for separations via passive transport

Membrane barrier structure	Trans-membrane gradient		
	Concentration	Pressure	Electrical field
Non-porous	Pervaporation (PV)	Gas separation (GS) Reverse Osmosis (RO)	Electrodialysis (ED)
Microporous pore diameter $d_p \leq 2$nm	Dialysis (D)	Nanofiltration (NF)	
Mesoporous pore diameter d_p=2-50nm	Dialysis	Ultrafiltration (UF)	Electrodialysis
Macroporous pore diameter d_p=50-500nm		Microfiltration (MF)	

solutes with the membrane (pore) surface may significantly alter the membrane performance. Examples include the GS using micro- and mesoporous membranes due to surface and Knudsen diffusion, and the rejection of charged substances in aqueous mixtures by microporous NF membranes due to their Donnan potential. Furthermore, with meso- and macroporous membranes, selective adsorption can be used for an alternative separation mechanism, (affinity) membrane adsorbers are the most important example [109]. In theory, porous barriers could be used for very precise continuous permselective separations based on subtle differences in size, shape and/or functional groups.

Membrane separation technologies commercially established in large scale are:

- D for blood detoxification and plasma separation ('medical devices');
- RO for the production of ultrapure water, including potable water ('water treatment');
- MF for particle removal, including sterile filtration (various industries);
- UF for many concentration, fractionation or purification processes (various industries including 'water treatment');
- GS for air separation or natural gas purification.

The following general strategies will lead to a higher separation's performance:

- non-porous membranes—composed of a selective transport and a stable matrix phase at an optimal volume ratio along with a minimal tortuosity of the transport pathways, thus combining high selectivity and permeability with high stability;
- porous membranes—with narrow pore size distribution, high porosity and minimal tortuosity (ideally: straight aligned pores though the barrier);
- additional functionalities for selective interactions (based on charge, molecular recognition or catalysis) combined with non-porous or porous membrane barriers;
- membrane surfaces (external, internal or both) which are 'inert' towards uncontrolled adsorption and adhesion processes.

3. Performance of Advance Functional Membrane

The performance criteria for advanced membranes obviously depend on the state of development and technical implementation of the respective membrane process

3.1. Gas Separation

GS with membranes is established in large scale for selected processes such as the separation of oxygen and nitrogen, hydrogen and nitrogen, or carbon dioxide and methane. Nevertheless, GS had not yet been implemented in the large scales envisioned a decade ago. Active research and development is still devoted to the removal of carbon dioxide from various streams. Other important separations are

the conditioning of natural gas or the purification of process gases. The separation of (organic) vapors, for the recovery for valuable material or for the removal of undesired components, is another opportunity

3.2. Reverse Osmosis

Over the last decades polyamide membranes for reverse osmosis (RO) have found many successful uses in desalination of sea and brackish water, waste treatment and various separations in chemical, food, pharmaceutical and other industries. Despite the commercial success, current understanding of separation of multicomponent mixtures, especially of electrolytes, by these membranes is still insufficient for predictive modeling and motivates search for novel characterization approaches.

Customarily, models employ a set of extended Nernst-Planck (ENP) differential equations. The ENP equations are obtained when a convection term is added to the Nernst-Planck equations for each ion in solution with an additional condition of electroneutrality [110-112]. Thermodynamic relations must be added to link the ion activity to local solution composition based on relevant mechanisms of ion exclusion—steric, Donnan and/or dielectric.

Even at the most basic level the models require a large number of phenomenological parameters such as the absolute ionic permeabilities ω_i and the reflection coefficients σ_i that must be known for *each individual ion* present in solution. However, in standard experiments with RO filtration of single salts only

lump "salt" parameters ω_s and σ_s may be obtained. For results, a significant number of assumptions are usually made regarding the exclusion mechanism(s) and the values of relevant parameters, e.g., effective fixed charge density for Donnan exclusion [110-112]. Obviously, this largely reduces the capability of the models to predict performance in complex cases. The difficulties to obtain individual ion characteristics for salts are mostly associated with two problems. The first is *coupling of the ion fluxes via electrostatic interactions*, which occurs even in the case of a single salt. For charged unsupported membranes (e.g., ion-exchange membranes), the standard way of splitting the salt parameters to individual ionic parameters is measuring some electrical characteristics, i.e., diffusion potential or high-frequency electrical resistance. However, in the case of composite RO membranes an additional difficulty arises due to the *presence of the supporting layers*, whose diffusional and electrical resistances overwhelm those of the active layer [113]. The largest progress using whole supported membranes has been achieved so far by Yaroshchuk et al. using non-steady state measurements, such as potential transients after a sudden change of current, pressure or concentration. In this way, contributions from the active and support layers may be separated at certain time scales [113-116].

3.3. Nanofiltration

Transport through nanofiltration membranes merge size and electrical effects, as total charge density, dielectric exclusion, etc., with solution diffusion

mechanisms. Actually it joins factors typically relevant in reverse osmosis with those usually controlling ultrafiltration. The pore size of nanofiltration membranes is typically below 1 nm in diameter. They have fixed charges developed by dissociation of appropriate groups present in the membrane materials. Due to these charges and sizes, a nanofiltration membrane retains multivalent complex ions and transmits relatively well small uncharged solutes and low charged ions. The low energy consumption and the high fluxes attained by the process, makes nanofiltration very useful in fractionation and selective removal of solutes from complex process streams [117].

Transport of solutes takes place by convection due to the applied pressure difference and by diffusion due to the concentration gradient that appears across the membrane. A sieving-friction mechanism explains the retention of uncharged solutes [118,119].

In order to take into account both the steric and electrical interactions on charged solutes, a space charge model is commonly used. The so-called Donnan steric pore model (DSPM) proposed by Bowen et al. [120] in 1996 has given useful results. This model is based on the extended Nernst–Planck equation, but includes steric or sieving effects along the Donnan equilibrium to give the equilibrium partition of ions between the solutions in and outside the membrane.

More recent developments include a description of dielectric exclusion whose effects are very relevant for such narrow pores. Non-uniformity of membranes can also be taken into account by introducing information on actual pore size

distribution, leading to slight modifications on retention if such distributions are wide enough [121].

Attending to the extremely relevant influence of pore size and pore size distribution for nanofiltration membranes, an adequate elucidation of such porometric properties [122] are discussed.

NF membranes possess a molecular weight cut-off of about a few hundreds to a few thousands Dalton which is intermediate between reverse osmosis and ultrafiltration membranes. Nanofiltration has attracted increasing attention over recent years due to the development of new applications in several areas, e.g. textile industry (removal of dye from waste rinse water), paper and plating industries (limitation of the consumption of clean water by recycling waste water), drinking water production, etc.

Some recent works devoted to the influence of electrolytes on the transfer of neutral solutes through NF organic membranes have shown a decrease in the rejection coefficient of neutral solutes in the presence of ions [123-126]. For instance, Bouchoux et al. studied the potentialities of NF as a purification step in the production process of lactic acid from sodium lactate fermentation broth [123].Working with single-solute solutions, these authors showed that the rejection coefficient of glucose (contained in the fermentation broth) was sufficiently greater than that of sodium lactate so that the purification was expected to be feasible. However, the experiments they carried out with the mixed-solute solutions revealed a sharp decrease in the glucose rejection

coefficient. Actually, the retention lowering was such that the rejection coefficients of both solutes became very close so that purification of anyone was unachievable. Several hypotheses have been postulated to explain this phenomenon. The first one was that the retention lowering may have been caused by an increase in the average pore size due to the repulsive interaction between the counterions inside the pores. This phenomenon is usually referred as pore swelling [123,124]. The second hypothesis was that ions may have decrease the effective size of the neutral species because water preferentially solvate ions (this would be a kind of salting out effect as first observed by Hofmeister in his work on the influence of the nature of the background salt on the precipitation of hen-egg-white protein [127]).

3.4. Pervaporation

Pervaporation (PV) is providing the method in separating liquid mixture of volatile ingredients. The efficiency of PV has been approved in eliminating water from organic solutions, concentrating or recovering the organic from aqueous solution, separation of organic mixture, etc. So far, the explorations of PV process have been widely focused in the fields of wastewater treatment [128-131], pharmaceutical industry, and removal of the products from fermentation broth in bioreactors [132,133], condensation of the natural aroma in extraction solution [134] and so on. One of the key rules in selecting PV membrane is the compatibility between the membrane and the separations mixtures. For example,

for the PV processes with preferential permeation of the lower polar organics, the membrane material should have lower polarity nature. Contrarily, the membrane material should have higher polarity for the PV with permeation preference in water or the polar organics [135,136]. At the same time, the membranes were usually fabricated into asymmetric or composite structures with skin layer to increase the flux [137]. So, the asymmetrically polymeric membranes with selecting skin layer were of the key considerations in pervaporation. Currently, the efforts are still focused on the skin layer materials with excellent balanced performances. Among the great varieties of investigated polymers for PV, the fluorine-containing polymer has been noted. The lower polarity/ surface energy/crystallinity, the higher hydrophobicity and stability could generate fluorine-containing polymer into membrane materials for PV with organic permeating preference, especially in the separation of organic/water mixtures [138-140].

3.5. Dialysis and Ultrafiltration

D and UF membranes have analogous porous barrier structures. For established materials prepared via the NIPS process, the pore size distribution with diameters in the lowest nanometer range is rather broad. Due to the different driving forces the separation in D and UF are much influenced by the early commercialization of hollow fiber membrane dialyzers, D which has now become a separate field.

D is mainly applied as hemodialysis for the treatment of patients, what lead to very strict requirements with respect to material's safety [141]. For the same reason, significant efforts are devoted to the improvement of biocompatibility of the membranes. A more precise filtration is also still a target for membrane improvement; however, the 'ideal' selectivity curve of a hemodialysis membrane is still not known based on a fundamental understanding of all critical components to be removed or retained [142]. Recently, the combination of D with selective adsorption had been actively developed, and the integration of useful adsorber functionalities in the membrane can also be achieved [143]. Finally, the well-developed D membranes and modules are a comfortable basis for the development of other (novel) membrane technologies, e.g. membrane contactors [144] or enzyme-membrane reactors.

Ultrafiltration (UF) membranes have been widely applied in molecular separation technologies such as those used in low concentration effluent treatment, water purification, and virus removal [145,146]. UF membranes with pore sizes in the range of 1–100 nm are classified by molecular weight cutoff (MWCO), which is typically defined as the molecular weight of a solute that has a rejection coefficient of 90% or greater. The pore geometry of UF membranes consists of an interconnected three dimensional network of channels of non-uniform size and shape. A prominent feature of UF membranes is their thin skin layer on the surface, which is usually 0.1–1 μm in thickness. This skin layer permits high hydraulic permeability while the more open/porous sublayer (typically 125 μm in

thickness) provides good mechanical support; additional strength is sometimes provided by casting the membrane on a spun-bonded polyethylene or polypropylene backing [147]. Therefore, the small pores in the thin and dense skin layer are mainly responsible for the separation characteristics of the membrane and the open sublayer does not usually influence the membrane performance. Thus, when developing a UF membrane for a particular molecular separation process, it is of prime importance to determine the size and distribution of the pores of the membrane, as accurately as possible [147,148].

Various methods have been employed to determine the pore size distribution (PSD) of porous membranes, including the microscopic observation method [149,150], bubble pressure method [151], mercury intrusion porosimetry [152], permporometry [153], gas adsorption–desorption [154], and differential scanning calorimetry (DSC) thermoporometry [155,156]. These methods vary widely in applicability, sensitivity, and information that they yield. However, some methods have their specific disadvantages such as irreversible damage of the samples and time consuming, which limited their applications for porous materials having the small pores. In the case of mercury intrusion porosimetry and gas adsorption–desorption, it is necessary to suppose a structural model for the pores, making the interpretation of the results quite complex. DSC thermoporometry observes heat transfer in a measurement consisting of dynamic and isothermal steps, from which the amount of liquid molten within given temperature ranges can be calculated with the help of the known enthalpy of fusion. However, DSC thermoporometry is

somewhat limited in the pore size range detectable, implying that it is difficult to obtain detailed information about the pore size distribution with a few nanometer sizes in UF membranes. Several approaches have been developed for characterizing the PSD of porous materials by means of 1H nuclear magnetic resonance (NMR) [157,158].

ultrafiltration has mainly been used for protein concentration and desalting. Recent studies have demonstrated that ultrafiltration could potentially be used for high-resolution protein–protein fractionation [159,160] Feins and Sirkar [161] studied the separation of very close molecular weight proteins by using multilayered UF membranes and obtained excellent separation. However, there has been limited success in translating these advances into commercial processes; the main reason being the unsuitability of the currently used UF configurations and modes of operation for the high resolution fractionation [162]. In a recent theoretical study, Ghosh [162] has shown that it is possible to achieve high-resolution protein–protein fractionation by using a continuous three-stage cascade UF configuration based on stirred cell membrane modules. The work demonstrated that both purification factor and recovery were affected by the manner in which the internal recycle streams were handled. By suitably adjusting the various flow streams within the configuration it was possible to simultaneously achieve high recovery and high purity in binary protein fractionation. More recently, Lightfoot [163] reiterated the possibility of using cascade systems for efficient binary solute fractionation. While purifying monoclonal antibodies

(mAbs) from mammalian cell culture supernatant using ultrafiltration, most separation strategies rely on the preferential retention of the mAb and preferential transmission of the impurities [164,165]. The mAb concentration in the starting material is typically in the 0.1–1.0 mg/mL range though many recent reports have claimed much higher yields [166]. The major impurities present in the cell culture supernatant are media proteins such as bovine serum albumin (BSA), bovine transferrin and insulin. Traditionally IgG1 type mAbs are purified using three batch process steps in series: affinity chromatography by using protein-A, cation exchange chromatography followed by size-exclusion chromatography [165]. This is a very expensive, time-consuming procedure which is quite difficult to scale-up. Moreover, there is a chance of protein-A leaching out from the affinity media during the elution step, this being undesirable since protein-A is immunotoxic in nature [167]. The use of acidic buffer (pH 3.0) during the elution step of protein-A affinity chromatography is also known to cause mAb denaturation and dimerization [168].

3.6. Microfiltration

Microfiltration (MF) has been extensively used for the removal of COD and pigment from textile and pulp industry wastewaters, treatment of oil-containing wastewater, radioactive substances containing wastewater and activated sludge wastewater, and the purification of water for re-use and drinking [169-172]. A MF membrane can be regarded as a charged porous membrane to better understand its

separation performance. It cannot be taken simply as a sieve that leads to the rejection of the solutes such as ions, molecules, clusters, aggregates, and even particles in solution [173]. The charging of a porous membrane surface in a solution usually comes about in two ways: one is the ionization or dissociation of the groups on the surface of the membrane pores, and the other is the adsorption of ions from solution onto the surface of the membrane pores. These lead to the formation of an electrical double layer (EDL) that restores the electro neutrality in the solution [174,175]. Whatever the charging mechanism is, the charges of the surface are finally balanced by the isometric and opposite counter-ions, some of which are bound, usually transiently, to the surface within the well known Stern or Helmholtz layer, while others form an atmosphere of ions in rapid thermal motion close to the surface, known as the diffuse EDL [176].

4. Membrane Adsorber

Separations with membrane adsorbers (membrane chromatography [177-180], solid phase extraction) are a very attractive and rapidly growing application field for the functional macroporous membranes. Several reviews had dealt with membrane adsorbers; some authors had tried to cover all important aspects from the materials to the process engineering [109,181], others had focused on special membranes [182,183] or on the various applications [184-187]. It should be mentioned that polymeric monoliths—made by a different manufacturing technology but having similar pore morphology — compete with macroporous

membrane adsorbers in some applications, especially for ultra-fast high-resolution separations [188-190].

The key advantages in comparison with conventional porous adsorbers (particles, typically having a diameter of $\geq$ 50 μ m [191,192] result from the pore structure of the membrane which allows a directional (convective) flow through the majority of the pores. Thus, the characteristic distances (i.e. times) for pore diffusion is drastically reduced. The separation of substances is based on their reversible binding on the functionalized pore walls. Therefore, the internal surface area of the membrane and its accessibility is most important for the (dynamic) binding capacity. Typical specific surface areas of microfiltration membranes are only moderate (for a nominal pore diameter of 0.2μ m between 5 and 50 m^2/g; for larger pore diameters even much smaller). Consequently, the development of high-performance membrane adsorbers should proceed via an independent optimization of pore structure and surface layer functionality, providing a maximum number of binding sites with optimum accessibility. Surface functionalizations of suited porous membranes, mostly MF membranes or macroporous filter media, via 'grafting-to' [193] or via 'grafting-from' [194] can be efficient approaches. A 'tentacle' or 'brush' structure of the functional layer can be used for a significant increase of the binding capacity in comparison with binding on the plain pore wall. Finally, the chemistry of the functional layer determines the selectivity of the separation metal chelate [195], chiral recognition [196,197] or immunoaffinity [193,194,198].

5. Catalytically Active Membrane

The concept of the catalytic membrane reactor (CMR) is focused onto one of the most stimulating visions in reaction engineering, i.e. the integration of reaction and separation [199]. Excellent overviews on this rapidly developing field are available, either covering all types and configurations of CMR [200], or with a particular attention onto biocatalytic membrane reactors [201]. In the simplest type of a CMR, the membrane should only retain the catalyst in the reactor—the membrane is exclusively a barrier. An analysis of continuous reactor operation reveals that the retention of the catalyst should be very close to 100% in order to be economical [201-203].

6. Membrane in Sensor System

A chemo- or biosensor is a system consisting of a receptor coupled with a transducer to a detector, thus enabling the conversion of a chemical signal—binding to the receptor—into a physical signal. Many technically established sensor systems or sensors in the research lab involve membranes, their structure may be rather diverse but they should fulfill at least one of the following main functions (often, synthetic membranes will combine all these functions):

- barrier between the sensor system and its environment, allowing selective access (e.g. of the analyte only) to the receptor or/and protecting the receptor from disturbing influences of the environment;

- matrix for the immobilization of the receptor or/and tool for bringing it into proximity to the detector—if the transducer is a separate chemical species, the membrane is also the means to integrate the entire sensing system.

Hence, it becomes clear, that many different membrane principles, barrier structures, transport mechanisms, and hence materials and their processing can be used to develop sensors systems. Special reviews can provide comprehensive insights into this diverse and dynamic field [204].

7. Membrane Potential

Membrane potential that is defined as a potential difference arising between the solutions of an electrolyte with different concentrations at the constant temperature and pressure when they are separated by a uniform membrane with fixed ionizable groups [205]. At the interface between membrane and electrolyte solutions, the Donnan potential occurs due to the transfer of ions. Inside the membrane, the diffusion potential arises since ions would diffuse from the high concentration side to the low concentration side under a certain concentration gradient. Membrane potential is the summation of the Donnan potential and the diffusion potential, and it can be also named as the exclusion–diffusion potential [206]. Membrane potential can be measured directly by determining the electrical properties of a membrane or the activities of ions inside the membrane.

The earlier theoretical studies on membrane potential were almost based on the TMS model and developed by Kobatake and co-workers [205,207,208] and

Lakshminarayanaiah and co-workers [209,21]. Kobatake and co-workers [205,207,208] derived an equation of membrane potential for uni-univalent electrolyte solutions and first proved that the derived equation agreed well with typical corresponding experimental data. Nikonenko et al. [210] investigated the influence of the 1-1 salt concentration, and the ratio of the diffusion boundary layers length and the counter-ions diffusion coefficient on the membrane potential of an ion-exchange membrane. The research work concluded that the membrane potential carried out numerically by the TMS model were similar to those obtained experimentally by Dammak if the salt concentration is less than 100 $molm^{-3}$. Lefebvre et al. [211] derived the general equations of the membrane potential, and the filtration potential of a charged membrane in an arbitrary electrolyte solution using an analytical approach. The group has limited their studies to the related aspects of the comparison of normalized filtration potential calculated numerically and analytically with no discussion on membrane potential [211]. The above analysis demonstrates that most studies of membrane potential evaluated by the TMS model have been emphasized with attention being given to the uni-univalent electrolytes. Nevertheless, there is not enough convincing theoretical investigation concerning the other kinds of electrolytes. It is worthwhile clarifying the fact that it the TMS model can be employed to evaluate membrane potential in multivalent electrolyte solutions [212].

In contact with external electrolyte solutions of low or moderate concentration the membrane excludes the co-ions (Donnan exclusion) by

electrostatic repulsion while the counter ions are admitted to the membrane and experience negligible resistance in passing from one solution to the other. At higher concentration, the Donnan exclusion becomes less effective and thus permselectivety gets reduced. The permselectivity [213] is reflected not only in the differences in permeability, but also in the electric potential difference which arises between the two solutions.

In the absence of an electric field, the migration of as ionic species the membrane involves a transfer of electric charge due to the migration of ionic species and this charge transfer has be balanced by one or more other fluxes. The compensation of the fluxes is brought about by the electric potential gradient, called the diffusion potential, built up by the process of diffusion. These characteristics of the fluxes, the action of the diffusion in the membrane and the permselectivity for counter ions are the key to the understanding of diffusion phenomena in the membrane systems.

When a membrane is between two solutions of the same electrolytes of different concentrations, the membrane potential is called concentration potential. In such a concentration cell, the counter ions diffuse more rapidly than the coions, due to permselectivity resulting in a net transfer of electric charge. With cation selective membranes, the electric potential in the dilute solution is thus more positive than in the concentrated solution. With anion-selective membranes, the opposite is true.

The membrane potential in a bi-ionic cell, containing two electrolyte solutions AX and BX separated by a permselective membrane, is called bi-ionic potential. In this type of cell, inter-diffusion of two counter ions A and B takes places within the membrane and the films [214]. The magnitude of electric potential difference (interdiffusion potential) depends basically on the charge, sigh and the mobility ratio of the counter ions. The interdiffusion potential should not be taken equal to membrane potential because the latter also includes the Donnan potential which is dependent on the nature of the counter ion and the solution concentration. In case of cation selective membrane, the electric potential tends to be more positive in the solution of lower concentration or in solution that contains the counter ion of lower mobility, lower valence, or lower affinity for the membrane matrix.

In the case of a multi-ionic cell, in which either one or both the solution(s), separated by the membrane, contain(s) more than one counter ion, the membrane potential is called the multi-ionic potential and magnitude of the latter depends primarily on the entire factor on which bi-ionic potential depends.

8. Membrane Conductance

Transport phenomena in membranes have been one of the most important branches of research activities during the last few decades because of the complex mechanism of ion permeation involved in different systems and in various environments. The investigations have utilized various techniques, different

methods and consequently have obtained different parameters to explain the mechanism of ion transport through specific membrane system. Electrochemical techniques have frequently been utilized for this purpose.

Ion permeation in membranes is usually characterized by such measurable parameters as conductance, current-voltage relationship, ionic fluxes, impedance and membrane potentials. These parameters have been quite helpful in explaining the mechanism of ion transport in various membrane systems [213,215-217]. The measurement of the conductivity of membrane systems with conventional a.c. or d.c. methods, although straight forward, requires special attention due to some particular features not met within bulk electrolyte solutions.

Absolute reaction rate theory provides a model of the transfer process envisioning diffusion as the "jumping" of solute molecules with associated activation energy, between the vacancies within the solvent lattice [218]. This theory has been further extended to predict the ratio of diffusivity in a dilute solution to its rate in pure bulk liquid. This approach allows the difference in activation energy to be related to the intermolecular distances between the molecules in solution. Thus, the diffusive behavior of a solute is seen to be dependent upon the spacing of the solution around it [219].

9. Concept of Ion Pairs in Membrane

An ion pairing effects might be expected to be important in solid polyelectrolyte systems for the following reasons: (i) there is a locally large

concentration of membrane-fixed ions and a reduced availability of water is to provide for hydration of the internal ions relative to the dilute external electrolyte solution; (ii) the dielectric constant of the organic polymer chains where the membrane-fixed ions are attached is very low (also, the local dielectric constant of the oriented water in the primary hydration shell of ions takes values significantly lower than the bulk water value because of the dielectric saturation effect)[220]; (iii) counter ions and membrane fixed ions can be brought into mutual proximity because of the membrane architecture limitations, finite size hydrophilic clusters, etc. Ion pairing can also be important for non aqueous electrolyte solutions in charged membranes [221] and for liquid ion exchange membranes with mobile sites [222].

More recently, a four-state model for the hydration-mediated dissociation equilibrium between counter ions and fixed charge groups has been proposed and applied to Nafion membranes. The model is based on the assumption that a discrete set of well-specified states of ion-water complexes exits and leads to a theoretical expression for the membrane internal water activity [223].

10. Membrane Morphology

10.1. Scanning Electron Microscopy

The first SEM image was obtained by Max Knoll in 1935. Further pioneering work on the physical principles of the SEM and beam specimen interactions was performed by Manfred von Ardenne in 1937 that produced a British patent [224].

The SEM was further developed by Professor Sir Charles Oatley and his postgraduate student Gary Stewart and was first marketed in 1965 by the Cambridge Instrument Company as the "Stereoscan" and the first instrument was delivered to DuPont.

The world's highest SEM resolution is obtained with the Hitachi S-5500. Resolution is 0.4nm at 30kV and 1.6nm at 1kV [Figure 1]. The combination of higher magnification, larger depth of focus, greater resolution, and ease of sample observation makes the SEM one of the most widely used instruments in research areas today [225,226]. The first commercial development of the Environmental SEM (ESEM) in the late 1980s [227] allowed samples to be observed in low-pressure gaseous environments (e.g. 1-50 Torr) and high relative humidity (up to 100%). The first commercial ESEMs were produced by the ElectroScan Corporation in USA in 1988. ElectroScan were later taken over by Philips (now FEI Company) in 1996.

ESEM is especially useful for non-metallic and biological materials because coating with carbon or gold is unnecessary. Uncoated Plastics and Elastomers can be routinely examined, as can be uncoated biological samples.

10.2. Transmission Electron Microscopy

The first practical TEM Originally was installed at I.G Farben-Werke and now on a display at the Deutsches Museum in Munich, Germany. The most common mode of operation for a TEM utilizes bright field imaging, whereby the contrast

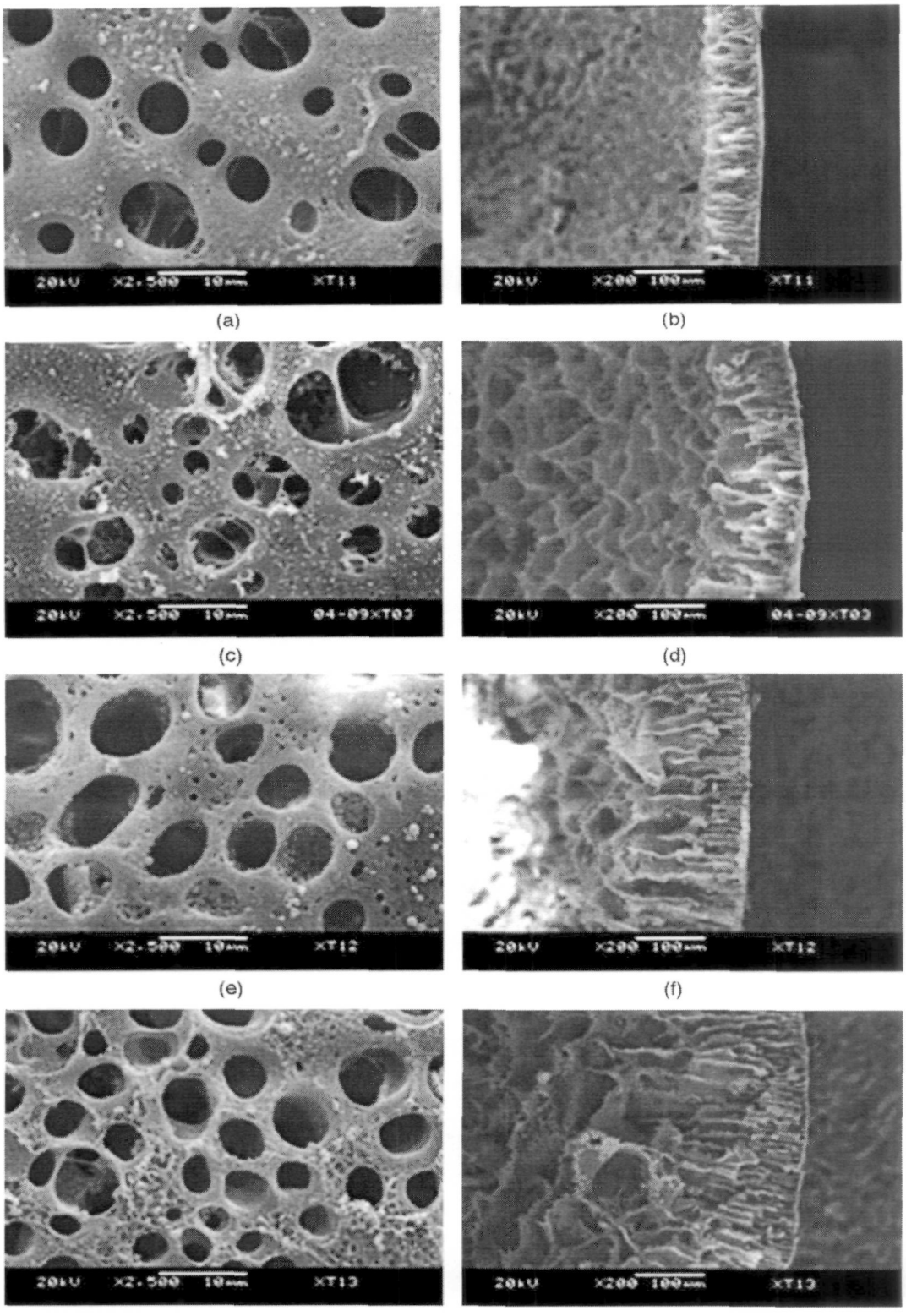

Figure 1 SEM micrographs of external surface (a, c, e and g) and cross-section (b, d, f and h)

formation, when considered classically, can be considered to be formed directly by occlusion. Thicker regions of the sample or regions with a higher atomic number will appear dark, whilst regions with no sample will appear bright [Figure 2].

An analytical TEM is the one equipped with detectors that can determine the elemental composition of the specimen by analyzing its X-ray spectrum or the energy-loss spectrum of the transmitted electrons. Modern research TEMs [228,229] may include aberration correctors, to reduce the amount of distortion in the image, allowing information on features on the scale of 0.1 nm to be obtained (resolutions down to 0.05 nm have been achieved) at magnifications of 50 million times. The TEM is used heavily in both material science/metallurgy and the biological sciences. In both cases the specimens must be very thin and able to withstand the high vacuum present inside the instrument [Figure 3].

10.3. Atomic Force Microscopy

The atomic force microscope (AFM) or scanning force microscope (SFM) is a very high-resolution type of scanning probe microscope, with demonstrated resolution of fractions of a nanometer, more than 1000 times better than the optical diffraction limit. The precursor to the AFM, the scanning tunneling microscope, was developed by Gerd Binnig and Heinrich Rohrer in the early 1980s, a development that earned them Nobel Prize in Physics in 1986. Binnig, Quate and Gerber invented the first AFM in 1986. The AFM is one of the foremost tools for imaging, measuring and manipulating matter at the nanoscale. The atom at the

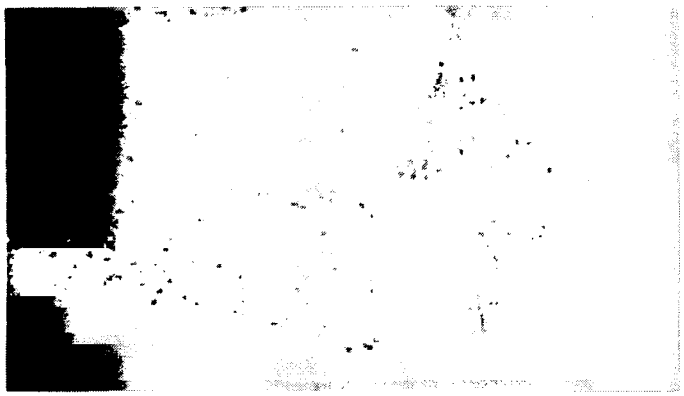

Figure 2 Transmission Electron Micrograph of a cobalt catalyst (darker spots) supported on coal carbonized at 850 °C and added by ion-exchange technique

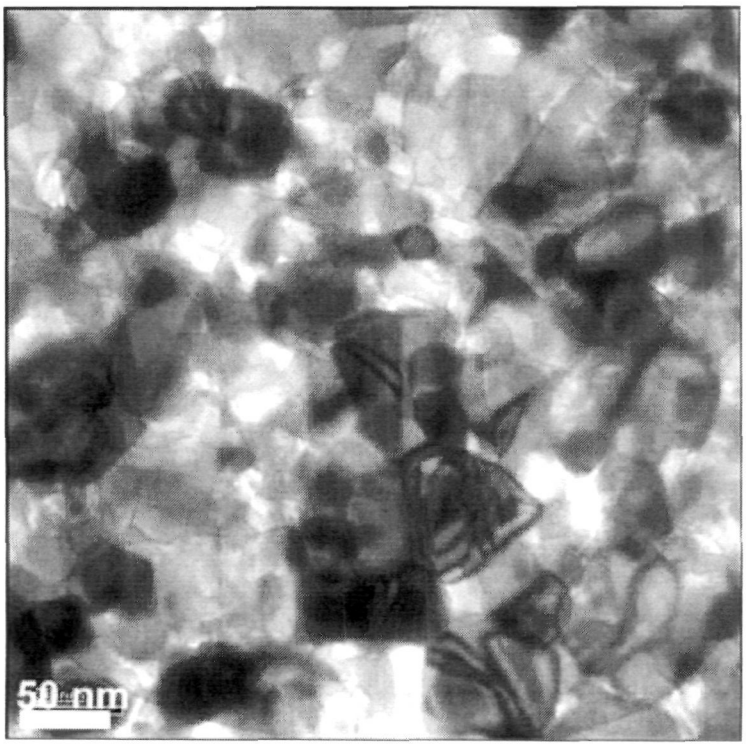

Figure 3 TEM image of a titania film composed of 3 layers and crystallized at 650°C.

apex of the tip "senses" individual atoms on the underlying surface when it forms incipient chemical bonds with each atom. Because these chemical interactions subtly alter the tip's vibration frequency, they can be detected and mapped. AFM is an excellent tool to study the topography of the membrane skin layer [230,231]. An AFM consists of an extremely sharp tip mounted to the end of a tiny cantilever spring, which is moved by a mechanical scanner over the surface to be observed. Every variation of the surface height varies the force acting on the tip and therefore varies the bending of the cantilever. This bending is measured and recorded line by line. The image is then reconstructed by computer software associated with the AFM. An AFM can be used to measure pore size and pore size distribution of some membranes [232-236]. One of the greatest advantages of AFM over traditional techniques such as optical and electron microscopes (SEM, TEM), is that the AFM directly produces three dimensional images [Figure 4], whereas traditional microscopes measure only two dimensional images.

10.4. Comparison of Techniques

- SEM has difficulty in resolving the feature due to the subtle variations in height [Figure 5]
- On most thin films, the SEM and AFM produce a similar representation of the Surface. But they differ in the other types of information.

  1. AFM provides with roughness with height.

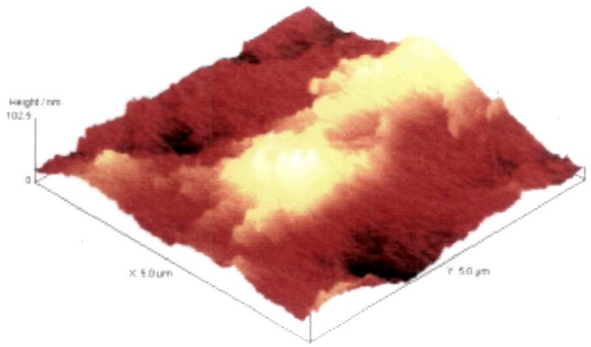

Figure 4 AFM image taken at the bottom of a deep trench

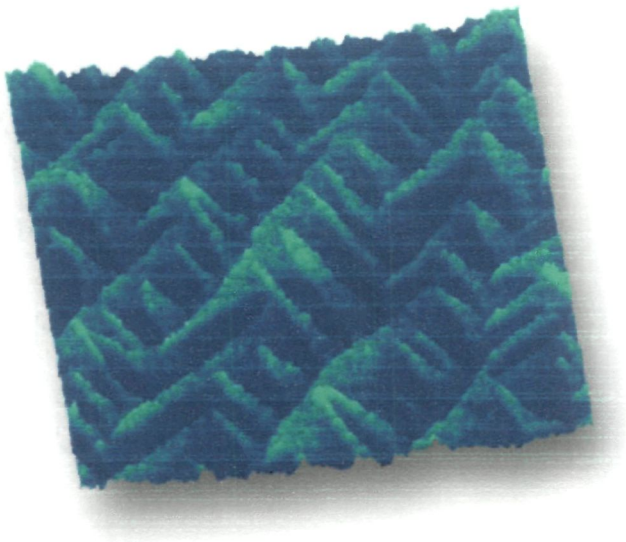

Figure 5 TM-AFM image of 0.14 nm monoatomic steps on epitaxial silicon deposited on (100) Si. 1 μm scan, RMS=0.07 nm

2. SEM provides a large view area.

- In the SEM image, it can be sometimes difficult to determine whether the feature is sloping up or down
- SEM provides measuring the undercuts of these lines
- With AFM one can measure the structure nondestructively, but without details on the sides.
- SEM has a large depth of field: Ability to image very rough surfaces
- SEM is conducted in a vacuum environment.
- AFM is conducted in vacuum, gas, liquid, vapor, and in an ambient environment.

Although SEM and AFM appear very different, they share a number of similarities

- Both techniques raster a probe across the surface
- Both techniques can produce artifacts.
- AFM can provide measurements in all three dimensions, with a vertical resolution of <0.05 nm dimensions,

References

[1] H.W. Blanch, D.S. Clark, Biochemical engineering, New York, Marcel Dekker, 1996.

[2] E. Damon, E. Morin, M.P. Belleyille, G.M. Rios, *Chem. Eng. Process* **42** (2003) 299.

[3] R.W. Baker, Membrane technology and applications, Chichester, Wiley, 2004

[4] R.K. Nagarale, G.S. Gohil, V.K. Shahi, *Adv. Colloid Interface Sci.* **119** (2006) 97.

[5] M. Ulbricht, *Polymer* **47** (2006) 2217.

[6] R.Vanreis, A.L. Zydney, *J. Membr. Sci.* **297** (2007) 1270.

[7] E.R.D.S. Miguel, J.C. Aquilar, J.D. Gyves, *J. Membr. Sci.* **307** (2008) 105.

[8] A. Jawor, E.M.V. Hock, *Desalination* **235** (2009) 44.

[9] A. Lindbåthen, M.B. Hägg, *Chem. Eng. Process* **48** (2009) 1.

[10] L. Chalakov, L.K.R. Struckmann, B. Munder, K. Sundmacher, *Chem. Eng. J.* **145** (2009) 385.

[11] E.K. Esbjörner, P. Lincolin, B. Nordén, *Biochim. Biophys. Acta* **1768** (2007) 1550.

[12] S.M. Cory, Y. Liu, M.I. Glavinović, *Biochim. Biophys. Acta* **1768** (2007) 2319.

[13] T.A. Desai, D. Hansford, L.Kulinsky, A.H. Nashat, G. Rasi, J. Tu, Y. Wang, M. Zhang, M. Ferrari, *J. Biomed. Microderices* **2** (1999) 11.

[14] T.A. Desai. D. Hansford, M. Ferrari, *J. Membr. Sci.* **159** (1999) 221.

[15] G.D. Luca, M.I. Glavinović, *Biochim. Biophys. Acta* **1768** (2007) 264.

[16] V.G. Shlyonsky, V.S. Markin. I. Andreeva, S.E. Pedersen, S.A. Simon, D.J. Benos, I.I. Ismailor, *Biochim. Biophys. Acta* **1758** (2006) 1723.

[17] J.H. Tay, J. Liu, D.D. Sun, *Water Research* **36** (2002) 585.

[18] N. Islam, N.A. Bulla, S. Islam, *Biochim. Biophys. Acta* **1667** (2004) 174.

[19] K. Sollner, *J. Phys. Chem.* **49** (1945) 47.

[20] K. Sollner, Electrochemistry in Biology and Medicine, John Wiley & Sons Inc., New York, 1955.

[21] N. Lakshminarayanaiah, Transport Phenomena in Membrane, Academic, Press, New York, 1969.

[22] N. Lakshminarayanaiah, *Proc. Indian Acad. Sci. A* **55** (1962) 200.

[23] G. Eder, *Z. Physik. Chem.* **39** (1963) 218.

[24] R. Schlögl, *Discuss Faraday Soc.* **21** (1956) 46.

[25] H.K. Lonsdale, B.P. Cross, F.M. Graber, C.E. Milstead, *J. Macromol. Sci. Phys. B* **5** (1971) 167.

[26] T. Sata, T. Sata, W. Yang, *J. Membr. Sci.* **206** (2002) 31.

[27] V.M. Volgin, A.D. Davydov, *J. Membr. Sci.* **259** (2005) 110.

[28] J. Balster, O. Krupenko, I. Punt, D.F. Stamatialis, M. Wessling, *J. Membr. Sci.* **263** (2005) 137.

[29] J. Lie, T. Xu. Y. Fu, *J. Membr. Sci.* **252** (2005) 165.

[30] T. Xu, *J. Membr. Sci.* **263** (2005) 1.

[31] T.W. Xu, W.H. Yang, *J. Membr. Sci.* **183** (2001) 193.

[32] C. Linder, O. Kedam, *J. Membr. Sci.* **181** (2001) 39.

[33] M. Takizawa, Y. Sugita, N. Ogumi, M. Nakamura, S. Horiguchi, T. Fukutomi, *J. Polymer. Sci.* **41** (2003) 1251.

[34] G.E. Molau, *J. Membr. Sci.* **8** (1981) 309.

[35] D.S. Flett, Chichester, Ellis Horwood, Ion exchange membranes, John Wiley & Sons Ltd., New York, 1983.

[36] P.V. Vyas, B.G.Shah, G.S. Trivedi, P. Ray, S.K. Adhikary, R. Rangarajan, *J. Membr. Sci.* **187** (2001) 39.

[37] N.P. Berezina, L.-V. Karpenko, *Colloid J.* **62167** (2000) 676.

[38] Z.V. Klimova, G.K. Saldadze, Zhurnal Prikladnoi Khimii **58** (1985) 524.

[39] A. Steck, O. Savadogo, P.R. Roberge, T.N. Veziroglu, Proceedings of the First International Symposium on New Materials for Fuel Cell Systems, Montreal, Canada, 9-13 July 1995, P-74.

[40] I. Honma, S. Nomura, H. Nakajima, *J. Membr. Sci.* **185** (2001) 83.

[41] P. Genova-Dimitrovo, B. Baradie, D. Foscallo, C. Poinsignon, J.Y. Sanchez, *J. Membr. Sci.* **185** (2001) 59.

[42] B. Tazi, O. Savadogo, *Electrochim. Acta* **45** (2000) 4329.

[43] S.M.J. Zaidi, S.D. Mikhailenko, G.P. Robertson, M.D. Guiver, S. Kaliaguine, *J. Membr. Sci.* **173** (2000) 17.

[44] M. Hogarth, X. Glipa, High temperature membranes for solid polymer fuel cells, Report ETSU F/02/00189/REP, DTI/Pub URN 01/893 prepared for Johnson Matthey Technology Centre, 2001.

[45] M. Tatsuo, M. Hironari, U.J. Ichi, K. Fukiko, K. Noriho, G. Masahiro, *Anal. Chem.* **76** (2004) 4495.

[46] R.-S. Juang, H.-C. Kao, W.-H. Wu, *J. Membr. Sci.* **228** (2004) 169.

[47] D. Nanda, M.S. Oak, M.P. Kumar, B. Maiti, P.K. Dutta, *Sep. Sci. Technol.* **36** (2001) 2489.

[48] M.B. Gholivand, S. Khorsandipoor, *J. Membr. Sci.* **180** (2000) 115.

[49] P.S. Kulkarni, S. Mukhopadhyay, M.P. Bellary, S.K. Ghost, *Hydrometallurgy* **64** (2002) 49.

[50] M. Shamsipur, M.H. Mashhadizadeh, G. Azimi, *Sep. Purif. Technol.* **27** (2002) 155.

[51] M. Ma, D.He, Q.Wang, Q. Xie, *Talanta* **55** (2001) 1109.

[52] J. Doležal, C. Moreno, A. Hrdlička, M. Valiente, *J. Membr. Sci.* **168** (2000) 175.

[53] S.C. Lee, *Chem. Eng. J.* **79** (2000) 61.

[54] P.F.M.M. Correia, J.M.R. de Carvalno, *J. Membr. Sci.* **179** (2002) 175.

[55] M.D. Luccio, B.D. Smith, T. Kida, C.P. Borges, T.L.M. Alves, *J. Membr. Sci.* **174** (2000) 217.

[56] D.He, M. Ma, Z. Zhao, *J. Membr. Sci.* **169** (2000) 53.

[57] A.A. Ensafi, H. Eskandari, *Sep. Sci. Technol.* **36** (2001) 81.

[58] J.C. Aquilar, M. Sánchez, Castellanos, E.R. de San Miguel, J. de Gyves, *J. Membr. Sci.* **190** (2001) 107.

[59] A. Safavi, F. Peiravian, E. Shams, *Sep. Purif. Technol.* **26** (2002) 221.

[60] M.B. Gholivand, S. Khorsandipoor, *J. Membr. Sci.* **180** (2000) 115.

[61] W.S.W. Ho, N.N. Li, Acs Sym. Ser, vol 642, American Chemical Society, Washington, DC, 1996.

[62] F. Luo, D. Li, Y. Wu, *Solvent. Extr. Ion Exch.* **22** (2004) 105.

[63] F. Schaffner, P.Y. Pontaloer, V. Sanchez, F. Lutin, *Desalination* **170** (2004) 113.

[64] L. Yu, J. Su, J. Wang, *Desalination* **177** (2005) 209.

[65] G.W. Meindersma, Effective Industrial Membrane Processes: Benefits and Opportunities, Elsevier Applied Science, New York, 1991.

[66] J. Haggin, New Generation of Membranes Developed for Industrial Separations, Chemical and Engineering News, 1988.

[67] K.S. Rajan, D.B. Boies, A.J. Casolo, J.L. Bregman, *Desalination* **1** (1966) 231.

[68] S.R. Caplain, *J. Electrochem. Soc.* **108** (1961) 577.

[69] R.J.R. Uhlhorn, A.J. Burggraff, Gas Separation with Inorganic Membranes in Inorganic Membranes Synthesis, Characterization and Application, B.V.N. Reinhold, New York, 1991.

[70] W.U. Malik, S.K. Srivastava, V.M. Bandari, Satish Kumar, *J. Colloid Interface Sci.* **47** (1974) 1.

[71] F.A. Siddiqi, N.I. Alvi, *Acta chimica Hungarica* **127** (1990) 759.

[72] N. Lakshminarayanaiah, Electrochemistry Specialist Periodical Reports, Vol. 4, Chemical Society, London, 1974.

[73] M.N. Beg, K. Ahmad, I. Altaf, M. Arshad, *J. Membr. Sci.* **9** (1981) 303.

[74] S. Kitao, M. Asaeda, *Key Eng. Mater.* **61-62** (1992) 267.

[75] S.D. Bruck, B. Raton, Controlled Drug Delivery, Ed., FLCRC Press, 1983.

[76] Y. Ikada, *Adv. Polym. Sci.* **57** (1984) 103.

[77] A.S. Michaels, *Pure Appl. Chem.* **46** (1976) 193.

[78] E.R. Edelman, R.J. Linhardt, H. Bobeck, J. Kost, H.B. Rosen, R. Langer, Polymers as Biomaterials, in: S.W. Shalably, A.S. Hoffman, B.D. Ratner, A. Horbett, Ed., Plenum Press, New York, 1984, P- 279.

[79] R. Duncan, J. Kopeček, *Adv. Polym. Sci.* **57** (1984) 51.

[80] A. Janshoff, C. Steinem, *Anal. Bioanal. Chem.* **385** (2006) 433.

[81] F. Giess, M.G. Friedrich, J. Heberle, R.L. Naumann, W. Knoll, *Biophys. J.* **87** (2004) 3213.

[82] L.J.C. Jeuken, S.D. Connell, P.J.F. Henderson, R.B. Gennis, S.D. Evans, R.J. Bushby, *J. Am. Chem. Soc.* **128** (2006) 1711.

[83] S. Terrettaz, M. Mayer, H. Vogel, *Langmuir* **19** (2003) 5567.

[84] A.T.A. Jenkins, R.J. Bushby, S.D. Evans, W. Knoll, A. Offenhausser, S.D. Ogier, *Langmuir* **18** (2002) 3176.

[85] L. He, J.W.F. Robertson, J. Li, I. Karcher, S.M. Schiller, W. Knoll, R. Naumann, *Langmuir* **21** (2005) 11666.

[86] G. Krishna, J. Schulte, B.A. Cornell, R. Pace, L. Wieczorek, P.D. Osman, *Langmuir* **17** (2001) 4858.

[87] L. Becucci, R. Guidelli, C. Peggion, C. Toniolo, M.R. Moncelli, *J. Electroanal. Chem* **576** (2005) 121.

[88] L. Becucci, M.R. Moncelli, R. Guidelli, *Langmuir* **22** (2006) 1341.

[89] L. Becucci, M.R. Moncelli, R. Naumann, R. Guidelli, *J. Am. Chem. Soc.* **127** (2005) 13316.

[90] G. Valincius, D.J. McGillivray, W. Febo-Ayala, D.J. Vanderah, J.J. Kasianowicz, M. Losche, *J. Phys. Chem. B* **110** (2006) 10213.

[91] F. Sneil, J. Wallker, G. Iverson, J. Lam, Physical Principle of Biological Membranes, Ed., Gordon & Breach, New York, 1970.

[92] K.H. Meyer, J.F. Sievers, *Helv Chim. Acta* **19** (1936) 649.

[93] V. Genesan, A. Walcarius, Langmuir **20** (2004) 3632.

[94] M.J. Percy, V. Michailidou, S.P. Armes, C. Perruchot, J.F. Watts, S.J. Greaves, *Langmuir* **19** (2003) 2072.

[95] L. Matějka, O. Dukh, B. Meissner, D. Hlavatá, J. Brus, A. Strachota, *Macromolecules* **36** (2003) 7977.

[96] A. Bhaumik, S. Inagaki, *J. Am. Chem. Soc.* **123** (2001) 691.

[97] D.E. de Vos, M. Dams, B.F. Sels, P.A. Jacobs, *Chem. Rev.* **102** (2002) 3615.

[98] Y. Park, M. Nagai, *Solid State Ionics* **145** (2001) 149.

[99] J.A. Kerres, *J. Membr. Sci.* **185** (2001) 3.

[100] Y. Yang, Z. Shi, S. Holdcroft, *Macromolecules* **37** (2004) 1678.

[101] B. Smitha, S. Sridhar, A.A. Khan, *Macromolecules* **37** (2004) 2233.

[102] P.G. Dimitrova, D.B. Baradic, D. Foscallo, C. Poinsignon, J.Y. Sanchez, *J. Membr. Sci.* **185** (2001) 59.

[103] C. Wu, T. Xu, W. Yang, *J. Membr. Sci.* **224** (2003) 117.

[104] M. Mulder, Basic Principles of membrane technology, 2nd ed., Dordrecht: Kluwer Academic Publishers, 1996.

[105] S.C. George, S. Thomas, *Prog. Polym. Sci.* **26** (2001) 985.

[106] J.G. Wijmans, R.W. Baker, *J. Membr. Sci.* **107** (1995) 1.

[107] W.J. Koros, A.H. Chan, D.R. Paul, *J. Membr. Sci.* **2** (1977) 165.

[108] R.D. Noble, *J. Membr. Sci.* **75** (1992) 121.

[109] D.K. Roper, E.N. Lightfoot, *J. Chromatography A* **702** (1995) 3.

[110] M.D. Afonso, M.N. de Pinho, *J. Membr. Sci.* **179** (2000) 137.

[111] W.R. Browen, J.S. Welfoot, *Desalination* **147** (2002) 197.

[112] A. Szymczyk, C. Labbez, P. Fievet, A.Vidonne, A. Foissy, J. Pagetti, *Adv. Colloid Interface Sci.* **103** (2003) 77.

[113] A.E. Yaroshchuk, A.L. Makovetskiy, Y.P. Boiko, E.W. Galinker, *J. Membr. Sci.* **172** (2000) 203.

[114] A. E. Yaroshchuk, Y.P Boiko, A.L. Makovetskiy, *Langmuir* **18** (2002) 5154.

[115] A.E. Yaroshchuk, L. Karpenko, V. Ribitsch, *J. Phys. Chem. B* **109** (2005) 7834.

[116] A.E. Yaroshchuk, Y.P. Boiko, A.L. Makovetskiy, *Langmuir* **21** (2005) 7680.

[117] W.R. Bowen, A.W. Mohammad, *AlChE J.* **44** (1998) 1799.

[118] B.V. Bruggen, C. Vandecasteele, *Environ. Pollut.* **122** (2003) 435.

[119] B.V. Bruggen, C. Vandecasteele, *Water Res.* **36** (2002) 1360.

[120] W.R. Bowen, H. Mukhtar, *J. Membr. Sci.* **112** (1996) 263.

[121] C. Labbez, P. Fievet, F. Thomas, A. Szymczyk, A. Vidonne, A. Foissy, J. Pagetti, *J. Colloid Interface Sci.* **262** (2003) 200.

[122] W.R. Bowen, J.S. Welfoot, *Chem. Eng. Sci.* **57** (2002) 1393.

[123] A. Bouchoux, H.R. Balmann, F. Lutin, *J. Membr. Sci.* **258** (2005) 123.

[124] G. Bargeman, J.M. Vollenbroek, J. Straatsma, C.G.P.H. Schorën, R.M. Boom, *J. Membr. Sci.* **247** (2005) 11.

[125] V. Fregen, T.C. Arnot, J.A. Howel, *J. Membr. Sci.* **178** (2000) 185.

[126] X.L. Wang, C. Zhang, P. Ouyang, *J. Membr. Sci.* **204** (2002) 271.

[127] W. Kunz, J. Henle, B.W. Ninham, *Curr. Opin. Colloid Interface Sci.* **9** (2004) 19.

[128] O. Trifunovic, G. Trägárdh, *Desalination* **149** (2002) 1

[129] A. Urkiaga, N. Bolaño, L.D. Fuentes, *Desalination* **149** (2002) 55.

[130] R. Maachi, Z. Bendjemaa, D. Legheraba, *Desalination* **139** (2001) 369.

[131] L.M. Vane, F.R. Alvarez, *J. Membr. Sci.* **202** (2002) 177.

[132] K. Bakó, N. Dörmő, O. Ulbert, L. Gubicza, *Desalination* **149** (2002) 267.

[133] A. Jonquières, R. Clèment, P. Lochon, J. Nèel, M. Dresch, B. Chrétien, *J. Membr. Sci.* **206** (2002) 87.

[134] H.O.E. Karlsson, G. Tragardh, *Tren. Food. Sci. Technol.* 7 (1996) 243,

[135] H.-H. Schwarz, G. Malsch, *J. Membr. Sci.* **247** (2005) 143.

[136] D.M. Sullivan, M.L. Bruening, *J. Membr. Sci.* **248** (2005) 161.

[137] T. Jin, K. Kuraoka, T. Yazawa, *Desalination* **148** (2002) 17.

[138] C.-L. Cheng, M.-S. Chang, *J. Membr. Sci.* **38** (2004) 117.

[139] J.-H. Kim, B.-J. Chang, S.-B. Lee, S.Y. Kim, *J. Membr. Sci.* **169** (2000) 185.

[140] A.M. Polyakov, L.E. Starannikova, Y.P. Yampolskii, *J. Membr. Sci.* **238** (2004) 21.

[141] B. Krause, M. Storr, T. Ertt, R. Buck, H. Hildwein, R. Deppisch, H. Göhl, *Chem. Ing. Tech.* **75** (2003) 1725.

[142] J. Vienken, Membranes- A key factor in the development of organ replacement medicine. Book of abstracts of Euromembrane, Hamburg, 2004.

[143] O. Pitiot, C. Legallais, L. Darnige, M.A. Vijayalakshmi, *J. Membr. Sci.* **166** (2000) 221.

[144] S.R. Wickramasinghe, M.J. Semmens, E.L. Cussler, *J. Membr. Sci.* **62** (1991) 371.

[145] J.G. Jacangelo, J.M. Laine, K.E. Carns, E.W. Cummings, J. Mallevialle, *J. Am. Water Works Assoc.* **83** (1991) 97.

[146] C. Cabassud, C. Anselme, J.L. Bersillon, P. Aptel, *Filtra. Sep.* **28** (1991) 194.

[147] M.C. Porter, Handbook of Industrial Membrane Technology, Noyes Publications, New Jersey, U.S.A. 1989.

[148] J. Zhou, L. Zhang, J. Cai, H. Shu, *J. Membr. Sci.* **210** (2002) 77.

[149] T.-S. Chung, J.-J. Qin, A. Huan, K.-C. Toh, *J. Membr. Sci.* **196** (2002) 251.

[150] J.Y. Kim, H.K. Lee, S.C. Kim, *J. Membr. Sci.* **163** (1999) 159.

[151] J.I. Calvo, A. Hernández, P. Prádanos, L. Matinez, W.R. Bowen, *J. Colloid Interface Sci.* **176** (1995) 467.

[152] C. Alié, R. Pirard, J.-P. Pirard, *Colloid Surf. A* **187-188** (2001) 367.

[153] P. Scheider, P. Uchytil, *J. Membr. Sci.* **95** (1994) 29.

[154] P. Prádanos, M.L. Rodriguez, J.I. Calvo, A. Hernandez, F. Tejerina, J.A. Saja, *J. Membr. Sci.* **117** (1996) 291.

[155] K. Ishikiriyama, M. Todoki, K. Motomura, *J. Colloid Interface Sci.* **171** (1995) 92.

[156] J.N. Hay, P.R. Laity, *Polymer* **41** (2000) 6171.

[157] R. Valckenborg, L. Pel, K. Kopinga, *Magn. Reson. Imaging* **19** (2001) 489.

[158] R.L. Kleinberg, *Magn. Reson. Imaging* **14** (1996) 761.

[159] R. Ghosh, Protein Bioseparation using Ultrafiltration: Theory, Applications and New Developments, Imperial College Press/World Scientific Publishing Ptv. Ltd., London, 2003

[160] Y. Wan, S. Vasan, R. Ghosh, G. Hale, Z. Cui, *Biotechnol. Bioeng.* **90** (2005) 422.

[161] M. Feins, K.K. Sirkar, *J. Membr. Sci.* **248** (2005) 137.

[162] R. Ghosh, *J. Membr. Sci.* **226** (2003) 85.

[163] E.N. Lightfoot, *Sep. Sci. Technol.* **40** (2005) 739.

[164] R. Ghosh, Y. Wan, Z. Cui, G. Hale, Biotechnol. Bioeng. **81** (2003) 673.

[165] Y. Wan, R. Ghosh, G. Hale, Z. Cui, *Biotechnol. Bioeng.* **90** (2005) 303.

[166] Y.J. Tang, R. Ohashi, J.F.P. Hamel, *Biotechnol. Prog.* **23** (2007) 255.

[167] K.L. Clarson, *Nat. Biotechnol.* **23** (2005) 1054.

[168] T. Arakawa, J.S. Philo, K. Tsumoto, R. Yumioka, D. Ejima, *Protein Exp. Purif.* **36** (2004) 244.

[169] A.L. Lim, R. Bai, *J. Membr. Sci.* **216** (2003) 279.

[170] M. Cheryan, N. Rajagopalan, *J. Membr. Sci.* **151** (1998) 13.

[171] H. Sato, P.S. Malchesky, S. Matsubara, Y. Nosé, *Artif. Organs* **7** (1983) 213.

[172] D. Vial, G. Doussau, *Desalination* **153** (2003) 141.

[173] J. Straatsma, G. Bargeman, H.C.V. Horst, J.A. Wesselingh, *J. Membr. Sci.* **198** (2002) 273.

[174] R.J. Hunter, Zeta Potential in Colloid Science; Principles and Applications, Academic Press, London, 1995.

[175] J. Lyklema, Fundamentals of Interface and Colloid Science, Vol. 11, Solid-Fluid Interface, Academic Press, London, 1995.

[176] J.N. Israelachvili, Intermolecular and Surfaces Forces, 2nd ed., Academic Press, London, 1992.

[177] R. Ghosh, *J. Chromatogr A* **952** (2002) 13

[178] H.N. Endres, J.A.C. Johnson, C.A. Ross, J.K. Welp, M.R. Etzel. *Biotechnol. Appl. Biochem.* **37** (2003) 259.

[179] M.R. Etzel, F. Svec, T.B. Tennikova, Z. Deyl, *J. Chromatogr Library* **67** (2003) 213.

[180] B. Kalbfuss, L.Wolff, G.A. Tappe, R.Wickramasinghe, V. Thom, U. Reichl, *J. Membr. Sci.* **299** (2007) 251.

[181] E. Klein, *J. Membr. Sci.* **179** (2000) 1

[182] X. Zeng, E.Ruckenstein, *Biotechnol Progr.* **15** (1999) 1003.

[183] T. Kawai, K. Saito, W. Lee, *J. Chromatogr. B* **790** (2003) 131.

[184] C. Charcosset, *J. Chem. Technol. Bitechnol.* **71** (1998) 95.

[185] H. Zou, Q. Luo, D. Zhou, *J. Bioochem. Biophys Methods* **49** (2001) 199.

[186] R. Ghosh, *J. Chromatogr. A* **952** (2002) 13.

[187] E.N. Lightfoot, J.S. Moscariello, *Biotechnol. Bioeng.* **87** (2004) 259.

[188] F. Svec, J.M.J. Fréchet, *Science* **273** (1996) 205.

[189] F. Svec, *J. Sep. Sci.* **27** (2004) 1419.

[190] D. Josic, A. Buchacher, A. Jungbauer, *J. Chromatogr. B* **752** (2001) 191.

[191] M. Leonard, *J. Chromatogr. B* **699** (1997) 3.

[192] M. Kaufmann, *J. Cromatogr. B* **699** (1997) 347.

[193] L.R. Catilho, W.-D. Deckwer, F.B. Anspach, *J. Membr. Sci.* **172** (2000) 269.

[194] H. Borcherding, H.G. Hicke, D. Jorcke, M. Ulbricht, *Ann. NY. Acad. Sci.* **984** (2003) 470.

[195] K. Rodermann, E. Staude, *Biotechnol. Bioeng.* **46** (1995) 503.

[196] M. Nakamura, S. Kiyohara, K. Saito, K. Sugita, T. Sugo, *Anal. Chem.* **71** (1999) 1323.

[197] Y. Goda, S. Fujirnoto, *Anal. Chem.* **74** (2002) 4933.

[198] R. Specht, B. Han, S.R. Wickramasinghe, J.O. Carlso, P. Czermak, A. Wolf, O.-W. Reif, *Biotechnol. Bioeng.* **88** (2004) 465.

[199] K. Sirkar, P.V. Shanbhag, A.S. Kowali, *Ind. Eng. Chem. Res.* **38** (1999) 3715.

[200] J.G.S. Marcano, T.T. Tsotsis, Catalytic membrane reactors and membrane reactors, Weinhein, Wiley& VCH, 2002.

[201] E. Drioli, L. Giorno, Biocatalytic membrane reactors, Taylor and Francis, London, 1999

[202] H.P. Dijkstra, G.P.M.V. Klink, G.V. Koten, *Acc. Chem. Res.* **35** (2002) 798.

[203] U. Kragl, T. Dwars, *Trends Biotechnol.* **19** (2001) 442.

[204] B. Adhikari, S. Majumdar, *Progr. Polym. Sci.* **29** (2004) 699.

[205] Y. Kobatake, *J. Chem. Phys.* **28** (1958) 146.

[206] T.-J. Chou, A. Tanioka, *J. Colloid Interface Sci.* **212** (1999) 293.

[207] Y. Kobatake, N. Takeguchi, Y. Toyoshima, H. Fujita, *J. Chem. Phys.* **69** (1965) 3981.

[208] Y. Toyoshima, Y. Kobatake, H. Fujita, *Trans. Faraday Soc.* **63** (1967) 2814.

[209] G.J. Hills, P.W.M. Jacobs, N. Lakshminarayanaiah, *Proc. Roy. Soc.* **262** (1961) 246.

[210] V.V. Nikonenko, K.A. Lebedev, V.I. Zabolotsky, L. Dammack, C. Larchet, *Eur. Polym. J.* **33** (1997) 1057.

[211] X. Lefebvre, J. Palmeri, P. David, *J. Phys. Chem. B* **108** (2004) 16811.

[212] W.J. Shang, X.L. Wang, Y.X. Yu, *J. Membr. Sci.* **285** (2006) 362.

[213] R.K. Nagarale, G.S. Gohil, V.K. Singh, *Adv. Colloid Interface Sci.* **119** (2006) 97.

[214] K. Singh, A.K. Tiwari, *J. Colloid Interface Sci.* **210** (1999) 241.

[215] G.S. Gohil, V.K. Shahi, R. Rangarajan, *J. Membr. Sci.* **240** (2004) 211.

[216] B. Auclair, V. Nikonenko, C. Larchet, M. Metayer, L. Dammak, *J. Membr. Sci.* **195** (2002) 89.

[217] J.-H. Choi, H.-J. Lee, S.-H. Moon, *J. Colloid Interface Sci.* **238** (2001) 188.

[218] K.E. Laidig, J.L. Gainer, V. Dagett, *J. Am. Chem. Soc.* **120** (1998) 36, 4394.

[219] S. Glasstone, K.J. Laidler, H. Eyring, Theory of Rate Processes, McGraw Hill, New York, 1941.

[220] J.Ó.M. Bockris, A.K.N. Reddy, Modern Electrochemistry, Plenum, New York, 1970.

[221] T.-J. Chou, A. Tanioka, *J. Membr. Sci.* **144** (1998) 275.

[222] R.P. Buck, F.S. Stover, D.E. Mathis, *J. Electroanal. Chem.* **100** (1979) 63.

[223] J.O.M. Bockris, B.E. Conway, R.E. White, Modern Aspects of Electrochemistry, Plenum Press, New York, 1999.

[224] M.V. Ardenne, Improvements in electron microscopes, GB Patent 511204, Germany, 1937.

[225] W. Shi, M.M. Benjamim, *J. Membr. Sci.* **331** (2009) 11.

[226] A. Gugliuzza, e. Drioli, *Desalination* **240** (2009) 14.

[227] G.D. Danilatos, *Adv. Electron. Electron. Phys.* **71** (1998) 109.

[228] A.C. Filemonowicz, P.A. Buffat, *J. Microscopy* **224** (2006) 21.

[229] D. Farrell, C.L. Dennis, J. Lim, S.A. Majetich, *J. Colloid Interface Sci.* **331** (2009) 394.

[230] Q. Yang, T.-S. Chung, M. Weber, *J. Membr. Sci.* **326** (2009) 322.

[231] Y. Mo, M. Bai, *J. Colloid Interface Sci.* **333** (2009) 304.

[232] M. Khayet, *Applied Surface Science* **238** (2004) 269.

[233] W.R. Bowen, T.A. Doneva, *Desalination* **129** (2000) 163.

[234] J.A. Otero, G. Lena, J.M. Colina, P.Prádanos, F. Tejerina, A. Hernández, *J. Membr. Sci.* **279** (2006) 410.

[235] J.A. Otero, R. Gutiérrez, I. Arnáez, P.Prádanos, L. Palacio, A. Hernández, *Desalination* **200** (2006) 354.

[236] A. Szymczyk, N.F. Rouge, P. Fievet, C. Ramseyer, A. Vidonne, *J. Membr. Sci.* **287** (2007) 102.

CHAPTER 2

Transport Studies of Nickel Arsenate Membrane

Introduction

Composite materials formed by mixing organic polymers and inorganic particles; possess all the good properties of both the constituents and an enhanced utility thereof. The combination of organic and inorganic precursors yields hybrid materials that have mechanical properties not present in the pure materials. The organic group can be reactive which implies that it is able to form an organic network as well as inorganic network. In designing composite materials scientists and engineers have ingeniously combined various metals, ceramics, and polymers to produce a new generation of extraordinary materials that encompass a wide variety of applications. Most composites have been created to improve combination of mechanical characteristics such as stiffness, toughness, and ambient and high temperature strength. Of particular interest is the molecular level combination of two different components that may lead to new composite materials that are expected to provide many possibilities termed 'organic inorganic hybrid' materials.

This type of hybrid composites prepared with electrically conducting polymers have emerged as fascinating materials due to a wide range of other desirable properties such as architectural flexibility, environmental stability, ease of fabrication, light weight, mechanical property and so on. Therefore, these materials are finding applications from coating to lubricants to solid-state technology to biotechnology. Conducting polymers possess good tuneable electrical conductivity and are organic electro chromic materials with chemically

active surface [1,2]. But they are chemically sensitive and have poor mechanical properties and thus pose a processibility problem. On the other hand, inorganic oxides or metal acid salts show the presence of more sites for surface reactivity and are highly porous in sol form. The metal oxides constitute a class of compounds widely used as cathode material in Li-ion batteries [3]. They also have good mechanical properties and are good dispersants too [4]. Thus composite materials formed through the incorporation of inorganic materials and organic polymers are attracted for the purpose of creating high performance or high functional polymeric materials. Recently, several groups have combined conductive polymers with metal oxides to generate hybrid composites that possess higher reversible capacity, redox cyclability and structural stability [5,6]. The properties of composites of such kind are strongly dependent on concentration of polymer. Polystyrene, one of the conducting polymers, has received lot of attention in the preparation of composites due to its high stability in conducting oxidized form [7,8].

The synthesis of polymeric–inorganic composite has received a great deal of attention because it provided new material with special mechanical, chemical, electrochemical, and optical as well as magnetic properties. In literature, various methods of preparing these hybrid materials have been reported [9,10]. The conversion of inorganic ion-exchangers has been taking place into composite ion exchange materials is the latest development in this discipline. These materials are used in the general areas of chemical sensors, chromatography, fabrication of

selective materials, and electrical and electronic applications. Efforts have been made to improve the chemical, mechanical and thermal stabilities of ion-exchangers and to make them high selective for certain heavy metal ions. Inorganic precipitate ion-exchanger based on organic polymeric matrix must be an interesting material, as it should possess the mechanical stability due to the presence of organic polymeric species and the basic characteristics of an inorganic ion-exchanger regarding its selectivity towards some particular metal ions.

In this paper, the evaluation of thermodynamically charge density of membrane, which is an important characteristic governing the membrane phenomena is described.

The methods used for the determination of charge densities are based on the equations for membrane potential developed recently by TMS [11] and Kobatake [12]. The selective membrane behavior has been explained in terms of thermodynamic activation parameters evaluated by utilizing the theory of absolute reaction rates.

Theory

Fixed charge theory of Teorell-Meyer-Sievers

In the TMS theory there is an equilibrium process at each solution membrane interface which has a formal analogy with the Donnan equilibrium. The assumptions made are (a) the cation and anion mobilities and fixed charge concentration are constant throughout the membrane phase and are independent of the salt concentration and (b) the transference of water may be neglected. The

implications of these assumptions have been discussed [13]. Further assumption must be made that the activity coefficient of the salt is the same in the membrane and solution phase at each interface. The introduction of activities for concentrations can only be correctly made for the Donnan potential using either the integration of Planck or Henderson.

According to TMS theory, the membrane potential $\Delta\phi$ (applicable to a highly idealized system) is given by the equation at 25° C

$$\Delta\phi = 59.2\left(\log\frac{C_2}{C_1}\frac{\sqrt{4C_1^2+\overline{D}^2}+\overline{D}}{\sqrt{4C_2^2+\overline{D}^2}+\overline{D}} + \overline{U}\log\frac{\sqrt{4C_2^2+\overline{D}^2}+\overline{D}\,\overline{U}}{\sqrt{4C_1^2+\overline{D}^2}+\overline{D}\,\overline{U}}\right), \overline{U} = \left(\frac{\overline{u}-\overline{v}}{\overline{u}+\overline{v}}\right) \qquad (1)$$

where $\overline{u}$ and $\overline{v}$ are the ionic mobilities of cation and anion ($m^2/v/s$) respectively, in the membrane phase, C_1 and C_2 are the concentrations of the membrane and $\overline{D}$ is the charge on the membrane expressed in equivalent per litre.

The graphical method of TMS determines the fixed charge $\overline{D}$ in equivalents/litre and the cation-to-anion mobility ratio in the membrane phase.

Kobatake Method

The system considered is composed of an ionizable membrane of uniform thickness which separates two bulk solutions of a uni-univalent electrolyte of concentrations C_1 and C_2. It is assumed that the system is isothermal and no pressure head is applied across the membrane. The ionizable groups are fixed on the polymer network which constitutes the given membrane. The expression for the membrane potential is given by

$$\Delta\phi = -\left(\frac{RT}{F}\right)\left[\frac{1}{\beta}\ln\frac{C_2}{C_1}\left(1+\frac{1}{\beta}-2\alpha\right)\ln\frac{C_2+\alpha\beta\theta}{C_1+\alpha\beta\theta}\right] \tag{2}$$

where

$$\alpha = \left(\frac{u}{u+v}\right)$$

$$\beta = 1+\left(\frac{KF\theta}{u}\right)$$

and parameters have been assumed to be independent of salt concentration.

Kobatake have derived two useful limiting forms of equation (2). These are (a) when C_2 becomes sufficiently small with γ fixed equation may be expanded to give

$$|\Delta\phi_r| = \frac{1}{\beta}\ln\gamma - \frac{\gamma-1}{\alpha\beta\gamma}\left(1+\frac{1}{\beta}-2\alpha\right)\frac{C_2}{\theta} \tag{3}$$

where $|\Delta\phi_r|$ is the absolute value of a reduced membrane potential defined by

$$|\Delta\phi_r| = \frac{F\Delta\phi}{RT} \tag{4}$$

(b) It has also been shown by Kobatake that at a fixed γ the inverse of an apparent transport number t_{-app} for the co-ion species in a negatively charged membrane is proportional to the inverse of the concentration C_2 in the region of high salt concentration. t_{-app} is defined by the relation

$$|\Delta\phi_r| = (1-2t_{-app})\ln\gamma \tag{5}$$

The derived transport number value has been called the apparent number i.e. t_{-app} because in this type of measurement water transport has not been taken into account. This apparent value will be close to the true value, when dilute solutions are used. Substituting for $\Delta\phi$ from equation (2) and expanding the resulting expression for $1/t_{-app}$ in powers of $1/C_2$ gives

$$\frac{1}{t_{-app}} = \frac{1}{(1-\alpha)} + \frac{(1+\beta-2\alpha\beta)}{2(1-\alpha)^2 \ln\gamma}\alpha\left(\frac{\theta}{C_2}\right) + ----- \quad (6)$$

Experimental

Preparation of membrane

Nickel arsenate precipitate was prepared by mixing 0.2M nickel (II) chloride (Otto Kemi, India with purity of 99.989%) with 0.2M sodium arsenate (E. Merck, India with purity of 99.90%) solutions. The precipitate was well washed with deionized water (Water purification systems, 'Integrate, whose RO conductivity 0-200μs/cm and UP resistivity 1-18.3 M Ω-CM) to remove free electrolyte and then dried and powdered. Membrane using suitable ratio of binder was prepared by the method used [14]. The precipitate having ion-exchange property was mixed with polystyrene (Otto Kemi, India, AR) granules of the size less than 200 meshes and pressed under suitable conditions of temperature and pressure for nickel arsenate 200 °C and 10MPa. Our effort has been to get the membrane of adequate chemical and mechanically stability. Thus, the membranes prepared by embedding 25% polystyrene were mechanically most stable and gave reproducible results. Those containing larger amount (>25%) of polystyrene did not give reproducible results.

while those containing lesser amount (<25%) were unstable. The membranes were subject to microscopic and electrochemical examinations for cracks and homogeneity of the surface and only those which had smooth surface and generated reproducible potentials were considered by carefully controlling the condition of fabrication.

Measurement of membrane potential

Membrane was cemented in Pyrex glass tube cell for measuring membrane potential. The half cell contained 25 ml of electrolyte solutions although the capacity of each of the half cells holding the membrane was about 35 ml. The various salt solutions (chlorides of K^+, Na^+, and Li^+) were prepared from B.D.H (A.R.) grade chemicals using deionized water. Saturated calomel electrodes were connected to a galvanometer (Osaw, spot reflecting galvanometer, Cat. No. 30241). The solutions in both the compartments were vigorously stirred by magnetic stirrers at constant 500 rpm to minimize the effect of boundary layers on potential [15]. The potential difference across the membrane was measured with the help of an Osaw Vernier Potentiometer (Cat. No. 30071), the concentration ratio $\left(\frac{C_2}{C_1}\right)$ was maintained at 10 throughout the experiment. The pressure and temperature were kept constant throughout the experiment. The electrochemical setup used for uni-ionic potential and membrane potential measurements may be represented as

SCE	Solution	Membrane	Solution	SCE
	C_1	Diffusion potential	C_2	
	Donnan potential		Donnan potential	

Measurement of membrane conductance

The electric conductance of the membrane was measured by the method used [16]. The membrane was sealed between two Pyrex glasses half cells. The half cells were first filled with electrolyte solutions of known concentration to equilibrate the membrane, and then the latter was replaced by purified mercury without removing the adhering surface liquid. Platinum electrodes dipping into mercury were used to established electrical contact. The membrane conductance was monitored on a direct reading conductivity meter (Model No L303). The solutions in both the compartments were vigorously stirred by magnetic stirrers at constant 500 rpm to minimize the effect of boundary layers on potential. The whole cells assembly was kept immersed in a water thermostat maintained at the required temperatures (10°C to 50°C).

Characterization of membrane

The pre-requisite for understanding the performance of an ion-exchange membrane is its complete physico-chemical characterization, which involves the determination of all such parameters that affects its electrochemical properties.

These parameters are membrane water content, porosity, thickness and swelling etc. and these were determined as described elsewhere [17].

Water content (%total wet weight)

The conditional membrane was first soaked in water to diffusible salt, blotted quickly with Whatmann filter paper to remove surface moisture and immediately weighted. These were further dried to a constant weight in a vacuum over P_2O_5 for 24h. The water content (total wet weight) was calculated as:

$$\% \text{ Total wet weight} = \left(\frac{W_w - W_d}{W_w}\right) \times 100$$

where W_w is the weight of the soaked / wet membrane and W_d the weight of the dry membrane.

Porosity

Porosity was determined as the volume of water incorporation in the cavities per unit membrane volume from the water content data:

$$\text{Porosity} = \left(\frac{W_w - W_d}{AL\rho_w}\right)$$

where W_d is the weight of the dry membrane, A the area of the membrane, L the thickness of the membrane and ρ_w is the density of water.

Thickness

The thickness of the membrane was measured by taking the average thickness of the membrane by using screw gauze.

Swelling

Swelling is measured as the difference between the average thickness of the membrane equilibrated with 1M NaCl for 24 h and the dry membrane.

Chemical stability

Chemical stability was evaluated on the basis of ASTM D543-95 method. Membrane was exposed to several media commonly utilized. Membrane was evaluated after 24, 48 and 168 h, analyzing alteration in color, texture, brightness, decomposition, splits, holes, bubbles, curving and stickiness [18].

SEM investigation of membrane morphology

Scanning Electron Microscope image was used to confirm the microstructure of fabricated porous membrane. The membrane morphology was investigated by Leo 4352 at an accelerating voltage of 20 kV. Sample was mounted on a copper stub and sputter coated with gold to minimize the charging.

Results and discussion

The results of thickness, swelling, porosity and water content capacity of nickel arsenate membrane are summarized in table 1.The water content of a membrane depends on the water vapor pressure of the surroundings. Knowledge of the pore size distribution and the water structure in a membrane might contribute to classify a special membrane resembling a solution-diffusion, a fine-porous, or a coarse-porous membrane [19]. In case of most of the transport measurements, only the membrane water content at saturation is needed, and that mostly as a function of solute concentration. Thus, low order of water content, swelling and porosity with

Table 1 Characterization of Nickel arsenate membrane

Thickness of the Membrane (cm)	Water Content as % weight of wet membrane	Porosity	Swelling of % weight wet membrane
0.075	0.038	0.057	No Swelling

less thickness of this membrane suggests that interstices are negligible and diffusion across the membrane would occur mainly through exchange sites. Membrane was tested for chemical resistance in acidic, alkaline and strongly oxidant media. In acidic (1M H_2SO_4) and in alkaline media (1M NaOH) few significant modifications were observed after 24, 48 and 168 h, demonstrating that the membrane is effective in such media. However, in strong oxidant media the synthesized membrane became fragile in 48 h and membrane was broken after 168 h, losing mechanical resistance. The nickel arsenate membrane using polystyrene as a binder was prepared by sol–gel process. The polystyrene was selected because its cross linked rigid framework provides adequate adhesion to the nickel arsenate which accounts for the mechanical stability to the membrane. Polystyrene based nickel arsenate membrane is better than a conventional membrane which degrades under harsh conditions and often encountered in industrial settings. Therefore, it is efficient, cost-effective material having solvent resistance and thermal resistance characteristics [20].

The characterization of membrane morphology has been studied by a number of investigators using scanning electron microscopy [21,22]. The composite pore structure, micro/ macro porosity, homogeneity, thickness, cracks and surface texture/morphology have been studied [23,24]. The cross-section of SEM micrograph of the surface is shown in figure 1. Membrane cross-section thickness was estimated to be around 30μm as observed in figure1. Membrane had random non-preferential orientation with no visible cracks and appeared to be composed of

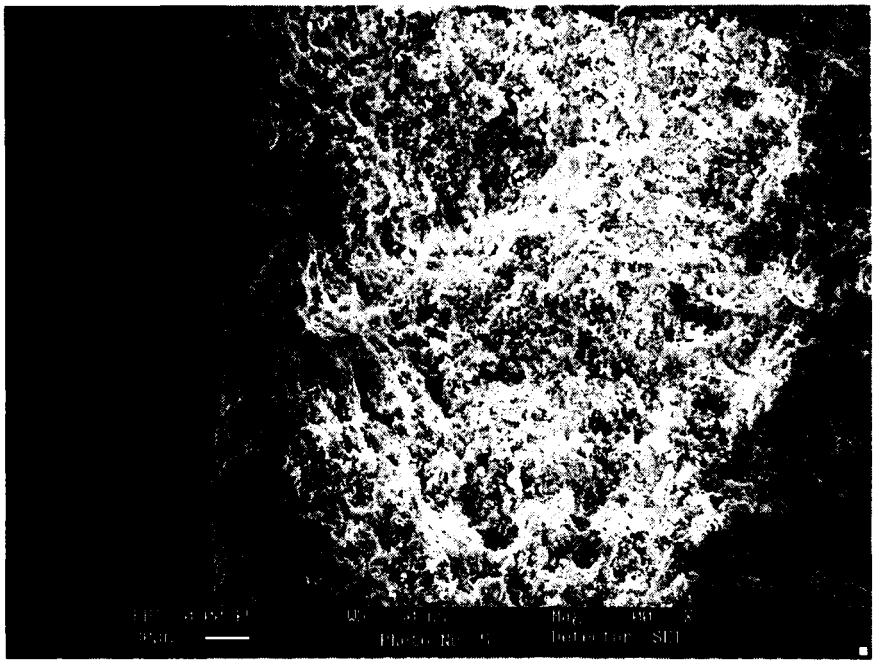

Figure 1 Cross-section SEM image of Polystyrene-based (25%) Nickel arsenate membrane

dense and loose aggregation of small particles. The membrane is macroscopically uniform in thickness and is porous in nature. The pores are modeled as uniform capillaries that extend throughout the membrane. These pores are evenly distributed throughout the surface of the membrane. Entrance and exit effects are ignored since the membrane thickness is large compared to the pore radius. However, the thickness is still large compared to the pore radius and it is assumed that the membrane and adjacent solution (interfaces) are in equilibrium. The distributions of charge density and mobile species within the pores are assumed to be uniform [25].

The values of observed membrane potential for the nickel arsenate membrane in contact with various 1:1 electrolyte solutions at 25 ± 1°C are given in table 2. The values for the membrane potential are of the order of positive mV and decrease with an increase of external electrolytes concentration. This shows that the membrane is negatively charged (cation selective) and the selectivity increases with dilution. The selectivity character of ion-exchange membrane with (1:1), (2:1) and (3:1) electrolytes has been reported [26,27]. In the case of (2:1) and (3:1) electrolytes, $\Delta\phi$ changes reverse sign (+ve to –ve). This indicates that the membrane has become anion selective. The change in the selectivity character of the membrane is evidently due to the adsorption of multivalent ions leading to a state where net positive charge left on the membrane surface making anion selective. Inorganic precipitate membrane was found to have the ability to generate potentials, when interposed between electrolyte solutions of different

Table 2 Observed membranes potentials $\Delta\phi$ in mV across the Nickel arsenate membrane in contact with various 1:1 electrolytes at different concentrations at 25±1° C

Electrolyte Concentration (mol/l)	Nickel Arsenate		
	KCl	NaCl	LiCl
10×10^{-1} / 1×10^{-1}	5.8	4.9	3.5
1×10^{-1} / 1×10^{-2}	8.7	7.8	6.4
7×10^{-2} / 7×10^{-3}	19.5	13.5	12.5
5×10^{-2} / 5×10^{-3}	24.2	20.1	18.6
2×10^{-2} / 2×10^{-3}	32.2	26.3	22.4
1×10^{-2} / 1×10^{-3}	36.5	30.2	28.5

concentrations due to the presence of a net charge on the membrane. Such charges play an important role in the sorption and transport of simple electrolytes in artificial as well as natural membranes [28], and impart some important electrochemical properties to the membrane, the most important being the differences in the permeabilities of co-ions, counter ions and neutral molecules. The quantity of charge required to generate the potentials, especially when dilute solution are used, is small. This of course, is dependent on the porosity of the membrane. In case the membrane pores are wide, any amount of charge on the membrane does little to generate good potentials. On the other hand, if the pores are narrow, a little amount of charge can give rise to good potential values. Hence, a detailed investigation of the mechanism of transport of simple electrolytes through a charged membrane seems to be incomplete without the evaluation of the thermodynamically effective fixed charge density of the membrane. The former can be evaluated by making uses of an equation derived on the basis of thermodynamics of irreversible processes. This approach employs a phenomenological coefficient to correlate the gradients that exits across a membrane and their resulting fluxes.

The membrane potential data obtained with nickel arsenate membrane using various 1:1 electrolytes are plotted as a function of $-\log C_2$ with the ratio γ fixed at 10. This plot is shown in figure 2.

The set of curves in figure 3 are the theoretical membrane potentials for a cation selective membrane, which is calculated from equation (1). The difference

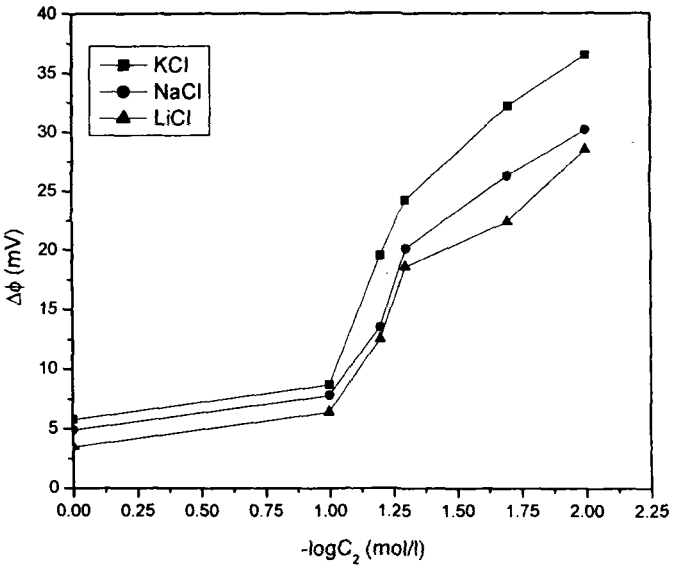

Figure 2 Plots of membrane potentials against $-\log C_2$ for Nickel arsenate membrane using various 1:1 electrolytes

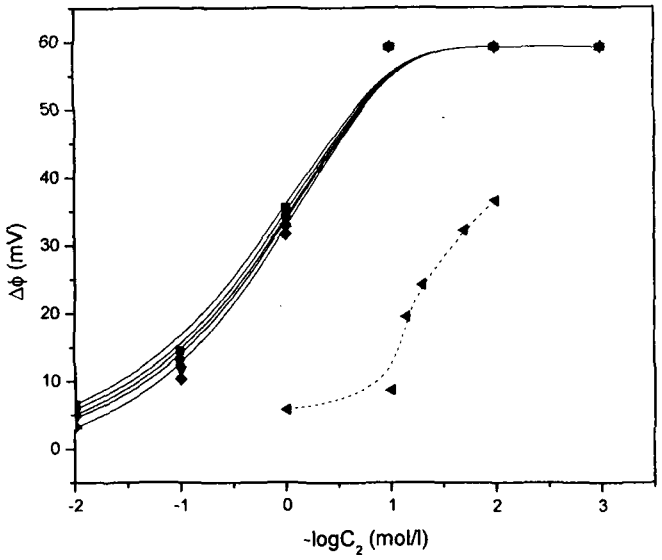

Figure 3 Plots of membrane potentials vs. $-\log C_2$ for Nickel arsenate membrane. Smooth curves are the theoretical concentration potentials for different mobility ratio. Broken line is the experimental values of membrane potential for different concentration of KCl solution.

curves are for different mobility ratios $\left(\frac{\bar{u}}{\bar{v}}\right)$, with a constant value of $\bar{D}$ is unity expressed in equivalent/litre. The experimental $\Delta\phi$ values for titanium arsenate membrane with KCI electrolyte were plotted in the same graph as a function of $-\log C_2$. The experimental curve was shifted horizontally and ran parallel to one of the theoretical curves. This shift gave $\log \bar{D}$, and the parallel theoretical curve gave the value for mobility ratio $\left(\frac{\bar{u}}{\bar{v}}\right)$ with the membrane phase. The values of $\bar{D}$ and $\left(\frac{\bar{u}}{\bar{v}}\right)$ derived in this way for the membrane and various 1:1 electrolytes are given in table 3. Thus, the order of fixed charge density for electrolytes used was found to be KCl > NaCl > LiCl.

Equation (3) indicates that a value of β and a relation between α and θ can be obtained by evaluation of the intercept and the initial slope of a plot of $|\Delta\phi_r|$ against C_2 which is shown in figure 4. The value of intercept is equal to $1/\beta \ln\gamma$ from which β is evaluated. Values are given in table 4.

Equation (6) indicate that the intercept of a plot of $1/t_{-app}$ against $1/C_2$ at fixed γ allows the value of α to be determined. Plots of $1/t_{-app}$ against $1/C_2$ for various uni-univalent electrolytes are shown in figure 5.The value of intercept is equal to $1/(1-\alpha)$, from which α may be evaluated. Values are given in table 4. If this value of α is inserted in the relation obtained from the initial slope for $|\Delta\phi_r|$ against C_2,

Table 3 Values of the thermodynamically charge density of Nickel arsenate membrane- electrolyte systems evaluated by various theories

Electrolyte	TMS		Kobatake	
	$\left(\frac{\bar{u}}{\bar{v}}\right)$	$\bar{D}$ (eq/l)	θ_c	θ_d
KCl	1.22	0.049	0.043	0.054
NaCl	1.17	0.034	0.026	0.040
LiCl	1.13	0.030	0.022	0.033

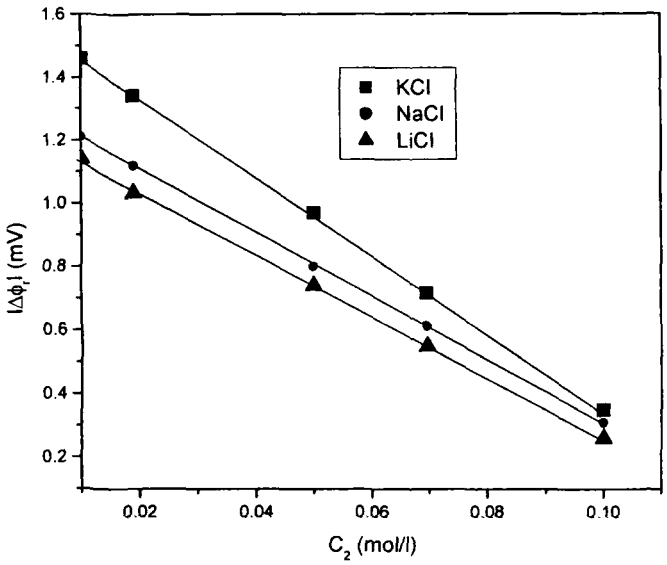

Figure 4 Plots of $|\Delta\phi_r|$ against C_2 for Nickel arsenate membrane using various 1:1 electrolytes

Table 4 Values of parameters α and β for Nickel arsenate membrane- electrolyte system

Electrolyte	Nickel Arsenate	
	α	β
KCl	0.55	1.58
NaCl	0.54	1.90
LiCl	0.53	2.02

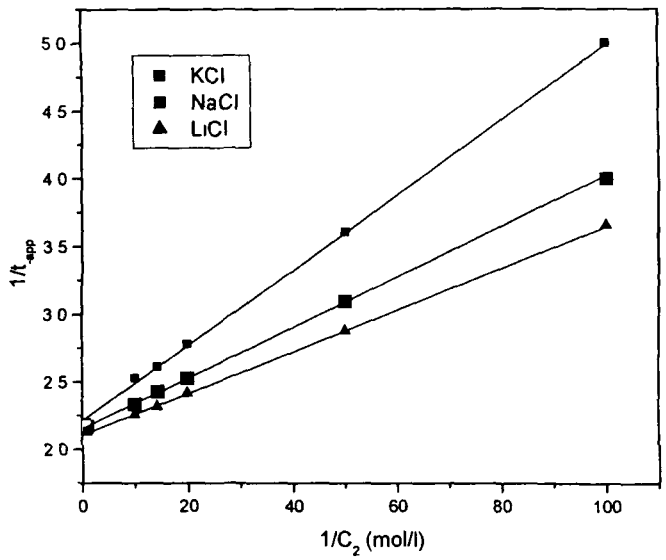

Figure 5 Plots of $1/t_{app}$ against $1/C_2$ for Nickel arsenate membrane using various 1:1 electrolytes

the desired value for θ_c can be determined. Once α and β are known in the manner described above, the values of θ_d may be evaluated from the initial slope for $1/t_{-app}$ against $1/C_2$.

Kobatake has suggested that provided his equation for the membrane potential is correct, then the two values of θ i.e. θ_c and θ_d thus determined from the opposite limits should agree with one another. The values are given in table 3 which are closed together thereby confirming the applicability of Kobatake's equation to these systems.

We have seen that the charge density is higher in the region of low concentrations (θ_d) than in high concentrations (θ_c) because the ionic atmosphere around fixed charges in the formal case is large compared with the later case. On the other hand, the charge density in the case of KCl is higher than in NaCl due to the size factor (the smaller size, the larger ionic atmosphere).

Inorganic membrane has the ability to generate potential [29,30]. When an ionic gradient is maintained using two solutions of different concentrations of same electrolyte on either side of the membrane, diffusion of electrolytes from the region of higher to lower concentration and flow of water in the opposite direction take place. In fact, the mobile species penetrate the membrane at different magnitude and various transport phenomena, including the development of potential across it, are induced into the system.

The TMS equation (1) can also be expressed by the sum of Donnan potential $\Delta\phi_{Don}$ between membrane surfaces and external solutions and the diffusion potential $\Delta\phi_{diff}$ within the membrane [31,32].

$$\Delta\phi_m = \Delta\phi_{Don} + \Delta\phi_{diff} \tag{7}$$

$$= -\frac{RT}{V_k F}\ln\left(\frac{\gamma''_{\pm}C_2\overline{C}_{1+}}{\gamma'_{\pm}C_1\overline{C}_{2+}}\right) - \frac{RT}{V_k F}\frac{\overline{\omega}-1}{\overline{\omega}+1}\times\ln\left(\frac{(\overline{\omega}+1)\overline{C}_{2+}+(V_x/V_k)\overline{D}}{(\overline{\omega}+1)\overline{C}_{1+}+(V_x/V_k)\overline{D}}\right) \tag{8}$$

The R, T and F have their usual significance; $\gamma'_{\pm}$ and $\gamma''_{\pm}$ are the mean ionic activity coefficients; $\overline{\omega} = \frac{\overline{u}}{\overline{v}}$ is the mobility ratio of the cation to the anion in the membrane phase and $\overline{C}_{1+}$ and $\overline{C}_{2+}$ are the cation concentrations in the membrane phase first and second, respectively. The cation concentration is given by the equation

$$\overline{C}_+ = \sqrt{\left(\frac{V_x\overline{D}}{2V_k}\right)^2 + \left(\frac{\gamma_{\pm}C}{q}\right)^2} - \frac{V_x\overline{D}}{2V_k} \tag{9}$$

Here V_k and V_x refer to the valency of cation and fixed-charge group on the membrane matrix, q is the charge effectiveness of the membrane and is defined by the equation

$$q = \sqrt{\frac{\gamma_{\pm}}{K_{\pm}}} \tag{10}$$

where $K_{\pm}$ is the distribution coefficient. It is expressed as

$$K_{\pm} = \frac{\overline{C}_i}{C_i}, \qquad \overline{C}_i = C_i - \overline{D} \tag{11}$$

where $\overline{C}_i$ is the *i*th ion concentration in the membrane phase and C_i is the *i*th ion concentration of the external solution. The transport properties of the membrane in various electrolyte solutions are important parameters to further investigate the membrane phenomena as shown in equation (12).

$$\Delta\phi = \frac{RT}{F}(t_+ - t_-)\ln\frac{C_2}{C_1} \tag{12}$$

$$\frac{t_+}{t_-} = \frac{\overline{u}}{\overline{v}} \tag{13}$$

Equation (13) was first used to calculate the values of transport numbers $t_\pm$, mobility ratio $\overline{\omega} = \frac{\overline{u}}{\overline{v}}$ and finally $\overline{U}$ as given in table 5. The values of mobility $\overline{\omega}$ of the electrolytes in the membrane phase were found to be high at lower concentration of all the electrolytes (KCl, NaCl and LiCl). Further increase in concentration of the electrolytes led to a sharp drop in the values of $\overline{\omega}$ as given in table 5. The high mobility is attributed to higher transport number of comparatively free cations of electrolytes and also be similar trend as the mobility in least concentrated solution. The values of the parameters $K_\pm$, q and $\overline{C}_+$ derived for the system have also been included in table 5. The values of $\gamma_\pm$ were the usual charted values for electrolytes. Using equation (11) it was found that the values of distribution coefficients increased at lower concentration of electrolytes. As the concentration of electrolytes increased, the values of distribution coefficients sharply dropped and, thereafter, a stable trend was observed as shown in table 5.

Table 5 The calculated values of the parameters t_+, $\overline{U}$, $\overline{\omega}$, $K_\pm$, q, and $\overline{C}_+$ of Nickel arsenate membrane with different concentration of electrolytes using eq. (12) and eq. (9) - (11)

C_2 (mol/l)	t_+	$\overline{U}$	$\overline{\omega}$	$K_\pm$	q	$\overline{C}_+$
KCl (Electrolyte)						
0.01	0.80	0.60	4.00	3.90	0.67	0.0024
0.02	0.77	0.54	3.35	1.45	0.80	0.0034
0.05	0.70	0.40	2.33	0.02	6.49	0.0058
0.07	0.66	0.32	1.94	0.30	1.64	0.0076
0.10	0.57	0.14	1.33	0.51	1.23	0.0411
1.00	0.55	0.10	1.22	0.97	0.80	0.7234
NaCl						
0.01	0.75	0.50	3.00	2.40	0.61	0.0021
0.02	0.72	0.44	2.57	0.70	1.12	0.0024
0.05	0.67	0.34	2.03	0.32	1.62	0.0062
0.07	0.61	0.22	1.56	0.51	1.23	0.0169
0.10	0.57	0.14	1.33	0.66	1.08	0.0366
1.00	0.54	0.08	1.17	0.96	0.79	0.7158
LiCl						
0.01	0.74	0.48	2.85	2.00	0.48	0.0020
0.02	0.69	0.38	2.23	0.50	1.33	0.0019
0.05	0.66	0.32	1.94	0.40	1.45	0.0086
0.07	0.60	0.20	1.50	0.57	1.19	0.0203
0.10	0.55	0.10	1.22	0.70	1.05	0.0410
1.00	0.53	0.06	1.13	0.96	0.79	0.6876

The large deviation in the value of $K_{\pm}$ at the lower concentration of electrolytes was attributed to the high mobility of comparatively free charges of the strong electrolyte and thus, reached into the membrane phase easily compared to higher concentrated electrolytes solution.

The charge effectiveness q, values for LiCl are the smallest of the electrolytes used in this study and order is KCl > NaCl > LiCl. The counter-ions Cl^-, is the same for all the electrolyte used therefore, the variation of charge effectiveness values are possibly due to increase in adsorption of co-ions on charged membrane [33,34].

When a permselective membrane happens to be in between the solutions of electrolytes of different concentrations, a steady electromotive force (e.m.f) develops due to difference in the relative permeabilities of various ionic species. This e.m.f, usually called the membrane potential, depends on the properties of the membrane and has been the subject of many theoretical and experimental studies. TMS theory and its modifications are inadequate to explain experimental results on non-ideal permselective membrane.

The perm selectivity [29] is a measure of the characteristic difference in the membrane of counter ions and co-ions and co-ions, which be expressed as

$$P_s = \left(\frac{\bar{t}_+ - t_+}{1 - t_+} \right) \tag{14}$$

where $\bar{t}_+$ is the counter-ion transport number through the membrane and t_+, is the counter ion transport number in the solution phase. Thus, the permselectivity

arises due to the nature of the membrane for differentiating between co-ions and counter ions and is not a membrane constant. Permselectivity can be calculated from the equation (14). It can be seen from figure 6 that permeslectivity decreased with the increase in the concentration of the salt solution. This is inconformity with the expectation based on increased deswelling of the ion exchange membrane resulting in progressively lowered co-ion exclusion with increase in concentration.

An ion exchange membrane undergoes swelling because of the osmotic intake of the solvent by the membrane network. This osmotic action depends on the solute concentration; it decrease with the increase in concentration [35] and as a result solvent uptake by the membrane matrix decreases leading to the deswelling of the membrane. Due of this membrane openness increases accompanied by lowered exclusion of co-ions. Permselectivity of the membrane therefore decreases. Thus, even electrolyte concentration remains unchanged; a reduction in membrane permselectivity is expected with increase in the concentration of the solution.

The values of observed membrane conductance for the nickel arsenate membrane in contact with various 1:1 electrolyte solutions at different temperature (10°C to 50°C) are given in table 6. The values for the membrane specific conductance are of the order of positive $m\Omega^{-1}cm^{-1}$ and increase with an increase of external electrolytes concentration as well as temperature (10°C to 50°C) in all the cases. This type of variation can be explained in terms of increased obstruction of

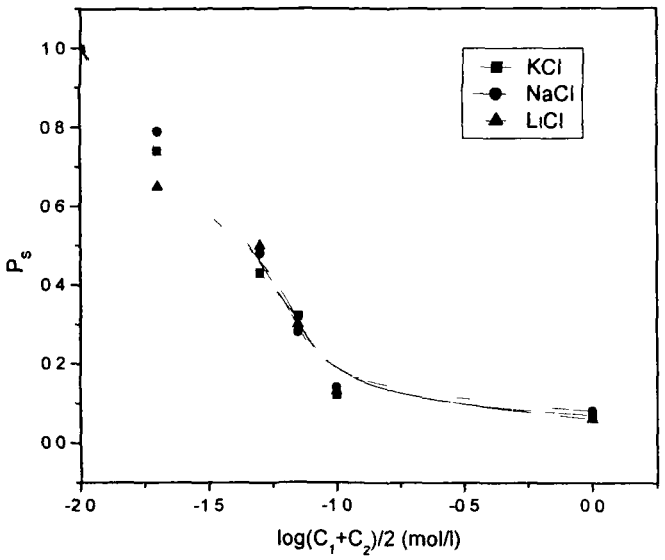

Figure 6 Plots of P_S against log $(C_1+C_2)/2$ for Nickel arsenate membrane using various 1:1 electrolytes

Table 6 Experimentally observed values of membrane conductance ($m\Omega^{-1}cm^{-1}$) for various 1:1 electrolytes at different temperature (10 to 50) ± 0.1°C

Temperature (°C)	**Concentration** (mol/l)				
	0.1	0.07	0.05	0.02	0.01
KCl					
10	9.00	5.40	4.30	3.40	2.70
20	9.45	6.70	4.80	3.60	2.95
30	10.10	7.10	5.50	3.75	3.20
40	10.75	7.50	6.05	4.10	3.50
50	11.20	8.30	6.60	4.70	4.00
NaCl					
10	8.45	4.15	3.50	2.70	2.50
20	8.90	4.60	3.95	3.05	3.20
30	9.40	5.25	5.70	4.50	3.80
40	10.15	6.20	5.90	4.30	4.00
50	10.95	7.10	6.40	3.80	4.40
LiCl					
10	5.75	3.40	2.40	2.10	1.90
20	6.35	3.80	2.90	2.50	2.30
30	7.10	4.30	3.60	3.00	2.80
40	7.90	4.70	4.25	3.50	3.35
50	8.45	5.05	4.65	3.90	4.50

the membrane matrix and increased salt uptake with an increase of external electrolyte concentration.

An examination of table 6 shows that the specific conductance not only increases with an increase in the electrolyte concentration but also attains a maximum limiting value at higher concentrations. Such a trend has been observed in all the above electrolytic solutions. This may be attributed to a progressive accumulation of ionic species within the membrane. The tendency to attain a limiting value seems to be due to the fact that an electrically neutral pore, which is specific for a particular ion, is unlikely to contain more than one type of ion. Consequently, at high electrolyte concentration, the pore saturates and the conductance approaches a limiting value. The values of specific conductance of the electrolytes follow the sequence for the cations:

$$K^+ > Na^+ > Li^+$$

The membrane specific conductance data obtained with nickel arsenate membrane using various 1:1 electrolytes at different temperature are plotted as a function of $\sqrt{C}$. This plot is shown in figure 7 for the KCl solutions. The remaining 2 plots (not shown here) based on the data contained in the table have also exhibited a similar behavior. The specific conductance of the membrane increases almost linearly with the square root of external electrolyte concentration. This behavior can be explained in terms of increased obstruction of the polymer matrix as diffusion pathways become more tortuous in concentrated solution. It is also observed that at higher concentration the uptake of salt by membrane is

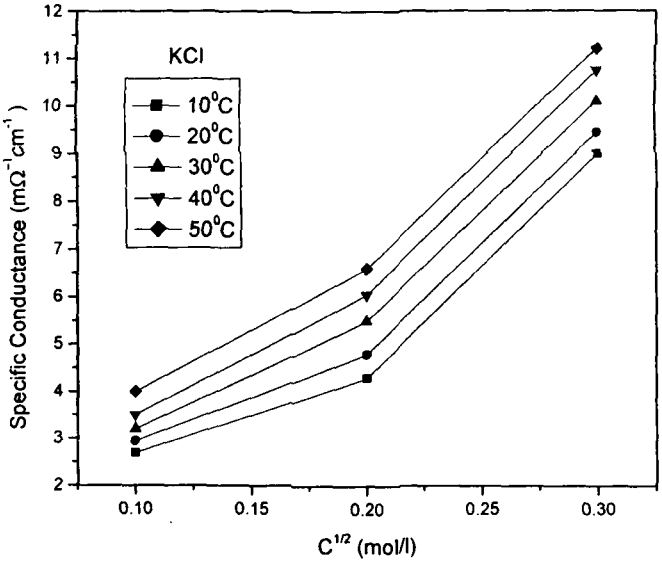

Figure 7 Plots of specific conductance ($m\Omega^{-1}cm^{-1}$) Vs square root of concentration for electrolytes at different temperature through Nickel arsenate membrane

higher which results in increased value of electrical conductance. These two opposing effects operate simultaneously at higher concentration as shown in figure 7 and a state is reached when membrane conductance attains a maximum value [36].

In addition, the diffusion of ions depends upon the charge on the membrane and its porosity. The membrane porosity in relation to the size of the hydrated species diffusing through the membrane appears to determine the above sequence. Several probable structures of water molecules under the condition of a given temperature may play an important role in determining the size of the hydrated ions [37]. As the diffusion paths in the membrane become more difficult in aqueous solutions, the mobility of large hydrated ions gets impeded by the membrane framework and the interaction with the fixed charge groups on the membrane matrix. Consequently, the membrane pores reduce the conductance of small ions, which is much hydrated. This is in accord with the earlier reported significance of the factors like pore size, hydration, etc. [38,39].

In figure 8, specific conductance increases with increase in temperature T, due to the state of hydration which implies that the activation energy decreases.

Table 7 shows that the activation energy decreases with increase in concentration of the bathing electrolyte solution and the sequence for energy of activation is

$$E_a K^+ > E_a Na^+ > E_a Li^+$$

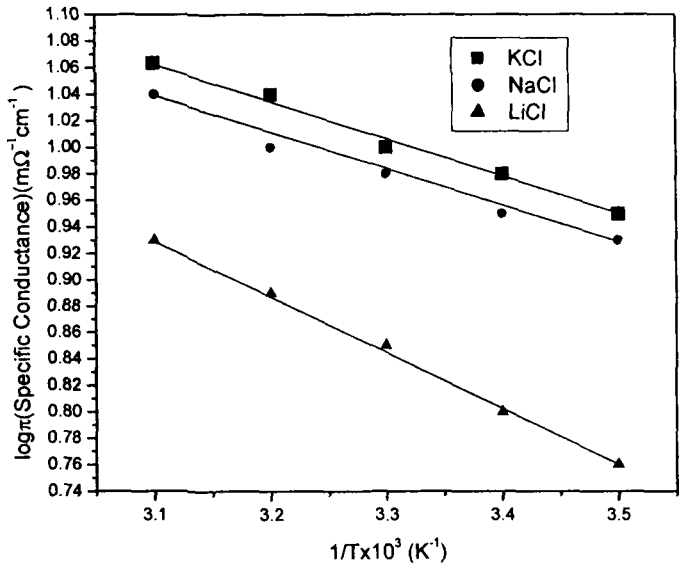

Figure 8 Arrhenius plots of specific conductance Vs 1/T 10^3 for 1:1 electrolytes through Nickel arsenate membrane

Table 7 Calculated values of Activation Parameters for 1:1 electrolytes through Nickel arsenate membrane

Electrolytes	Conc.(mol/l)	E_a (KJ/mole)	ΔH^*(KJ/mole)	ΔG^*(KJ/mole)	$-\Delta S^*(JK^{-1}mol^{-1})$
KCl	0.1	9.57	7.12	69.73	213.68
	0.01	12.05	9.60	76.64	228.81
NaCl	0.1	7.66	5.2	68.09	214.64
	0.01	11.67	9.22	76.37	229.19
LiCl	0.1	5.73	3.28	66.56	215.98
	0.01	10.92	8.47	75.96	230.34

Table 8 shows that an increase of activation energy with an increase of crystallographic radius confirms the applicability of Kumins [40] arguments for polystyrene based inorganic precipitate membrane systems

According to Eyring [41], the pores in the membranes may be considered as a sequence of energy barriers over which the ion has to jump in order to cross the barriers in the process of diffusion/transport of ions.

On the basis of absolute reaction rate [41]

$$\Lambda = \left(\frac{RT}{Nh}\right) e^{-\left(\frac{\Delta H^*}{RT}\right)} e^{\left(\frac{\Delta S^*}{R}\right)} \tag{15}$$

where Λ is the observed specific conductance, h the planck's constant, R the gas constant, N the Avogadro number, T the absolute temperature, ΔH^* the enthalpy of activation and ΔS^* the entropy of activation while the other terms have their usual meaning.

The enthalpy and entropy of activation are related to the free energy of activation, ΔG^*, by the Gibbs-Helmholtz equation

$$\Delta G^* = \Delta H^* - T\Delta S^* \tag{16}$$

The enthalpy of activation is also related to the Arrhenius energy of activation, E_a, as

$$E_a = \Delta H^* + RT \tag{17}$$

A plot of $\log\frac{\Lambda Nh}{RT}$ versus $\frac{1}{T}$ from experimental data, shown in Figure 9, RT gives the value of ΔH^* /R and ΔS^*/R. ΔG^* and E_a were obtained by using

Table 8 Relation between Crystallographic radius and activation energy of alkali chlorides

Ion	Crystallographic radii (Å)	Energy of activation (KJ/mole)
K^+	1.33	9.57
Na^+	0.93	7.66
Li^+	0.60	5.73

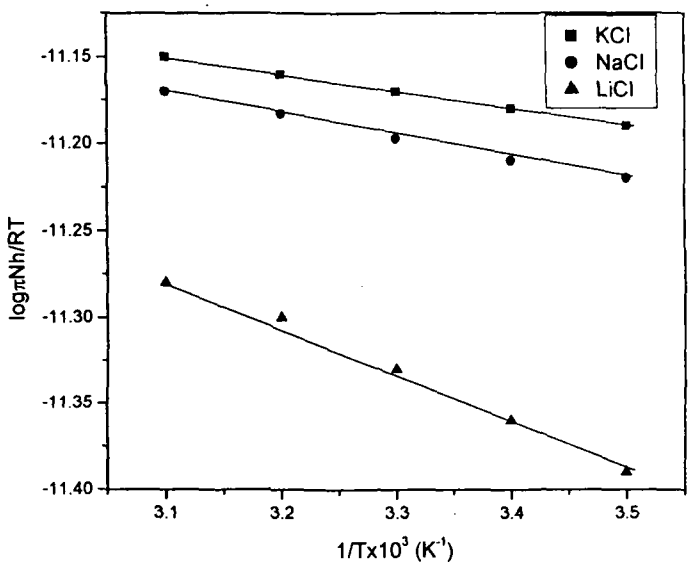

Figure 9 Plots of $\log \frac{\pi Nh}{RT}$ Vs 1/T 10^3 for 1:1 electrolytes through Nickel arsenate membrane

equations (16) and (17). The values of various kinetic activation parameters E_a, ΔH^*, ΔG^* and ΔS^*derived for the diffusion of various electrolytes in membrane are given in table 7. The results indicate that the electrolyte permeation gives rise to a negative value of ΔS^*. Amongst the ions of the same valence the order of ΔS^* is as follows

$$K^+ > Na^+ > Li^+$$

Thus, the negative values of ΔS^* indicated electrolyte diffusion with partial immobilization in the membrane, the relative partial immobility increasing with increase in the valence of ions constituting the electrolyte [42].

According to Eyring [41] , the values of ΔS^* indicate the mechanism of flow, the large positive ΔS^* is interpreted as reflecting bonds breaking, while low values indicate that permeation has taken place without bonds breaking. Negative ΔS^* values are considered to indicate either formation of a covalent bond between the permeating species and the membrane material or that the permeation through the membrane may not be the rate determining step.

Conclusions

The membrane potentials of inorganic membrane were measured with uni-univalent electrolyte (KCl, NaCl and LiCl) solution using saturated calomel electrodes. The membrane potential offered by electrolytes is in the order of KCl>NaCl> LiCl and the obtained data indicates that the behavior investigated membrane is cation selective. Fixed charge density is the central parameter governing transport phenomena in membrane and depends upon the feed

composition. The fixed charge concept of TMS model for charged membrane is an appropriate starting point for the investigations of the actual mechanisms of ionic or molecular processes which occur in membrane phase. Table 3 shows that the values of the charge densities evaluated from the various procedures are not much different from each other and a slight difference in the value may be ascribed to the different graphical procedures adopted for the evaluation. From the data in table 7 it can be inferred that the larger ions face more difficulties in crossing the membrane than the smaller ones. Thus, it can be explained that the magnitudes of E_a, $\Delta H^*$and ΔG^* must be higher for larger ions than the smaller ones. On the one hand, a high ΔS^* value associated with the high value of E_a for diffusion may suggest the existence of either a large zone of activation or loosening of more chain segments of the membrane. On the other hand, low value of ΔS^* implies either a small zone of activation or no loosening of the membrane structure upon permeation [42].

References

[1] A.G. MacDiarmid, A.J. Epstein, Conducting Polymers Science and Technology, Plenium Publishing Corp., Brazil, 1993

[2] S. Roth, W. Graupner, *Syn. Met.* **57** (1993) 3623.

[3] M. Broussely, P. Bieusan, B. Simon, *Electrochim. Acta* **45** (1999) 3.

[4] C.R. Martin, *Science* **266** (1994) 1961.

[5] F. Huguenin, M.T.D. Gambardella, R.M. Torresi, S.I.C. deTorresi, D.A. Buttry, *J. Electrochem. Sci.* **147** (2000) 2437.

[6] Z.F. Li, E. Ruckenstein, *Langmuir* **18** (2002) 6956.

[7] F.D.R. Amado, E. Gondran, J.Z. Ferreira, M.A.S. Rodrigues, C.A. Ferreira, *J. Membr. Sci.* **234** (2004) 139.

[8] V.K. Gupta, M.M. Antonijevie, S. Chandra, S. Agarwal, *Sensors* **2** (2002) 233.

[9] Y. Chujo, Curr. Opin. *Solid State Mater. Sci.* **1** (1996) 806.

[10] J.C. Douglas, H. Douglas, J.Z. Pamela, P.H. Robert, L. Robert, C.H. Robert, J. Zubieta, *Coord. Chem. Rev.* **737** (1999) 190.

[11] R.K. Nagarale, G.S. Gohil, V.K. Shahi, R. Rangarajan, *J. Colloid Interface Sci.* **287** (2005) 198.

[12] Y. Kobatake, T. Noriaki, Y. Toyoshima, H. Fujita, *J. Phys. Chem.* **69** (1965) 3981.

[13] A. Nakajima, T. Miyasaka, K. Sakai, T. Tsukahara, *J. Membr. Sci.* **187** (2001) 129.

[14] F. Jabeen, Rafiuddin, *J. Appl. Polym. Sci.* **110** (2008) 3023.

[15] A. Canas, M.J. Ariza, J. Benavente, *J. Colloid Interface Sci.* **246** (2002) 150.

[16] N. Lakshminarayanaih, Transport Phenomena in membrane, Academic Press, New York, 1969.

[17] A.A. Khan, A. Khan, Inamuddin, *Talanta* **72** (2007) 699.

[18] ASTM D543-95, Standard Particles for evaluating the resistance of plastics to chemical reagent, 1998.

[19] S. Koter, P.Piotrowski, J. Kerrs, *J. Membr. Sci.* **153** (1999) 83.

[20] U. Razdan, S.V. Joshi, U.J. Shah, *Current Science* **85 (6)** (2003) 761.

[21] Y. Wu, C. Wu, F. Yu, T. Xu, Y. Fu, *J. Membr. Sci.* **307** (2008) 28.

[22] B. Ernst, S. Haag, M. Burgard, *J. Membr. Sci.* **288** (2008) 208.

[23] J.O. Titiloye, I. Hussain, *J. Colloid Interface Sci.* **318** (2008) 50.

[24] M. Resina, J. Macanás, J. de Gyves, M. Muňoz, *J. Membr. Sci.* **289** (2007) 150.

[25] J.G. Aleman, J.M. Dicker, *J. Membr. Sci.* **235** (2004) 1.

[26] K. Singh, A.K. Tiwari, J.P. Rai, *Ind. J. Chem.* **24 (A)** (1985) 825.

[27] K. Singh, A.K. Tiwari, *Poc. Indian Natn. Sci. Acad.* **70 (A)** (2004) 477.

[28] J. Schaep, C. Vandecasteele, *J. Membr. Sci.* **188** (2001) 129.

[29] V.K. Shahi, G.S. Trivedi, S.K. Thampy, R. Rangarajan, *J. Colloid Interface Sci.* **262** (2003) 566.

[30] F. Jabeen, Rafiuddin, Rafiuddin, *J. Sol Gel Sci. Technol.* **44** (2007) 195.

[31] H. Matsumoto, A. Tanioka, T.J. Murata, M. Higa, K. Horiuchi, *J. Phys. Chem. B* **102** (1998) 5011.

[32] T.J. Chou, A. Tanioka, *J. Colloid Interface Sci.* **212** (1999) 293.

[33] W. Bowen, A. Mohammad, N. Hilal, *J. Membr. Sci.* **126** (1997) 91.

[34] X. Wang, T. Suru, M. Tagoh, S. Nakao, S. Kimura, *J. Chem. Eng, Jpn.* **28 (2)** (1995) 186.

[35] R.E. Kesting, Synthetic Polymeric Membrane, McGraw Hill Book Company, New Delhi, 1971.

[36] T. Iijima, T. Obara, M. Isshiki, T. Seki, K. Adachi, *J. Colloid Interface Sci.* **63** (1978) 421.

[37] S. Islam, B.N. Waris, *Thermochim Acta* **424** (2004) 165.

[38] J.L. Lovenam, Structure and Function in Biological Membranes, Holden-Day, San Fransisco, 1964.

[39] J.F. Danielli, H. Daysin, The Permeability of Natural Membranes, McMillan New York, 1943.

[40] C.A. Kumins, T.K. Kwei, J. Crank, GS. Park Diffusion in Polymers, Academic Press, New York, 1968.

[41] S. Glassto, K.J. Laider, H. Eyring, The Theory of Rate Processes, McGraw-Hill, New York, 1941.

[42] K.E. Shuler, C.A. Dames, K.J. Laidler, *J. Chem. Phys.* **17** (1949) 860.

CHAPTER 3

Transport Studies of Titanium Arsenate Membrane

Introduction

Organic–inorganic composite, a new class of materials is attractive for the creating high performance or high functional polymeric behaviors that are expected to provide many possibilities. Composite can be used to modify organic polymeric material or to modify inorganic materials that exhibit very different properties from their original component. The inorganic ion-exchange materials besides other advantages are important in being more stable to high temperature and radiation field than the organic ones [1]. In order to obtain a combination of these advantages associated with polymeric and inorganic materials as ion-exchangers, attempts have been made to develop polymeric-inorganic composite ion-exchangers by incorporation of organic monomers in the inorganic matrix [2]. An inorganic precipitate ion-exchanger based on organic polymeric matrix must be an interesting material, as it should possess the mechanical stability due to the presence of organic polymeric species and the basic characteristics of an inorganic ion-exchanger regarding its selectivity for some particular metal ions [3-5]. The basic applications of the ion-exchange membrane process are based on the Donnan membrane equilibrium principle and have been paid attention to solve two important environmental problems, for the recovery and enrichment of valuable ions, and the removal of undesirable ions from waste water [6].

In this paper we describe a series of electric potentials observed across titanium arsenate polystyrene based ion exchange membrane separating various 1:1 electrolytes at different concentrations for the evaluation of effective fixed

charge density by various method namely those of (a) Teorell-Meyer-Sievers and (b) Kobatake.

The transport numbers of ions, mobility, distribution coefficient, charge effectiveness, permselectivity and other parameters studies theory have also been carried out. To calculate the theoretical membrane potentials $\Delta\phi$ at different electrolyte concentrations using the TMS theory [7,8] and Kobatake method to test the applicability of these developed equations for membrane potentials for the system under investigation.

Various thermodynamics parameters, namely, energy of activation, E_a, free energy of activation, ΔG^*, enthalpy of activation, ΔH^*, entropy of activation, ΔS^*, of the membrane-electrolyte system have been determined at different temperatures in order to understand the mechanism of ion transport through the membrane. The assembly used in the investigation provides data for various membrane parameters, with reasonable accuracy.

Theory

Fixed charge theory of Teorell-Meyer-Sievers

In the TMS theory there is an equilibrium process at each solution membrane interface which has a formal analogy with the Donnan equilibrium. The assumptions made are (a) the cation and anion mobilities and fixed charge concentration are constant throughout the membrane phase and are independent of the salt concentration and (b) the transference of water may be neglected. The implications of these assumptions have been discussed [9]. Further assumption

must be made that the activity coefficient of the salt is the same in the membrane and solution phase at each interface. The introduction of activities for concentrations can only be correctly made for the Donnan potential using either the integration of Planck or Henderson.

According to TMS theory, the membrane potential $\Delta\phi$ (applicable to a highly idealized system) is given by the equation at 25° C

$$\Delta\phi = 59.2\left(\log\frac{C_2}{C_1}\frac{\sqrt{4C_1^2+\overline{D}^2}+\overline{D}}{\sqrt{4C_2^2+\overline{D}^2}+\overline{D}} + \overline{U}\log\frac{\sqrt{4C_2^2+\overline{D}^2}+\overline{D}\,\overline{U}}{\sqrt{4C_1^2+\overline{D}^2}+\overline{D}\,\overline{U}}\right), \overline{U} = \left(\frac{\overline{u}-\overline{v}}{\overline{u}+\overline{v}}\right) \qquad (1)$$

where $\overline{u}$ and $\overline{v}$ are the ionic mobilities of cation and anion (m^2/v/s) respectively, in the membrane phase, C_1 and C_2 are the concentrations of the membrane and $\overline{D}$ is the charge on the membrane expressed in equivalent per litre.

The graphical method of TMS determines the fixed charge $\overline{D}$ in equivalents/litre and the cation-to-anion mobility ratio in the membrane phase.

Kobatake Method

The system considered is composed of an ionizable membrane of uniform thickness which separates two bulk solutions of a uni-univalent electrolyte of concentrations C_1 and C_2. It is assumed that the system is isothermal and no pressure head is applied across the membrane. The ionizable groups are fixed on the polymer network which constitutes the given membrane. The expression for the membrane potential is given by

$$\Delta\phi = -\left(\frac{RT}{F}\right)\left[\frac{1}{\beta}\ln\frac{C_2}{C_1}\left(1+\frac{1}{\beta}-2\alpha\right)\ln\frac{C_2+\alpha\beta\theta}{C_1+\alpha\beta\theta}\right] \tag{2}$$

where

$$\alpha = \left(\frac{u}{u+v}\right)$$

$$\beta = 1+\left(\frac{KF\theta}{u}\right)$$

and parameters have been assumed to be independent of salt concentration.

Kobatake [10] have derived two useful limiting forms of equation (2). These are (a) when C_2 becomes sufficiently small with γ fixed equation may be expanded to give

$$|\Delta\phi_r| = \frac{1}{\beta}\ln\gamma - \frac{\gamma-1}{\alpha\beta\gamma}\left(1+\frac{1}{\beta}-2\alpha\right)\frac{C_2}{\theta} \tag{3}$$

where $|\Delta\phi_r|$ is the absolute value of a reduced membrane potential defined by

$$|\Delta\phi_r| = \frac{F\Delta\phi}{RT} \tag{4}$$

(b) It has also been shown by Kobatake that at a fixed γ the inverse of an apparent transport number t_{-app} for the co-ion species in a negatively charged membrane is proportional to the inverse of the concentration C_2 in the region of high salt concentration. t_{-app} is defined by the relation

$$|\Delta\phi_r| = (1-2t_{-app})\ln\gamma \tag{5}$$

The derived transport number value has been called the apparent number i.e. t_{-app} because in this type of measurement water transport has not been taken into

account. This apparent value will be close to the true value, when dilute solutions are used. Substituting for $\Delta\phi$ from equation (2) and expanding the resulting expression for $1/t_{-app}$ in powers of $1/C_2$ gives

$$\frac{1}{t_{-app}} = \frac{1}{(1-\alpha)} + \frac{(1+\beta-2\alpha\beta)}{2(1-\alpha)^2 \ln\gamma}\alpha\left(\frac{\theta}{C_2}\right) + ------ \quad (6)$$

Experimental

Preparation of membrane

Titanium arsenate precipitate was prepared by mixing 0.2M titanium (III) chloride with 0.2M sodium arsenate solution. The precipitate was well washed with deionized water to remove free electrolyte and then dried and powdered. Membrane using suitable ratio of binder was prepared by the method used [11]. The precipitate having ion-exchange property was mixed with polystyrene granules of the size less than 200 meshes and pressed under suitable conditions of temperature and pressure for titanium arsenate 200 °C and 10 MPa. Our effort has been to get the membrane of adequate chemical and mechanically stability. Thus, the membranes prepared by embedding 25% polystyrene were mechanically most stable and gave reproducible results. Those containing larger amount (>25%) of polystyrene did not give reproducible results, while those containing lesser amount (<25%) were unstable. The membranes were subject to microscopic and electrochemical examinations for cracks and homogeneity of the surface and only those which had smooth surface and generated reproducible potentials were considered by carefully controlling the condition of fabrication.

Measurement of membrane potential

Membrane was cemented in Pyrex glass tube cell for measuring membrane potential. The half cell contained 25 ml of electrolyte solutions although the capacity of each of the half cells holding the membrane was about 35 ml. The various salt solutions (chlorides of K^+, Na^+, and Li^+) were prepared from B.D.H (A.R.) grade chemicals using deionized water. Saturated calomel electrodes were connected to a galvanometer (Osaw, spot reflecting galvanometer, Cat. No. 30241). The solutions in both the compartments were vigorously stirred by magnetic stirrers at constant 500 rpm to minimize the effect of boundary layers on potential [12]. The potential difference across the membrane was measured with the help of an Osaw Vernier Potentiometer (Cat. No. 30071), the concentration ratio $\left(\frac{C_2}{C_1}\right)$ was maintained at 10 throughout the experiment. The pressure and temperature were kept constant throughout the experiment. The electrochemical setup used for uni-ionic potential and membrane potential measurements may be represented as

SCE	Solution	Membrane	Solution	SCE
	C_1	Diffusion potential	C_2	

Donnan potential Donnan potential

Measurement of membrane conductance

The electric conductance of the membrane was measured by the method used [13]. The membrane was sealed between two Pyrex glasses half cells. The half cells were first filled with electrolyte solutions of known concentration to equilibrate the membrane, and then the latter was replaced by purified mercury without removing the adhering surface liquid. Platinum electrodes dipping into mercury were used to established electrical contact. The membrane conductance was monitored on a direct reading conductivity meter (Model No L303). The solutions in both the compartments were vigorously stirred by magnetic stirrers at constant 500 rpm to minimize the effect of boundary layers on potential [12]. The whole cells assembly was kept immersed in a water thermostat maintained at the required temperatures (10°C to 50°C).

Characterization of membrane

The pre-requisite for understanding the performance of an ion-exchange membrane is its complete physico-chemical characterization, which involves the determination of all such parameters that affects its electrochemical properties. These parameters are membrane water content, porosity, thickness and swelling etc. and these were determined as described elsewhere [14]

Water content (%total wet weight)

The conditional membrane was first soaked in water to diffusible salt, blotted quickly with Whatmann filter paper to remove surface moisture and immediately

weighted. These were further dried to a constant weight in a vacuum over P_2O_5 for 24 h. The water content (total wet weight) was calculated as:

$$\% \text{ Total wet weight} = \left(\frac{W_w - W_d}{W_w}\right) \times 100$$

where W_w is the weight of the soaked / wet membrane and W_d the weight of the dry membrane.

Porosity

Porosity was determined as the volume of water incorporation in the cavities per unit membrane volume from the water content data:

$$\text{Porosity} = \left(\frac{W_w - W_d}{AL\rho_w}\right)$$

where W_d the weight of the dry membrane, A the area of the membrane, L the thickness of the membrane and ρ_w is the density of water.

Thickness

The thickness of the membrane was measured by taking the average thickness of the membrane by using screw gauze.

Swelling

Swelling is measured as the difference between the average thickness of the membrane equilibrated with 1M NaCl for 24 h and the dry membrane.

Chemical stability

Chemical stability was evaluated on the basis of ASTM D543-95 method. Membrane was exposed to several media commonly utilized. Membrane was

evaluated after 24, 48 and 168 h, analyzing alteration in color, texture, brightness, decomposition, splits, holes, bubbles, curving and stickiness [15].

SEM investigation of membrane morphology

Scanning Electron Microscope image was used to confirm the microstructure of fabricated porous membrane. The membrane morphology was investigated by Leo 4352 at an accelerating voltage of 20 kV. Sample was mounted on a copper stub and sputter coated with gold to minimize the charging.

Results and discussion

The values of observed membrane potential for the titanium arsenate membrane in contact with various 1:1 electrolyte solutions at 25 ± 1°C are given in table1. The values for the membrane potential are of the order of positive mV and decrease with an increase of external electrolytes concentration. This shows that the membrane is negatively charged (cation selective) and the selectivity increases with dilution due to structural changes produced in the electrical double layer at the solution membrane interface. The selectivity character of ion-exchange membrane with (1:1), (2:1) and (3:1) electrolytes has been reported [16,17]. In the case of (2:1) and (3:1) electrolytes, $\Delta\phi$ changes reverse sign (+ve to –ve). This indicates that the membrane has become anion selective. The change in the selectivity character of the membrane is evidently due to the adsorption of multivalent ions leading to a state where net positive charge left on the membrane surface making anion selective .Inorganic precipitate membrane was found to have the ability to generate potentials [18,19], when interposed between electrolyte

Table 1 Observed membranes potentials $\Delta\phi$ in mV across the Titanium arsenate membrane in contact with various 1:1 electrolytes at different concentrations at 25±1° C

Electrolyte Concentration (mol/l)	Titanium Arsenate		
	KCl	NaCl	LiCl
$10\times10^{-1}/1\times10^{-1}$	14.2	10.5	9.3
$1\times10^{-1}/1\times10^{-2}$	19.2	13.2	12.3
$7\times10^{-2}/7\times10^{-3}$	27.6	20.5	18.5
$5\times10^{-2}/5\times10^{-3}$	32.5	25.6	23.4
$2\times10^{-2}/2\times10^{-3}$	36.2	30.2	28.2
$1\times10^{-2}/1\times10^{-3}$	39.2	34.5	33.5

solutions of different concentrations due to the presence of a net charge on the membrane. Such charges play an important role in the sorption and transport of simple electrolytes in artificial as well as natural membranes [20], and impart some important electrochemical properties to the membrane, the most important being the differences in the permeabilities of co-ions, counter ions and neutral molecules. The quantity of charge required to generate the potentials, especially when dilute solution are used, is small. This of course, is dependent on the porosity of the membrane. In case the membrane pores are wide, any amount of charge on the membrane does little to generate good potentials. On the other hand, if the pores are narrow, a little amount of charge can give rise to good potential values. Hence, a detailed investigation of the mechanism of transport of simple electrolytes through a charged membrane seems to be incomplete without the evaluation of the thermodynamically effective fixed charge density of the membrane. The former can be evaluated by making uses of an equation derived on the basis of thermodynamics of irreversible processes. This approach employs a phenomenological coefficient to correlate the gradients that exits across a membrane and their resulting fluxes.

The membrane potential data obtained with titanium arsenate membrane using various 1:1 electrolytes are plotted as a function of $-\log C_2$ with the ratio γ fixed at 10. This plot is shown in figure1.

The results of thickness, swelling, porosity and water content capacity of titanium arsenate membrane are summarized in table 2. The water content of a

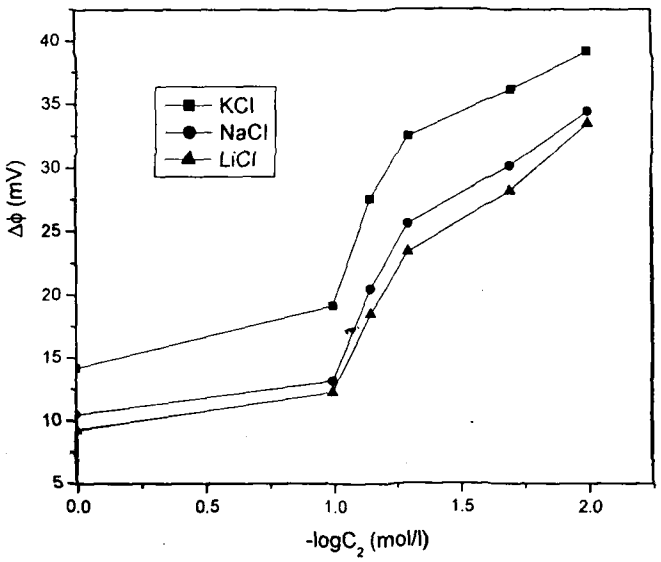

Figure 1 *Plots of membrane potentials against* $-\log C_2$ *for titanium arsenate* membrane using various 1:1 electrolytes

Table 2 Characterization of Titanium arsenate membrane

Thickness of the membrane (cm)	0.075
Water Content as % weight of wet membrane	0.074
Porosity	0.113
Swelling of %weight wet membrane	No Swelling

membrane depends on the water vapor pressure of the surroundings. Knowledge of the pore size distribution and the water structure in a membrane might contribute to classify a special membrane resembling a solution-diffusion, a fine-porous, or a coarse-porous membrane. In general membrane having the same chemical composition absorb same amount of water, where density ionizable groups are same throughout the membrane [21]. In case of most of the transport measurements, only the membrane water content at saturation is needed, and that mostly as a function of solute concentration. Thus, low order of water content, swelling and porosity with less thickness of this membrane suggests that interstices are negligible and diffusion across the membrane would occur mainly through exchange sites. Membrane was tested for chemical resistance in acidic, alkaline and strongly oxidant media. In acidic (1M H_2SO_4) and in alkaline media (1M NaOH) few significant modifications were observed after 24, 48 and 168 h, demonstrating that the membrane is effective in such media. However, in strong oxidant media the synthesized membrane became fragile in 48 h and membrane was broken after 168 h, losing mechanical resistance.

The characterization of membrane morphology has been studied by a number of investigators using scanning electron microscopy [22,23]. The composite pore structure, micro/ macro porosity, homogeneity, thickness, cracks and surface texture/morphology have been studied [24,25]. The cross-section of SEM micrograph of the surface is shown in figure 2. Membrane cross-section thickness was estimated to be around 30μm as observed in figure 2. Membrane had random

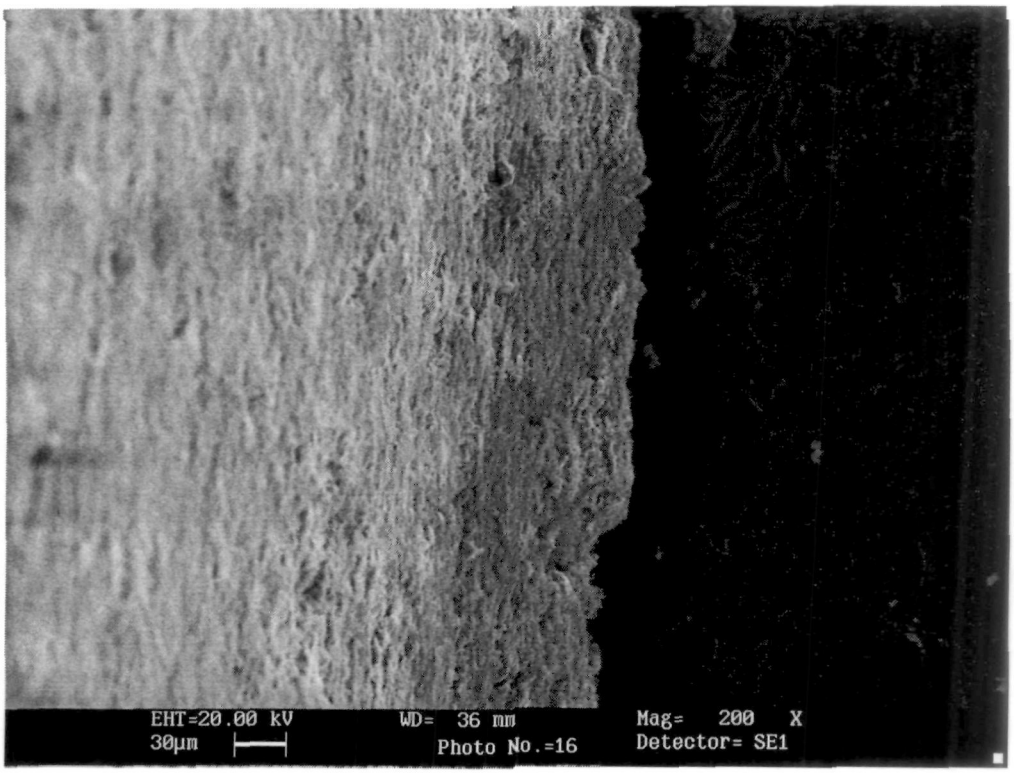

Figure 2 Cross-section SEM image of Polystyrene-based (25%) Titanium arsenate membrane

non-preferential orientation with no visible cracks and appeared to be composed of dense and loose aggregation of small particles. The membrane is macroscopically uniform in thickness and is porous in nature. The pores are modeled as uniform capillaries that extend throughout the membrane. These pores are evenly distributed throughout the surface of the membrane. Entrance and exit effects are ignored since the membrane thickness is large compared to the pore radius. However, the thickness is still large compared to the pore radius and it is assumed that the membrane and adjacent solution (interfaces) are in equilibrium. The distributions of charge density and mobile species within the pores are assumed to be uniform [26].

The set of curves in figure 3 are the theoretical membrane potentials for a cation selective membrane, which is calculated from equation (1). The difference curves are for different mobility ratios $\left(\frac{\bar{u}}{\bar{v}}\right)$, with a constant value of $\bar{D}$ is unity expressed in equivalent/litre. The experimental $\Delta\phi$ values for titanium arsenate membrane with KCI electrolyte were plotted in the same graph as a function of $-\log C_2$. The experimental curve was shifted horizontally and ran parallel to one of the theoretical curves. This shift gave $\log \bar{D}$, and the parallel theoretical curve gave the value for mobility ratio $\left(\frac{\bar{u}}{\bar{v}}\right)$ with the membrane phase. The values of $\bar{D}$ and $\left(\frac{\bar{u}}{\bar{v}}\right)$ derived in this way for the membrane and various 1:1 electrolytes are

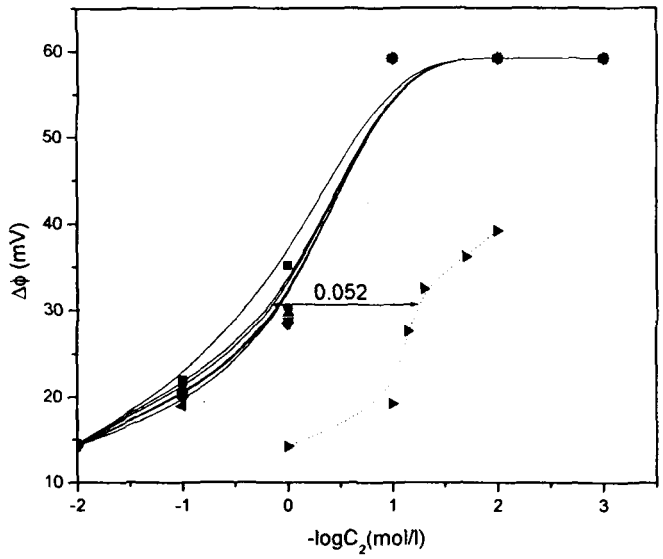

Figure 3 Plots of membrane potentials vs. $-\log C_2$ for titanium arsenate membrane. Smooth curves are the theoretical concentration potentials for different mobility ratio. Broken line is the experimental values of membrane potential for different concentration of KCl solution

given in table 3. Thus, the order of fixed charge density for electrolytes used was found to be KCl > NaCl > LiCl.

Equation (3) indicates that a value of β and a relation between α and θ can be obtained by evaluation of the intercept and the initial slope of a plot of $|\Delta\phi_r|$ against C_2 which is shown in figure 4. The value of intercept is equal to $1/\beta \ln\gamma$ from which β is evaluated. Values are given in table 4.

Equation (6) indicate that the intercept of a plot of $1/t_{-app}$ against $1/C_2$ at fixed γ allows the value of α to be determined. Plots of $1/t_{-app}$ against $1/C_2$ for various uni-univalent electrolytes are shown in figure 5.The value of intercept is equal to $1/(1-\alpha)$, from which α may be evaluated. Values are given in table 4. If this value of α is inserted in the relation obtained from the initial slope for $|\Delta\phi_r|$ against C_2, the desired value for θ_c can be determined. Once α and β are known in the manner described above, the values of θ_d may be evaluated from the initial slope for $1/t_{-app}$ against $1/C_2$.

Kobatake has suggested that provided his equation for the membrane potential is correct, then the two values of θ i.e. θ_c and θ_d thus determined from the opposite limits should agree with one another. The values are given in table 3 which are closed together thereby confirming the applicability of Kobatake's equation to these systems.

Table 3 Values of the thermodynamically charge density of Titanium arsenate membrane - electrolyte systems evaluated by various theories

Electrolyte Concentration (mol/l)	TMS		Kobatake	
	$\left(\frac{\bar{u}}{\bar{v}}\right)$	$\bar{D}$ (eq/l)	θ_c	θ_d
KCl	1.63	0.052	0.049	0.059
NaCl	1.44	0.045	0.039	0.048
LiCl	1.38	0.040	0.038	0.043

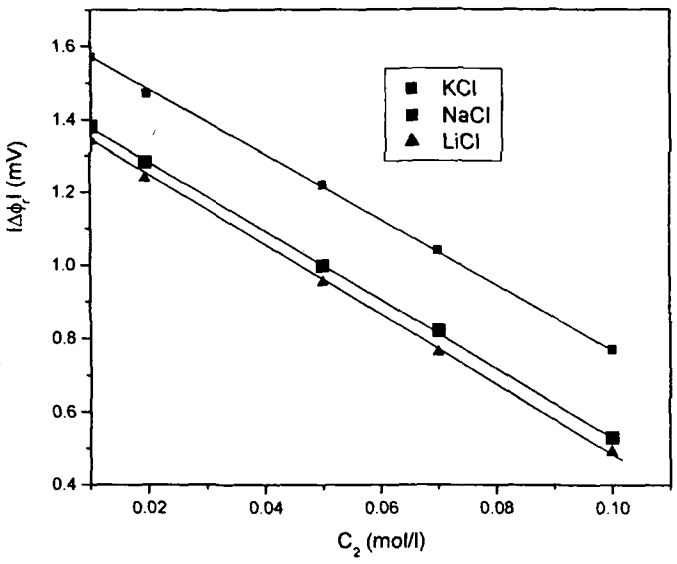

Figure 4 Plots of $|\Delta\phi_r|$ against C_2 for Titanium arsenate membrane using various 1:1 electrolytes

Table 4 Values of parameters α and β for Titanium arsenate membrane-electrolyte system

Electrolyte	Titanium Arsenate	
	α	β
KCl	0.62	1.47
NaCl	0.60	1.67
LiCl	0.58	1.72

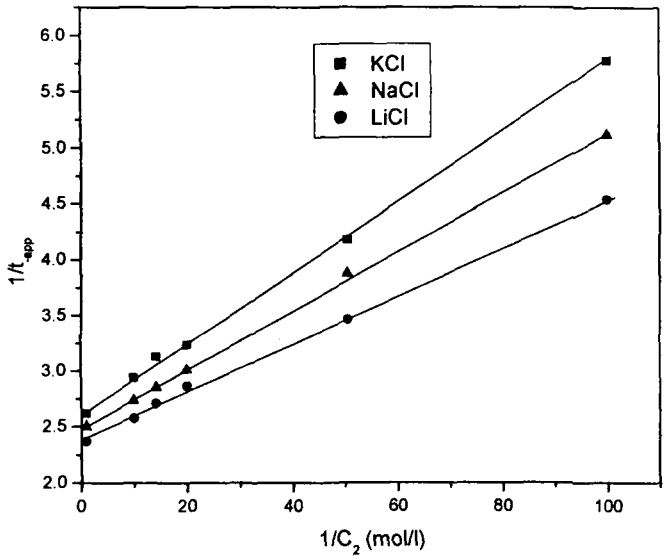

Figure 5 Plots of $1/t_{-app}$ against $1/C_2$ for Titanium arsenate membrane using various 1:1 electrolytes

We have seen that the charge density is higher in the region of low concentrations (θ_d) than in high concentrations (θ_c) because the ionic atmosphere around fixed charges in the formal case is large compared with than in the later case. On the other hand, the charge density in the case of KCl is higher than in NaCl case due to the size factor (the smaller size, the larger ionic atmosphere).

The advantage of the determination of the potential between two solutions of different concentrations is that the tests are not obscured by concentration polarization effect at the membrane surface. When an ionic gradient is maintained using two solutions of different concentrations of same electrolyte on either side of the membrane, diffusion of electrolytes from the region of higher to lower concentration and flow of water in the opposite direction take place. In fact, the mobile species penetrate the membrane at different magnitude and various transport phenomena, including the development of potential across it, are induced into the system. The nature of fixed charge in the membrane matrix greatly influences the counter ion than co-ion as well as the transport phenomena.

The TMS equation (1) can also be expressed by the sum of Donnan potential $\Delta\phi_{Don}$ between membrane surfaces and external solutions and the diffusion potential $\Delta\phi_{diff}$ within the membrane [27,28].

$$\Delta\phi_m = \Delta\phi_{Don} + \Delta\phi_{diff} \tag{7}$$

$$= -\frac{RT}{V_k F}\ln\left(\frac{\gamma''_{\pm}C_2\overline{C}_{1+}}{\gamma'_{\pm}C_1\overline{C}_{2+}}\right) - \frac{RT}{V_k F}\frac{\overline{\omega}-1}{\overline{\omega}+1}\times\ln\left(\frac{(\overline{\omega}+1)\overline{C}_{2+}+(V_x/V_k)\overline{D}}{(\overline{\omega}+1)\overline{C}_{1+}+(V_x/V_k)\overline{D}}\right) \tag{8}$$

The R, T and F have their usual significance; $\gamma'_{\pm}$ and $\gamma''_{\pm}$ are the mean ionic activity coefficients; $\overline{\omega} = \frac{\overline{u}}{\overline{v}}$ is the mobility ratio of the cation to the anion in the membrane phase and $\overline{C}_{1+}$ and $\overline{C}_{2+}$ are the cation concentrations in the membrane phase first and second, respectively. The cation concentration is given by the equation

$$\overline{C}_{+} = \sqrt{\left(\frac{V_x \overline{D}}{2V_k}\right)^2 + \left(\frac{\gamma_{\pm} C}{q}\right)^2} - \frac{V_x \overline{D}}{2V_k} \tag{9}$$

Here V_k and V_x refer to the valency of cation and fixed-charge group on the membrane matrix, q is the charge effectiveness of the membrane and is defined by the equation

$$q = \sqrt{\frac{\gamma_{\pm}}{K_{\pm}}} \tag{10}$$

where $K_{\pm}$ is the distribution coefficient. It is expressed as

$$K_{\pm} = \frac{\overline{C}_i}{C_i}, \qquad \overline{C}_i = C_i - \overline{D} \tag{11}$$

where $\overline{C}_i$ is the ith ion concentration in the membrane phase and C_i is the ith ion concentration of the external solution. The transport properties of the membrane in various electrolyte solutions are important parameters to further investigate the membrane phenomena as shown in equation (12).

$$\Delta\phi = \frac{RT}{F}(t_+ - t_-)\ln\frac{C_2}{C_1} \tag{12}$$

$$\frac{t_+}{t_-} = \frac{\bar{u}}{\bar{v}} \tag{13}$$

Equation (13) was first used to calculate the values of transport numbers t_+, mobility ratio $\bar{\omega} = \frac{\bar{u}}{\bar{v}}$ and finally $\bar{U}$ as given in table 5. The values of mobility $\bar{\omega}$ of the electrolytes in the membrane phase were found to be high at lower concentration of all the electrolytes (KCl, NaCl and LiCl). Further increase in concentration of the electrolytes led to a sharp drop in the values of $\bar{\omega}$ as given in table 5. The high mobility is attributed to higher transport number of comparatively free cations of electrolytes and also be similar trend as the mobility in least concentrated solution. The values of the parameters $K_{\pm}$, q and $\bar{C}_+$ derived for the system have also been included in table 5. The values of $\gamma_{\pm}$ were the usual charted values for electrolytes. Using equation (11) it was found that the values of distribution coefficients increased at lower concentration of electrolytes. As the concentration of electrolytes increased, the values of distribution coefficients sharply dropped and, thereafter, a stable trend was observed as shown in table 5. The large deviation in the value of $K_{\pm}$ at the lower concentration of electrolytes was attributed to the high mobility of comparatively free charges of the strong electrolyte and thus, reached into the membrane phase easily compared to higher concentrated electrolytes solution.

The charge effectiveness q, values for LiCl are the smallest of the electrolytes used in this study and order is KCl > NaCl > LiCl. The charge

Table 5 The calculated values of the parameters $t_+, \overline{U}, \overline{\omega}, K_\pm$, q, and $\overline{C}_+$ of Titanium arsenate membrane with different concentration of electrolytes using eq. (12) and eq. (9) - (11)

C_2 (mol/l)	t_+	$\overline{U}$	$\overline{\omega}$	$K_\pm$	q	$\overline{C}_+$
KCl (Electrolyte)						
0.01	0.83	0.66	4.88	4.20	0.55	0.0023
0.02	0.80	0.60	4.00	1.60	0.74	0.0035
0.05	0.77	0.54	3.35	0.04	4.59	0.0053
0.07	0.73	0.46	2.70	0.26	1.77	0.0062
0.10	0.66	0.32	1.94	0.48	1.27	0.0306
1.00	0.62	0.24	1.63	0.97	0.81	0.7055
NaCl						
0.01	0.79	0.58	3.76	3.50	0.51	0.0023
0.02	0.75	0.50	2.00	1.25	0.84	0.0032
0.05	0.71	0.42	2.49	0.01	2.90	0.0052
0.07	0.67	0.34	2.03	0.36	1.50	0.0057
0.10	0.61	0.22	1.56	0.55	1.18	0.0262
1.00	0.59	0.18	1.44	0.96	0.80	0.6967
LiCl						
0.01	0.78	0.56	3.55	3.00	0.46	0.0022
0.02	0.74	0.48	2.85	1.00	0.94	0.0028
0.05	0.70	0.40	2.33	0.20	2.90	0.0050
0.07	0.65	0.30	1.86	0.43	1.37	0.0056
0.10	0.60	0.20	1.50	0.60	1.13	0.0208
1.00	0.58	0.16	1.38	0.95	0.79	0.6842

effectiveness depends upon the hydration of the solute–solute interaction and ionic radii of the counter-ions. Structural hydration interaction model (SHI) based on the effect to account for many thermodynamic properties of small solutes in water. The counter-ions Cl^-, is the same for all the electrolyte used therefore, the variation of charge effectiveness values are possibly due to increase in adsorption of co-ions on charged membrane [29,30].

When a permselective membrane happens to be in between the solutions of electrolytes of different concentrations, a steady electromotive force (e.m.f) develops due to difference in the relative permeabilities of various ionic species. This e.m.f, usually called the membrane potential, depends on the properties of the membrane and has been the subject of many theoretical and experimental studies. TMS theory and its modifications are inadequate to explain experimental results on non-ideal permselective membrane.

The perm selectivity [18] is a measure of the characteristic difference in the membrane of counter ions and co-ions, which be expressed as

$$P_s = \left(\frac{\bar{t}_+ - t_+}{1 - t_+} \right) \tag{14}$$

where $\bar{t}_+$ is the counter-ion transport number through the membrane and t_+, is the counter ion transport number in the solution phase. Thus, the permselectivity arises due to the nature of the membrane for differentiating between co-ions and counter ions and is not a membrane constant. An ideal permselectivity cation – exchange membrane would transmit positively charge ions only. Permselectivity

can be calculated from the equation (14). It can be seen from figure 6 that permselectivity decreased with the increase in the concentration of the salt solution. This is inconformity with the expectation based on increased deswelling of the ion exchange membrane resulting in progressively lowered co-ion exclusion with increase in concentration.

An ion exchange membrane undergoes swelling because of the osmotic intake of the solvent by the membrane network. This osmotic action depends on the solute concentration; it decrease with the increase in concentration [31] and as a result solvent uptake by the membrane matrix decreases leading to the deswelling of the membrane. Due to this increased membrane openness this is accompanied by lowered exclusion of co-ions and Permselectivity of the membrane therefore decreases. Thus, even when electrolyte concentration remains unchanged; a reduction in membrane permselectivity is expected with the increase in the concentration of the solution.

Increase in concentration results in decreases in the magnitude of the counter ion transport number as expected because of deswelling of the membrane.

The values of observed membrane conductance for the titanium arsenate membrane in contact with various 1:1 electrolyte solutions at different temperature (10°C to 50°C) are given in table 6. The values for the membrane specific conductance are of the order of positive $m\Omega^{-1}cm^{-1}$. The overall behavior of specific conductance of 1:1 electrolytes as a function of concentration and temperature is displayed by taking one of the representative plots shown in figure

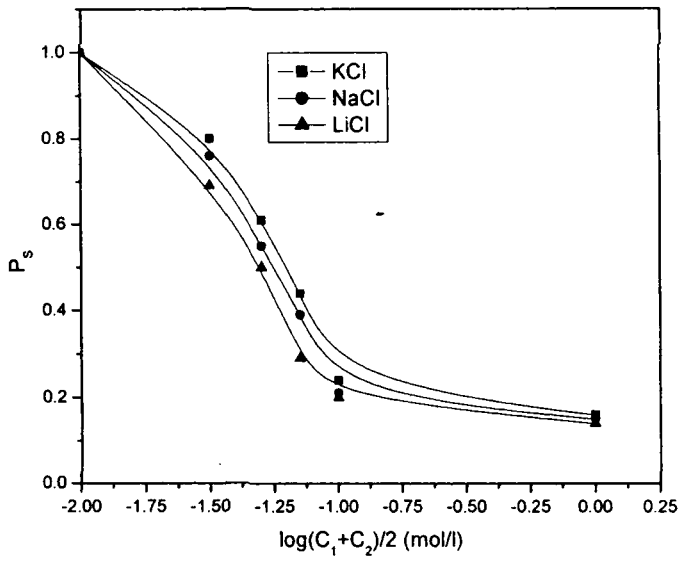

Figure 6 Plots of P_S against log $(C_1+C_2)/2$ for Titanium arsenate membrane using various 1:1 electrolytes

Table 6 Experimentally observed values of membrane conductance ($m\Omega^{-1}cm^{-1}$) for various 1:1 electrolytes at different temperature (10 to 50) ± 0.1°C

Temperature (°C)	**Concentration** (mol/l)				
	0.1	0.07	0.05	0.02	0.01
KCl					
10	8.25	4.0	3.48	2.05	1.40
20	9.15	5.20	3.60	2.10	1.50
30	9.95	5.70	4.50	2.15	1.55
40	10.40	6.30	4.90	2.25	1.60
50	10.90	7.10	5.50	2.70	1.70
NaCl					
10	7.60	3.85	3.20	1.65	1.35
20	8.05	4.30	3.45	1.72	1.42
30	8.50	4.75	4.35	2.00	1.45
40	9.20	5.25	4.65	2.20	1.50
50	9.85	6.20	5.20	2.65	1.65
LiCl					
10	6.70	2.95	3.15	1.60	1.30
20	7.10	3.15	3.40	1.65	1.35
30	7.50	3.60	3.95	1.95	1.40
40	7.85	4.00	4.35	2.10	1.45
50	8.20	4.40	4.75	2.50	1.50

7 for the KCl solutions. The remaining 2 plots (not shown here) based on the data contained in the table have also exhibited a similar behavior. The conductance values have been found to increase with increase in concentration as well as temperature (10°C to 50°C) in all the cases. These results are in accord with those found for the pericardial membrane in respect of their conductance behavior with varying electrolytic concentrations. An examination of these plots shows that their slope values decrease at relatively higher concentrations compared to those of extremely dilute solutions. Also, such slopes keep on increasing with increase in temperature as one may envisage.

Table 6 shows that the specific conductance not only increases with an increase in the electrolyte concentration but also attains a maximum limiting value at higher concentrations. Such a trend has been observed in all the above electrolytic solutions. This may be attributed to a progressive accumulation of ionic species within the membrane. The tendency to attain a limiting value seems to be due to the fact that an electrically neutral pore, which is specific for a particular ion, is unlikely to contain more than one type of ion. Consequently, at high electrolyte concentration, the pore saturates and the conductance approaches a limiting value. The values of specific conductance of the electrolytes follow the sequence for the cations:

$$K^+ > Na^+ > Li^+$$

In addition, the diffusion of ions depends upon the charge on the membrane and its porosity. The membrane porosity in relation to the size of the hydrated species

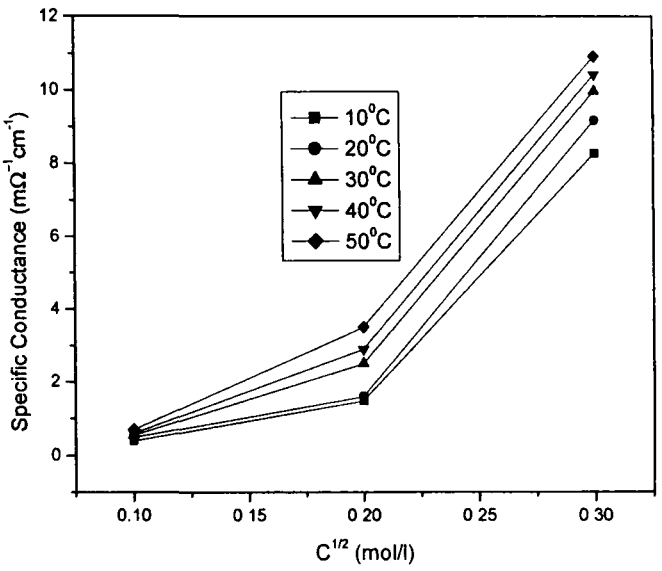

Figure 7 *Plots of specific conductance* ($m\Omega^{-1}cm^{-1}$) *Vs square root of concentration* for electrolytes at different temperature through Titanium arsenate membrane

diffusing through the membrane appears to determine the above sequence. Several probable structures of water molecules under the condition of a given temperature may play an important role in determining the size of the hydrated ions [32]. As the diffusion paths in the membrane become more difficult in aqueous solutions, the mobility of large hydrated ions gets impeded by the membrane framework and the interaction with the fixed charge groups on the membrane matrix. Consequently, the membrane pores reduce the conductance of small ions, which is much hydrated. This is in accord with the earlier reported significance of the factors like pore size, hydration, etc. [33-35].

In figure 8, specific conductance increases with increase in temperature T, due to the state of hydration which implies that the activation energy decreases.

Table 7 shows that the activation energy decreases with increase in concentration of the bathing electrolyte solution and the sequence for energy of activation is

$$E_a K^+ > E_a Na^+ > E_a Li^+$$

Table 8 shows that an increase of activation energy with an increase of crystallographic radius confirms the applicability of Kumins [36] arguments for polystyrene based inorganic precipitate membrane systems

The rate theory describes any process from diffusion to chemical reaction in terms of elementary jumps over energy barriers. The permeant encounters energy maxima (barriers) and minima (wells) in its journey from one side of the membrane of the other side. The energy maxima represent the energies of

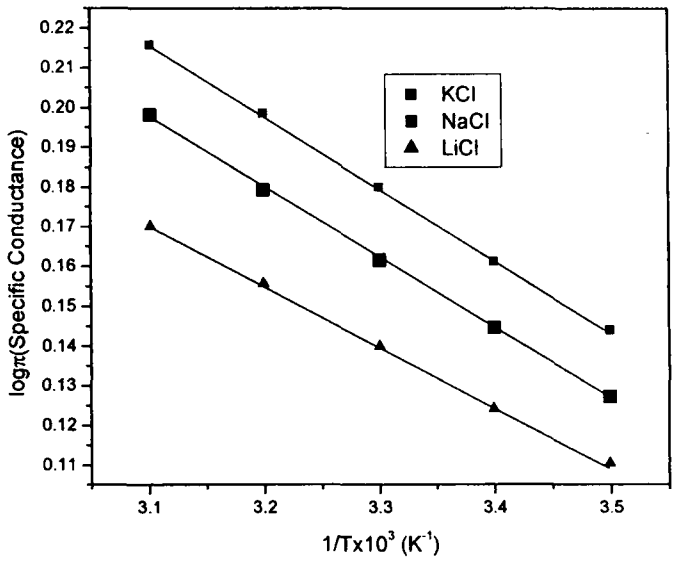

Figure 8 Arrhenius plots of specific conductance Vs 1/T 10^3 for 1:1 electrolytes through Titanium arsenate membrane

Table 7 Calculated values of Activation Parameters for 1:1 electrolytes through Titanium arsenate membrane

Electrolytes	Conc. (mol/l)	E_a (KJ/mole)	ΔH^* (KJ/mole)	ΔG^* (KJ/mole)	$-\Delta S^*$ ($JK^{-1}mole^{-1}$)
KCl	0.1	4.77	2.32	64.93	213.68
	0.01	8.64	6.19	73.23	228.81
NaCl	0.1	3.44	0.98	63.87	214.64
	0.01	7.68	5.22	72.38	230.78
LiCl	0.1	2.68	0.23	63.51	215.98
	0.01	7.30	4.85	72.33	231.20

Table 8 Relation between Crystallographic radius and activation energy of alkali chlorides

Ion	Crystallographic radii (Å)	Energy of activation (KJ/mole)
K^+	1.33	4.77
Na^+	0.93	3.44
Li^+	0.60	2.68

transition states and diffusion past these unfavorable locations can be represented by single jumps over the corresponding barriers. The progress over each barrier is proportional to the number of ions attaining the energy needed to surmount the barrier. The rate constant K for crossing a barrier is related to standard Gibbs free energy of activation, ΔG^*, as

$$K = A \exp(-\Delta G^*/RT) \quad (15)$$

where A represents the frequency of attempted hops. The ΔG^* is related to ΔH^* and ΔS^* as

$$\Delta G^* = \Delta H^* - T\Delta S^* \quad (16)$$

ΔH^* and ΔS^* can be evaluated with the help of experimentally observed values of specific conductance,Λ by making use of the following relationship:

$$\Lambda = \left(\frac{RT}{Nh}\right) e^{-\left(\frac{\Delta H^*}{RT}\right)} e^{\left(\frac{\Delta S^*}{R}\right)} \quad (17)$$

The obtained values of ΔH^* can be used to evaluate the Arrhenius activation energy, E_a, on the basis of the equation

$$E_a = \Delta H^* + RT \quad (18)$$

A plot of $\log\frac{\Lambda Nh}{RT}$ versus $\frac{1}{T}$ from experimental data, shown in figure 9, RT gives the value of ΔH^* /R and ΔS^*/R. ΔG^* and E_a were obtained by using equations (16) and (18). The values of various kinetic activation parameters E_a, ΔH^*, ΔG^* and ΔS^*derived for the diffusion of various electrolytes in membrane are given in table 7.

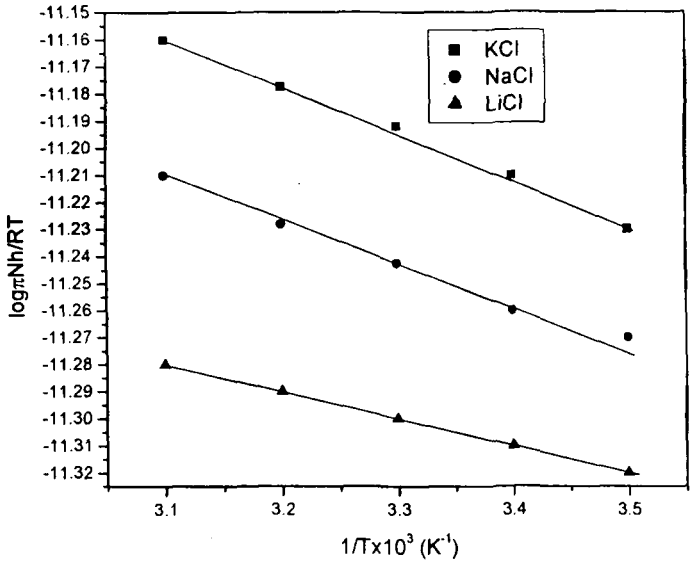

Figure 9 Plots of $\log\frac{\pi Nh}{RT}$ Vs 1/T 10^3 for 1:1 electrolytes through Titanium arsenate membrane

Table 7 shows that a larger ion has more difficulty in crossing the membrane than a smaller one. This type of variation can be explained the heights of the energy barriers (i.e., the differences between outer wells and peaks). It has been found that the larger ion encounters a bigger entrance barrier lying very close to the surface of the membrane. The entrance barrier for the smaller ion is not only of lesser height [37]. The location of the outermost well has been assumed to be same for all the ions, while that of the inner well found to be much further in for smaller ions than the larger ones. In the light of these findings, it can be argued that the magnitudes of E_a, ΔH^* and ΔG^* must be higher for larger ions than the smaller ones.

ΔS^* indicates the mechanism of flow, and has been interpreted in a number of ways [38,39]. Negative ΔS^* values are considered to indicate either formation of a covalent bond between the permeating species and the membrane material or that the permeation through the membrane may not be the rate determining step. The data in table 7 also shows that the values of ΔH^* are correlated to the values of ΔS^*, as ΔH^* values increases; ΔS^* values increases. This phenomenon is known as "enthalpy–entropy compensation".

Conclusions

The polystyrene based titanium arsenate membrane was prepared after preliminary investigations and it was found that membrane was quite stable and did not show any dispersion in water and other electrolyte solutions. The surface charge model work as a tool to improve the performance of the membrane filtration process and

selectivity of ion exchange. The hydrated size of Li^+ ion is large compared with K^+ ion; therefore, the passage of the formal ion was relatively hard especially at high concentrations. Membrane with higher fixed charged density offered high membrane potential for a given electrolyte solution. The distribution coefficient values were found to be diminished with the increasing electrolyte concentration and their order found to be, LiCl > NaCl > KCl. Table 3 shows that the values of the charge densities evaluated from the various procedures are not much different from each other and a slight difference in the values may be ascribed to the different graphical procedures adopted for the evaluation. The experimental values were found to be quite close to the theoretical values. Therefore, the extended-TMS equation may be utilized for obtaining the membrane potential and derived parameters for the membrane under investigation. From the data in table 7, it can be inferred that the larger ions face more difficulties in crossing the membrane than the smaller ones. Thus, it can be explained that the magnitudes of E_a, $\Delta H^*$and ΔG^* must be higher for larger ions than the smaller ones. On the one hand, a high ΔS^* value associated with the high value of E_a for diffusion may suggest the existence of either a large zone of activation or loosening of more chain segments of the membrane. On the other hand, low value of ΔS^* implies either a small zone of activation or no loosening of the membrane structure upon permeation [40].

References

[1] C.B. Amphlett, Inorganic Ion Exchangers, Elsevier, Amsterdam, 1964.

[2] A. Clearfied, *Solv. Extrn. Ion Exch.* **18** (2000) 655.

[3] A.A. Khan, M.M. Alam, *React. Funct. Polym.* **55** (2003) 277.

[4] K.G. Varshney, N. Tayal, A.A. Khan, R. Niwas, *Colloid Surf. A: Physicochem. Eng. Asp.* **181** (2001) 123.

[5] A.P. Gupta, H. Agarwal, S. Ikram, *J. Indian Chem. Soc.* **80** (2003) 57.

[6] S.A. Nabi, M. Naushad, Inamuddin, *J. Hazard. Mater.* **142** (2007) 404.

[7] R.K. Nagarale, G.S. Gohil, V.K. Shahi, R. Rangarajan, *J. Colloid Interface Sci.* **287** (2005) 198.

[8] R.K. Nagarale, G.S. Gohil, V.K. Shahi, G.S. Trivedi, R. Rangarajan, *J. Colloid Interface Sci.* **277** (2004) 162.

[9] A. Nakajima, T. Miyasaka, K. Sakai, T. Tsukahara, *J. Membr. Sci.* **187** (2001) 129.

[10] Y. Kobatake, T. Noriaki, Y. Toyoshima, H. Fujita, *J. Phys. Chem.* **69** (1965) 3981.

[11] F. Jabeen, Rafiuddin, *J. Sol. Gel Sci. Technol.* **44** (2007) 195.

[12] A. Canas, M.J. Ariza, J. Benavente, *J. Colloid Interface Sci.* **246** (2002) 150.

[13] N. Lakshminarayanaiah, Transport Phenomena in Membrane, Academic Press, New York, 1969.

[14] A.A. Khan, A. Khan, Inamuddin, *Talanta* **72** (2007) 699.

[15] ASTM D543-95, Standard particles for evaluating the resistance of plastics to chemical reagents, 1998.

[16] K. Singh, A.K. Tiwari, J.P. Rai, *Ind. J. Chem.* **24** (1985) 825.

[17] K. Singh, A.K. Tiwari, *Poc. Indian Natn. Sci. Acad.* **70 (A)** (2004) 477.

[18] V.K. Shahi, G.S. Trivedi, S.K. Thampy, R. Ranrarajan, *J. Colloid Interface Sci.* **262** (2003) 566.

[19] J.H. Chai, S.H. Moon, *J. Membr. Sci.* **191** (2001) 225

[20] J. Schaep, C. Vandecasteele, *J. Membr. Sci.* **188** (2001) 129.

[21] S. Koter, P. Piotrowski, J. Kerrs, *J. Membr. Sci.* **153** (1999) 83.

[22] J. Liu, T. Xu, M. Gong, F. Yu, Y. Fu, *J. Membr. Sci.* **283** (2006) 190.

[23] V.S. Silva, B. Ruffmann, S. Vetter, A. Mendes, L.M. Madeira, S.P. Nunes, *Catalysis Today* **104** (2005) 205.

[24] J.O. Titiloye, I. Hussain, *J. Colloid Interface Sci.* **318** (2008) 50.

[25] M. Resina, J. Macanás, J.D. Gyves, M. Muňoz, *J. Membr. Sci.* **289** (2007) 150.

[26] J.G. Aleman, J.M. Dicker, *J. Membr. Sci.* **235** (2004) 1.

[27] H. Matsumoto, A. Tanioka, T.J. Murata, M. Higa, K. Horiuchi, *J. Phys. Chem. B* **102** (1998) 5011.

[28] T.J. Chou, A. Tanioka, *J. Colloid Interface Sci.* **212** (1999) 293.

[29] W. Bowen, A. Mohammad, N. Hilal, *J. Membr. Sci.* **126** (1997) 91.

[30] X. Wang, T. Suru, M. Togoh, S. Nakao, S. Kimura, *J. Chem. Eng. Jpn.* **28** (1995) 186.

[31] R.E. Kesting, Synthetic Polymeric Membrane, McGraw Hill Book Company, New Delhi, 1971.

[32] S. Islam, B.N. Waris, *Thermochim Acta* **424** (2004) 165.

[33] T. Teorell, *Prog. Biophys. Biophys. Chem.* **3** (1953) 305.

[34] D.E. Danielli, H. Davson, *J. Cell. Comp. Physiol.* **5** (1935) 495.

[35] D.E. Goldmann, *Biophys. J.* **4** (1964) 167.

[36] C.A. Kumins, T.K. Kwei, J. Crank, G.S. Park, Diffusion in Polymers, Academic Press, New York, 1968.

[37] G. Eisenman, R. Horn, *J. Membr. Biol.* **76** (1983) 197.

[38] M.N. Beg, K. Ahmad, I. Altaf, M. Arshad, *J. Membr. Sci.* **9** (1981) 303.

[39] F.A. Siddiqi, N.I. Alvi, *J. Membr. Sci.* **46** (1989) 185.

[40] K.E. Schuler, C.A. Dames, K.J. Laidler, *J. Chem. Phys.* **17** (1949) 760

CHAPTER 4

Transport Studies of Cobalt Arsenate Membrane

Introduction

There has been substantial research on the inorganic ion exchangers as well as organic resins commonly known as ion exchange media for the remediation of wastewater containing heavy metal ions as a by product of various industries. However, the practical use of organic and inorganic ion-exchange media are still limited by two major obstacles, one of the important limitations of organic resin is its poor thermal and radiation stability than inorganic ion-exchangers and other is the non-reproducible character, less stability in high acidic and basic medium and high cost of inorganic ion-exchangers. Further more inorganic ion-exchangers cannot be used in convenient way in case when the impurities from a large volume of effluent are to be removed In this connection, research has motivated to the investigators to study of organic–inorganic hybrid ion-exchangers with better mechanical, chemical, thermal and radiation stabilities, reproducibility and possessing good selectivity for heavy toxic metals [1–3], indicating its useful environmental applications [4,5]. Membrane potential and conduction has been found to depend on a variety of factors such as: fixed charge concentration on the membrane matrix, water content, porosity, electrolyte uptake of the membrane, temperature, concentration, and composition of the external electrolyte solution [6,7]. Ion permeation in membranes is usually characterized by such measurable parameters as conductance, current-voltage relationship, ionic fluxes, impedance and membrane potentials. These parameters have been quite helpful in explaining the mechanism of ion transport in various membrane systems [8,9].

In this paper, the membrane potential measurements across cobalt arsenate membrane are described. The membrane potential data have been used to examine the validity of TMS [10,11] and Kobatake [12] theory based on the thermodynamics of irreversible processes.

The theory of absolute reaction rates [13] has been utilized for the evaluation of energy of activation, E_a, free energy of activation, ΔG^*, enthalpy of activation, ΔH^*, entropy of activation, ΔS^*, by making use of conductance data observed for the membrane in contact with various univalent electrolytes.

Theory

Fixed charge theory of Teorell-Meyer-Sievers

In the TMS theory there is an equilibrium process at each solution membrane interface which has a formal analogy with the Donnan equilibrium. The assumptions made are (a) the cation and anion mobilities and fixed charge concentration are constant throughout the membrane phase and are independent of the salt concentration and (b) the transference of water may be neglected. The implications of these assumptions have been discussed [14]. Further assumption must be made that the activity coefficient of the salt is the same in the membrane and solution phase at each interface. The introduction of activities for concentrations can only be correctly made for the Donnan potential using either the integration of Planck or Henderson.

According to TMS theory, the membrane potential $\Delta\phi$ (applicable to a highly idealized system) is given by the equation at 25° C

$$\Delta\phi = 59.2\left(\log\frac{C_2}{C_1}\frac{\sqrt{4C_1^2 + \overline{D}^2} + \overline{D}}{\sqrt{4C_2^2 + \overline{D}^2} + \overline{D}} + \overline{U}\log\frac{\sqrt{4C_2^2 + \overline{D}^2} + \overline{D}\,\overline{U}}{\sqrt{4C_1^2 + \overline{D}^2} + \overline{D}\,\overline{U}} \right), \overline{U} = \left(\frac{\overline{u} - \overline{v}}{\overline{u} + \overline{v}} \right) \qquad (1)$$

where $\overline{u}$ and $\overline{v}$ are the ionic mobilities of cation and anion (m^2/v/s) respectively, in the membrane phase, C_1 and C_2 are the concentrations of the membrane and $\overline{D}$ is the charge on the membrane expressed in equivalent per litre.

The graphical method of TMS determines the fixed charge $\overline{D}$ in equivalents/litre and the cation-to-anion mobility ratio in the membrane phase.

Kobatake Method

The system considered is composed of an ionizable membrane of uniform thickness which separates two bulk solutions of a uni-univalent electrolyte of concentrations C_1 and C_2. It is assumed that the system is isothermal and no pressure head is applied across the membrane. The ionizable groups are fixed on the polymer network which constitutes the given membrane. The expression for the membrane potential is given by

$$\Delta\phi = -\left(\frac{RT}{F}\right)\left[\frac{1}{\beta}\ln\frac{C_2}{C_1}\left(1 + \frac{1}{\beta} - 2\alpha\right)\ln\frac{C_2 + \alpha\beta\theta}{C_1 + \alpha\beta\theta}\right] \qquad (2)$$

where

$$\alpha = \left(\frac{u}{u+v}\right)$$

$$\beta = 1 + \left(\frac{KF\theta}{u}\right)$$

and parameters have been assumed to be independent of salt concentration.

Kobatake have derived two useful limiting forms of equation (2). These are (a) when C_2 becomes sufficiently small with γ fixed equation may be expanded to give

$$|\Delta\phi_r| = \frac{1}{\beta}\ln\gamma - \frac{\gamma-1}{\alpha\beta\gamma}\left(1+\frac{1}{\beta}-2\alpha\right)\frac{C_2}{\theta} \tag{3}$$

where $|\Delta\phi_r|$ is the absolute value of a reduced membrane potential defined by

$$|\Delta\phi_r| = \frac{F\Delta\phi}{RT} \tag{4}$$

(b) It has also been shown by Kobatake that at a fixed γ the inverse of an apparent transport number t_{-app} for the co-ion species in a negatively charged membrane is proportional to the inverse of the concentration C_2 in the region of high salt concentration. t_{-app} is defined by the relation

$$|\Delta\phi_r| = (1-2t_{-app})\ln\gamma \tag{5}$$

The derived transport number value has been called the apparent number i.e. t_{-app} because in this type of measurement water transport has not been taken into account. This apparent value will be close to the true value, when dilute solutions are used. Substituting for $\Delta\phi$ from equation (2) and expanding the resulting expression for $1/t_{-app}$ in powers of $1/C_2$ gives

$$\frac{1}{t_{-app}} = \frac{1}{(1-\alpha)} + \frac{(1+\beta-2\alpha\beta)}{2(1-\alpha)^2\ln\gamma}\alpha\left(\frac{\theta}{C_2}\right) + ----- \tag{6}$$

Experimental

Preparation of membrane

Cobalt arsenate precipitate was prepared by mixing a 0.2M cobalt chloride with 0.2M sodium arsenate solution. The precipitate was well washed with deionized water to remove free electrolyte and then dried and powdered. Membrane using suitable ratio of binder was prepared by the method used [15]. The precipitate having ion-exchange property was mixed with polystyrene granules of the size less than 200 meshes and pressed under suitable conditions of temperature and pressure for cobalt arsenate 200 °C and 10MPa. Our effort has been to get the membrane of adequate chemical and mechanically stability. Thus, the membranes prepared by embedding 25% polystyrene were mechanically most stable and gave reproducible results. Those containing larger amount (>25%) of polystyrene did not give reproducible results, while those containing lesser amount (<25%) were unstable. The membranes were subject to microscopic and electrochemical examinations for cracks and homogeneity of the surface and only those which had smooth surface and generated reproducible potentials were considered by carefully controlling the condition of fabrication.

Measurement of membrane potential

Membrane was cemented in Pyrex glass tube cell for measuring membrane potential. The half cell contained 25 ml of electrolyte solutions although the capacity of each of the half cells holding the membrane was about 35 ml. The various salt solutions (chlorides of K^+, Na^+, and Li^+) were prepared from B.D.H

(A.R.) grade chemicals using deionized water. Saturated calomel electrodes were connected to a galvanometer (Osaw, spot reflecting galvanometer, Cat. No. 30241). The solutions in both the compartments were vigorously stirred by magnetic stirrers at constant 500 rpm to minimize the effect of boundary layers on potential [16]. The potential difference across the membrane was measured with the help of an Osaw Vernier Potentiometer (Cat. No. 30071), the concentration ratio $\left(\frac{C_2}{C_1}\right)$ was maintained at 10 throughout the experiment. The pressure and temperature were kept constant throughout the experiment. The electrochemical setup used for uni-ionic potential and membrane potential measurements may be represented as

SCE Solution Membrane Solution SCE

C_1 Diffusion potential C_2

Donnan potential Donnan potential

Measurement of membrane conductance

The electric conductance of the membrane was measured by the method used [17]. The membrane was sealed between two Pyrex glasses half cells. The half cells were first filled with electrolyte solutions of known concentration to equilibrate the membrane, and then the latter was replaced by purified mercury without

removing the adhering surface liquid. Platinum electrodes dipping into mercury were used to established electrical contact. The membrane conductance was monitored on a direct reading conductivity meter (Model No L303). The solutions in both the compartments were vigorously stirred by magnetic stirrers at constant 500 rpm to minimize the effect of boundary layers on potential. The whole cells assembly was kept immersed in a water thermostat maintained at the required temperatures (10°C to 50°C).

Characterization of membrane

The pre-requisite for understanding the performance of an ion-exchange membrane is its complete physico-chemical characterization, which involves the determination of all such parameters that affects its electrochemical properties. These parameters are membrane water content, porosity, thickness and swelling etc. and these were determined as described elsewhere [18].

Water content (%total wet weight)

The conditional membrane was first soaked in water to diffusible salt, blotted quickly with Whatmann filter paper to remove surface moisture and immediately weighted. These were further dried to a constant weight in a vacuum over P_2O_5 for 24h. The water content (total wet weight) was calculated as:

$$\% \text{ Total wet weight} = \left(\frac{W_w - W_d}{W_w}\right) \times 100$$

where W_w is the weight of the soaked / wet membrane and W_d the weight of the dry membrane.

Porosity

Porosity was determined as the volume of water incorporation in the cavities per unit membrane volume from the water content data:

$$\text{Porosity} = \left(\frac{W_w - W_d}{AL\rho_w} \right)$$

where W_d is the weight of the dry membrane, A the area of the membrane, L the thickness of the membrane and ρ_w is the density of water.

Thickness

The thickness of the membrane was measured by taking the average thickness of the membrane by using screw gauze.

Swelling

Swelling is measured as the difference between the average thickness of the membrane equilibrated with 1M NaCl for 24 h and the dry membrane.

Chemical stability

Chemical stability was evaluated on the basis of ASTM D543-95 method. Membrane was exposed to several media commonly utilized. Membrane was evaluated after 24, 48 and 168 h, analyzing alteration in color, texture, brightness, decomposition, splits, holes, bubbles, curving and stickiness [19].

SEM investigation of membrane morphology

Scanning Electron Microscope image was used to confirm the microstructure of fabricated porous membrane. The membrane morphology was investigated by Leo

4352 at an accelerating voltage of 20 kV. Sample was mounted on a copper stub and sputter coated with gold to minimize the charging.

Results and discussion

The cobalt arsenate membrane using polystyrene as a binder was prepared by sol–gel process. The polystyrene was selected because its cross linked rigid framework provides adequate adhesion to the cobalt arsenate which accounts for the mechanical stability to the membrane. Polystyrene based cobalt arsenate membrane is better than a conventional membrane which degrades under harsh conditions and often encountered in industrial settings [20]. The results of thickness, swelling, porosity and water content capacity of cobalt arsenate membrane are summarized in table 1. The water content of a membrane depends on the water vapor pressure of the surroundings. Knowledge of the pore size distribution and the water structure in a membrane might contribute to classify a special membrane resembling a solution-diffusion, a fine-porous, or a coarse-porous membrane [21]. In case of most of the transport measurements, only the membrane water content at saturation is needed, and that mostly as a function of solute concentration. Thus, low order of water content, swelling and porosity with less thickness of this membrane suggests that interstices are negligible and diffusion across the membrane would occur mainly through exchange sites. Membrane was tested for chemical resistance in acidic, alkaline and strongly oxidant media. In acidic (1M H_2SO_4) and in alkaline media (1M NaOH) few significant modifications were observed after 24, 48 and 168 h, demonstrating that

Table 1 Characterization of Cobalt arsenate membrane

Thickness of the membrane (cm)	0.075
Water Content as % weight of wet membrane	0.057
Porosity	0.085
Swelling of %weight wet membrane	No Swelling

the membrane is effective in such media. However, in strong oxidant media the synthesized membrane became fragile in 48 h and membrane was broken after 168 h, losing mechanical resistance.

The characterization of membrane morphology has been studied by a number of investigators using scanning electron microscopy [22,23]. The composite pore structure, micro/ macro porosity, homogeneity, thickness, cracks and surface texture/morphology have been studied [24,25]. The cross-section of SEM micrograph of the surface is shown in figure 1. Membrane cross-section thickness was estimated to be around 30μm as observed in figure1. Membrane had random non-preferential orientation with no visible cracks and appeared to be composed of dense and loose aggregation of small particles. The membrane is macroscopically uniform in thickness and is porous in nature. The pores are modeled as uniform capillaries that extend throughout the membrane. These pores are evenly distributed throughout the surface of the membrane. Entrance and exit effects are ignored since the membrane thickness is large compared to the pore radius. However, the thickness is still large compared to the pore radius and it is assumed that the membrane and adjacent solution (interfaces) are in equilibrium. The distributions of charge density and mobile species within the pores are assumed to be uniform [26].

The values of observed membrane potential for the cobalt arsenate membrane in contact with various 1:1 electrolyte solutions at 25 ± 1°C are given in table 2. The values for the membrane potential are of the order of positive mV. The

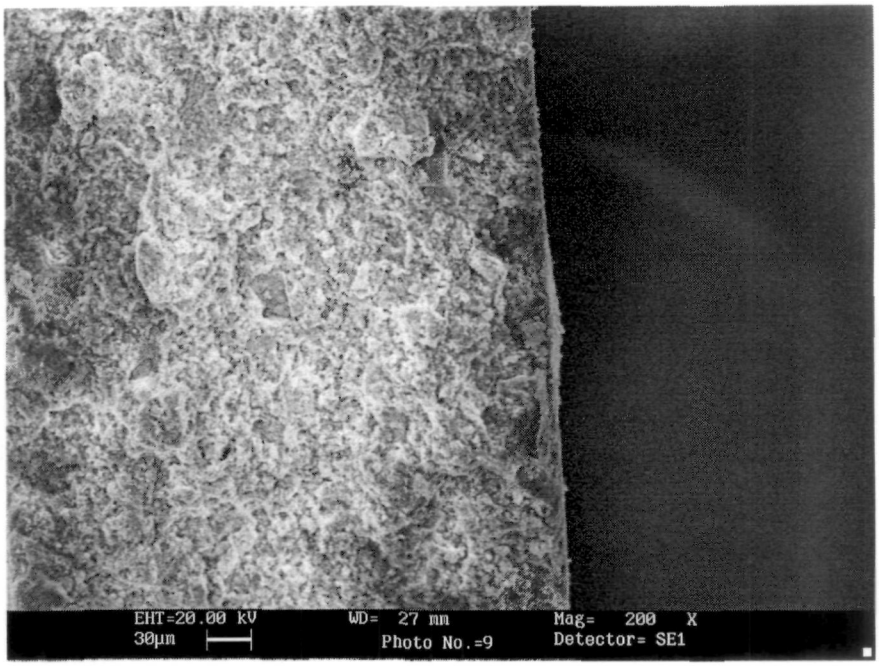

Figure 1 Cross-section SEM image of Polystyrene-based (25%) Cobalt arsenate membrane

Table 2 Observed membranes potentials $\Delta\phi$ in mV across the Cobalt arsenate membrane in contact with various 1:1 electrolytes at different concentrations at 25±1° C

Electrolyte Concentration (mol/l)	Cobalt Arsenate		
	KCl	NaCl	LiCl
$10\times10^{-1}/1\times10^{-1}$	25.5	12.2	10.5
$1\times10^{-1}/1\times10^{-2}$	36.6	25.0	15.0
$5\times10^{-2}/5\times10^{-3}$	40.9	29.0	25.5
$2\times10^{-2}/2\times10^{-3}$	45.0	34.5	30.0
$1\times10^{-2}/1\times10^{-3}$	47.5	36.5	33.0

observed values of membrane potential have been plotted against $-\log C_2$ in figure 2. The decrease in the magnitude of membrane potential with an increase of bathing electrolyte concentration shows that the membrane is negative charged (cation selective) and its selectivity increases with the increase of dilution due to structural changes produced in the electrical double layer at the solution membrane interface [27].The fixed charge concentration in the membrane is due to cobalt, which interacts with hydrated counter-ion and form the ion-pairs by loosing much of the water content while repelling the co-ions because of the same charge as that of the fixed charged group. The concentration difference of these charged ions generates an electrical potential difference in order to maintain electrochemical equilibrium between the membrane and electrolyte solution [15].

In the absence of a pressure or temperature gradient, the generation of a steady e.m.f. between two solutions of an electrolyte of different concentrations, separated by a membrane, can be attributed to the presence of a net charge on the membrane. Such charges play an important role in the sorption and transport of simple electrolytes in artificial as well as natural membranes [28], and impart some important electrochemical properties to the membrane, the most important being the differences in the permeabilities of co-ions, counter ions and neutral molecules.

The set of curves in figure 3 are the theoretical membrane potentials for a cation selective membrane, which is calculated from equation (1). The difference

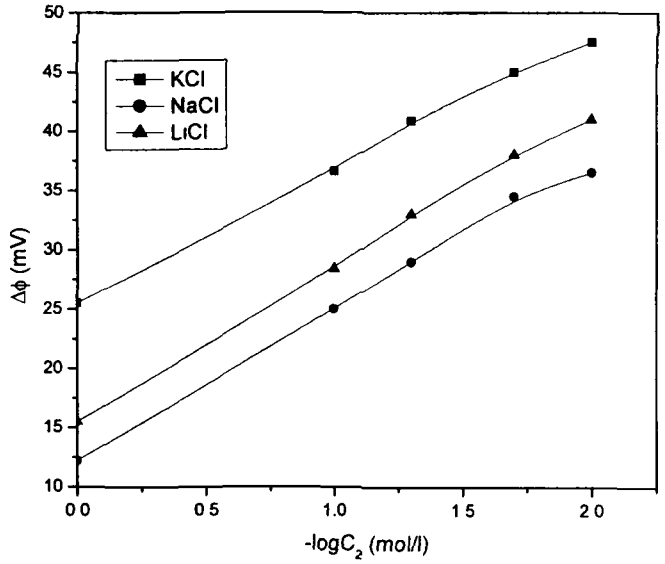

Figure 2 Plots of membrane potentials against $-\log C_2$ for Cobalt arsenate membrane using various 1:1 electrolytes

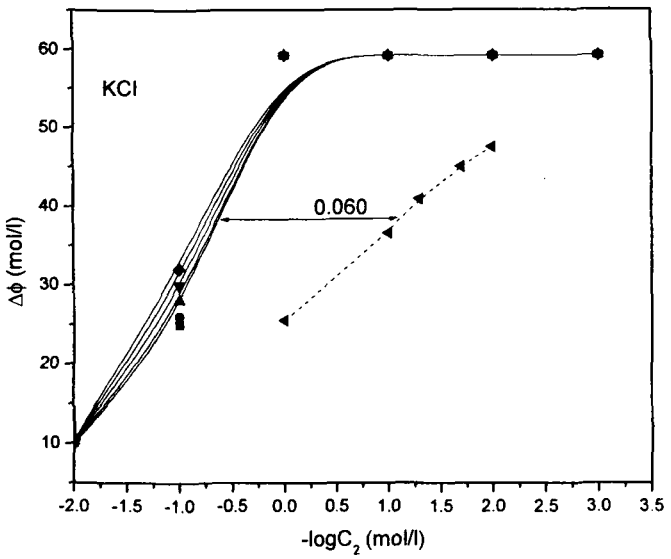

Figure 3 Plots of membrane potentials vs. $-\log C_2$ for Cobalt arsenate membrane. Smooth curves are the theoretical concentration potentials for different mobility ratio. Broken line is the experimental values of membrane potential for different concentration of KCl solution

curves are for different mobility ratios $\left(\frac{\bar{u}}{\bar{v}}\right)$, with a constant value of $\bar{D}$ is unity expressed in equivalent/litre. The experimental $\Delta\phi$ values for cobalt arsenate membrane with KCI electrolyte were plotted in the same graph as a function of $-\log C_2$. The experimental curve was shifted horizontally and ran parallel to one of the theoretical curves. This shift gave $\log \bar{D}$, and the parallel theoretical curve gave the value for mobility ratio $\left(\frac{\bar{u}}{\bar{v}}\right)$ with the membrane phase. The values of $\bar{D}$ and $\left(\frac{\bar{u}}{\bar{v}}\right)$ derived in this way for the membrane and various 1:1 electrolytes are given in table 3. Thus, the order of fixed charge density for electrolytes used was found to be KCl > NaCl > LiCl. The charge model may work as a tool to improve the performance of the membrane filtration process. Since, the charge density is an important parameter governing transport phenomena and the charge property of the membrane dominates the electrostatics interaction between the membrane and particles in the feed solution due to the prefential adsorption of some ions. Therefore, by controlling the solution physico- chemistry, the optimum charge property of the membrane can be obtained as desired [29].

Equation (3) indicates that a value of β and a relation between α and θ can be obtained by evaluation of the intercept and the initial slope of a plot of $|\Delta\phi_r|$ against C_2 which is shown in figure 4. The value of intercept is equal to $1/\beta \ln \gamma$ from which β is evaluated. Values are given in table 4.

Table 3 Values of the thermodynamically charge density of Cobalt arsenate membrane- electrolyte systems evaluated by various theories

Electrolyte	TMS		Kobatake	
	$\left(\frac{\bar{u}}{\bar{v}}\right)$	$\overline{D}$(eq/l)	θ_c	θ_d
KCl	2.45	0.060	0.042	0.068
NaCl	1.50	0.054	0.039	0.066
LiCl	1.44	0.052	0.032	0.061

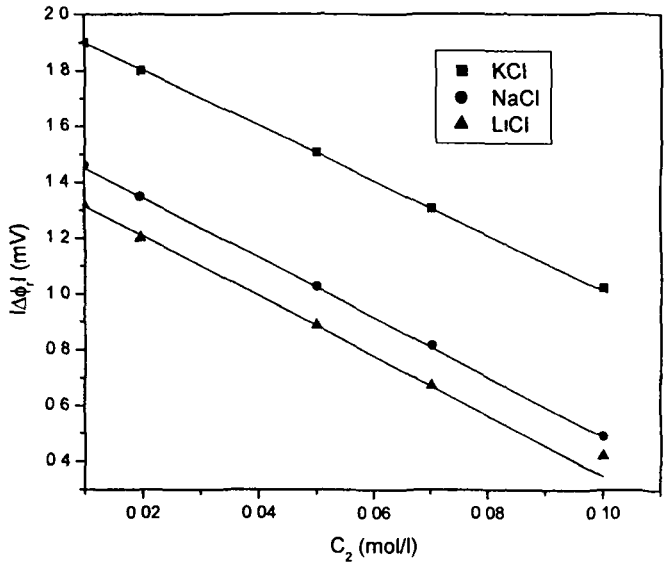

Figure 4 Plots of $|\Delta\phi_r|$ against C_2 for Cobalt arsenate membrane using various 1:1 electrolytes

Table 4 Values of parameters α and β for Cobalt arsenate membrane- electrolyte system

Electrolyte	Cobalt Arsenate	
	α	β
KCl	0.71	1.21
NaCl	0.60	1.58
LiCl	0.59	1.74

Equation (6) indicate that the intercept of a plot of $1/t_{-app}$ against $1/C_2$ at fixed γ allows the value of α to be determined. Plots of $1/t_{-app}$ against $1/C_2$ for various uni-univalent electrolytes are shown in figure 5.The value of intercept is equal to $1/(1-\alpha)$, from which α may be evaluated. Values are given in table 4. If this value of α is inserted in the relation obtained from the initial slope for $|\Delta\phi_r|$ against C_2, the desired value for θ_c can be determined. Once α and β are known in the manner described above, the values of θ_d may be evaluated from the initial slope for $1/t_{-app}$ against $1/C_2$.

Kobatake has suggested that provided his equation for the membrane potential is correct, then the two values of θ i.e. θ_c and θ_d thus determined from the opposite limits should agree with one another. The values are given in table 3 which are closed together thereby confirming the applicability of Kobatake's equation to these systems. We have seen that the charge density is higher in the region of low concentrations (θ_d) than in high concentrations (θ_c) because the ionic atmosphere around fixed charges in the formal case is large compared with than in the later case. On the other hand, the charge density in the case of KCl is higher than in NaCl case due to the size factor (the smaller size, the larger ionic atmosphere).

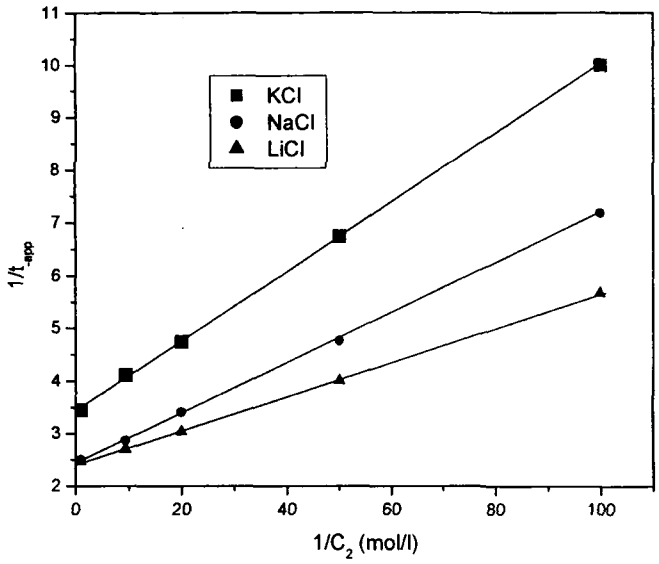

Figure 5 Plots of $1/t_{app}$ against $1/C_2$ for Cobalt arsenate membrane using various 1:1 electrolytes

The TMS equation (1) can also be expressed by the sum of Donnan potential $\Delta\phi_{Don}$ between membrane surfaces and external solutions and the diffusion potential $\Delta\phi_{diff}$ within the membrane [30,31].

$$\Delta\phi_m = \Delta\phi_{Don} + \Delta\phi_{diff} \tag{7}$$

$$= -\frac{RT}{V_k F}\ln\left(\frac{\gamma''_{\pm}C_2\overline{C}_{1+}}{\gamma'_{\pm}C_1\overline{C}_{2+}}\right) - \frac{RT}{V_k F}\frac{\overline{\omega}-1}{\overline{\omega}+1}\times\ln\left(\frac{(\overline{\omega}+1)\overline{C}_{2+}+(V_x/V_k)\overline{D}}{(\overline{\omega}+1)\overline{C}_{1+}+(V_x/V_k)\overline{D}}\right) \tag{8}$$

The R, T and F have their usual significance; $\gamma'_{\pm}$ and $\gamma''_{\pm}$ are the mean ionic activity coefficients; $\overline{\omega} = \frac{\overline{u}}{\overline{v}}$ is the mobility ratio of the cation to the anion in the membrane phase and $\overline{C}_{1+}$ and $\overline{C}_{2+}$ are the cation concentrations in the membrane phase first and second, respectively. The cation concentration is given by the equation

$$\overline{C}_+ = \sqrt{\left(\frac{V_x\overline{D}}{2V_k}\right)^2 + \left(\frac{\gamma_{\pm}C}{q}\right)^2} - \frac{V_x\overline{D}}{2V_k} \tag{9}$$

Here V_k and V_x refer to the valency of cation and fixed-charge group on the membrane matrix, q is the charge effectiveness of the membrane and is defined by the equation

$$q = \sqrt{\frac{\gamma_{\pm}}{K_{\pm}}} \tag{10}$$

where $K_{\pm}$ is the distribution coefficient. It is expressed as

$$K_{\pm} = \frac{\overline{C}_i}{C_i}, \qquad \overline{C}_i = C_i - \overline{D} \tag{11}$$

where $\overline{C}_i$ is the *i*th ion concentration in the membrane phase and C_i is the *i*th ion concentration of the external solution. The transport properties of the membrane in various electrolyte solutions are important parameters to further investigate the membrane phenomena as shown in equation (12)

$$\Delta\phi = \frac{RT}{F}(t_+ - t_-)\ln\frac{C_2}{C_1} \tag{12}$$

$$\frac{t_+}{t_-} = \frac{\overline{u}}{\overline{v}} \tag{13}$$

Equation (13) was first used to calculate the values of transport numbers t_+, mobility ratio $\overline{\omega} = \frac{\overline{u}}{\overline{v}}$ and finally $\overline{U}$ as given in table 5. The values of mobility $\overline{\omega}$ of the electrolytes in the membrane phase were found to be high at lower concentration of all the electrolytes (KCl, NaCl and LiCl). Further increase in concentration of the electrolytes led to a sharp drop in the values of $\overline{\omega}$ as given in table 5. The high mobility is attributed to higher transport number of comparatively free cations of electrolytes and also be similar trend as the mobility in least concentrated solution. The values of the parameters $K_\pm$, q and $\overline{C}_+$ derived for the system have also been included in table 5. The values of $\gamma_\pm$ were the usual charted values for electrolytes. Using equation (11) it was found that the values of distribution coefficients increased at lower concentration of electrolytes. As the concentration of electrolytes increased, the values of distribution coefficients sharply dropped and, thereafter, a stable trend was observed as shown in table 5.

Table 5 The calculated values of the parameters $t_+, \overline{U}, \overline{\omega}, K_\pm$, q, and $\overline{C}_+$ of Cobalt arsenate membrane with different concentration of electrolytes using eq. (12) and eq. (9) - (11)

C_2 (mol/l)	t_+	$\overline{U}$	$\overline{\omega}$	$K_\pm$	q	$\overline{C}_+$
KCl (Electrolyte)						
0.01	0.90	0.80	9.00	5.00	0.463	0.0025
0.02	0.88	0.76	7.33	2.00	0.664	0.0038
0.05	0.84	0.68	5.25	0.20	2.054	0.0056
0.10	0.81	0.62	4.26	0.40	1.386	0.0200
1.00	0.71	0.42	2.45	0.95	0.803	0.6839
NaCl						
0.01	0.80	0.60	4.00	4.40	0.453	0.0024
0.02	0.79	0.58	3.76	1.70	0.720	0.0036
0.05	0.74	0.48	2.85	0.08	3.244	0.0054
0.10	0.71	0.42	2.49	0.46	1.293	0.0194
1.00	0.60	0.20	1.50	0.94	0.800	0.6805
LiCl						
0.01	0.78	0.56	3.55	4.20	0.424	0.0022
0.02	0.75	0.50	3.00	0.62	1.192	0.0034
0.05	0.71	0.42	2.49	0.04	4.588	0.0053
0.10	0.63	0.26	1.70	0.48	1.266	0.0157
1.00	0.59	0.18	1.44	0.94	0.799	0.6701

The large deviation in the value of $K_{\pm}$ at the lower concentration of electrolytes was attributed to the high mobility of comparatively free charges of the strong electrolyte and thus, reached into the membrane phase easily compared to higher concentrated electrolytes solution.

The charge effectiveness q, values for LiCl are the smallest of the electrolytes used in this study and order is KCl > NaCl > LiCl. The counter-ions Cl^-, is the same for all the electrolyte used therefore, the variation of charge effectiveness values are possibly due to increase in adsorption of co-ions on charged membrane [32,33].

When a permselective membrane happens to be in between the solutions of electrolytes of different concentrations, a steady electromotive force (e.m.f) develops due to difference in the relative permeabilities of various ionic species. This e.m.f, usually called the membrane potential, depends on the properties of the membrane and has been the subject of many theoretical and experimental studies. TMS theory and its modifications are inadequate to explain experimental results on non-ideal permselective membrane.

The perm selectivity [34] is a measure of the characteristic difference in the membrane of counter ions and co-ions, which be expressed as

$$P_s = \left(\frac{\bar{t}_+ - t_+}{1 - t_+} \right) \tag{14}$$

where $\bar{t}_+$ is the counter-ion transport number through the membrane and t_+, is the counter ion transport number in the solution phase. Thus, the permselectivity

arises due to the nature of the membrane for differentiating between co-ions and counter ions and is not a membrane constant. An ideal permselectivity cation – exchange membrane would transmit positively charge ions only. Permselectivity can be calculated from the equation (14). It can be seen from figure 6 that permselectivity decreased with the increase in the concentration of the salt solution. This is inconformity with the expectation based on increased deswelling of the ion exchange membrane resulting in progressively lowered co-ion exclusion with increase in concentration.

An ion exchange membrane undergoes swelling because of the osmotic intake of the solvent by the membrane network. This osmotic action depends on the solute concentration; it decrease with the increase in concentration [35] and as a result solvent uptake by the membrane matrix decreases leading to the deswelling of the membrane. Due to this increased membrane openness this is accompanied by lowered exclusion of co-ions and Permselectivity of the membrane therefore decreases. Thus, even when electrolyte concentration remains unchanged; a reduction in membrane permselectivity is expected with the increase in the concentration of the solution.

Increase in concentration results in decreases in the magnitude of the counter ion transport number as expected because of deswelling of the membrane.

The values of observed membrane conductance for the cobalt arsenate membrane in contact with various 1:1 electrolyte solutions at different temperature (10°C to 50°C) are given in table 6. The values for the membrane specific

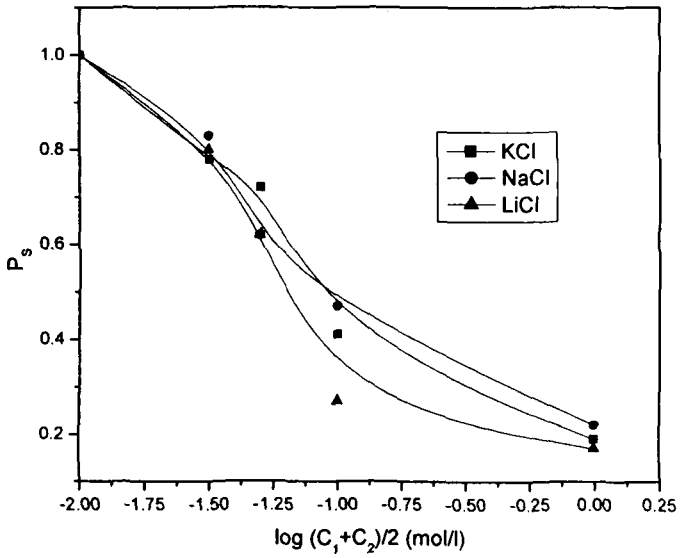

Figure 6 Plots of P_S against log $(C_1+C_2)/2$ for Cobalt arsenate membrane using various 1:1 electrolytes

Table 6 Experimentally observed values of membrane conductance ($m\Omega^{-1}cm^{-1}$) for various 1:1 electrolytes at different temperature (10 to 50) ± 0.1°C

Concentration, C (mol/l)	**Temperature (°C)**														
	10			20			30			40			50		
	KCl	NaCl	LiCl	KCl	NaCl	LiCl	KCl	NaCl	LiCl	KCl	NaCl	LiCl	KCl	NaCl	LiCl
0.1	9.82	8.92	8.50	10.30	9.44	8.97	10.53	9.69	9.25	10.79	9.95	9.50	11.03	10.25	9.74
0.07	7.56	6.98	6.50	7.92	7.39	6.98	8.12	7.63	7.25	8.33	7.90	7.51	8.56	8.14	7.80
0.05	5.12	5.00	4.85	5.54	5.42	5.33	5.70	5.63	5.50	5.84	5.68	5.58	6.00	5.89	5.68
0.02	3.39	3.12	2.98	3.70	3.48	3.39	3.94	3.68	3.59	4.10	3.92	3.85	4.30	4.18	4.10
0.01	1.96	1.84	1.64	2.08	1.90	1.85	2.25	2.10	2.00	2.42	2.22	2.10	2.58	2.42	2.35

conductance are of the order of positive $m\Omega^{-1}cm^{-1}$ and increase with an increase of external electrolytes concentration. This type of variation can be explained in terms of increased obstruction of the membrane matrix and increased salt uptake with an increase of external electrolyte concentration.

From the table 6, under identical conditions of temperature and concentration, it is clear that the membrane's conductance is highest when in contact with KCl and lowest when in contact with LiCl, and for various alkali metal ions give the sequence,

$$K^+ > Na^+ > Li^+$$

which follows the order of their ionic radii and also from the selectivity sequence observed [36,37].

In addition, the diffusion of ions depends upon the charge on the membrane and its porosity. The membrane porosity in relation to the size of the hydrated species diffusing through the membrane appears to determine the above sequence. Several probable structures of water molecules under the condition of a given temperature may play an important role in determining the size of the hydrated ions [38]. As the diffusion paths in the membrane become more difficult in aqueous solutions, the mobility of large hydrated ions gets impeded by the membrane framework and the interaction with the fixed charge groups on the membrane matrix. Consequently, the membrane pores reduce the conductance of small ions, which is much hydrated [39,40].

The membrane specific conductance data obtained with cobalt arsenate membrane using various 1:1 electrolytes at different temperature are plotted as a function of $\sqrt{C}$. This plot is shown in figure 7. The specific conductance of the membrane increases almost linearly with the square root of external electrolyte concentration. This behavior can be explained in terms of increased obstruction of the polymer matrix as diffusion pathways become more tortuous in concentrated solution. It is also observed that at higher concentration the uptake of salt by membrane is higher which results in increased value of electrical conductance. These two opposing effects operate simultaneously at higher concentration as shown in figure 7 and a state is reached when membrane conductance attains a maximum value [41].

In figure 8, specific conductance increases with increase in temperature T, this implies that activation energy decreases.

Table 7 shows that the activation energy decreases with increase in concentration of the bathing electrolyte solution and the sequence for energy of activation is

$$E_a K^+ > E_a Na^+ > E_a Li^+$$

Table 8 shows that an increase of activation energy with an increase of crystallographic radius confirms the applicability of Kumins [42] arguments for polystyrene based inorganic precipitate membrane systems.

On the basis of absolute reaction rate, Eyring [43]

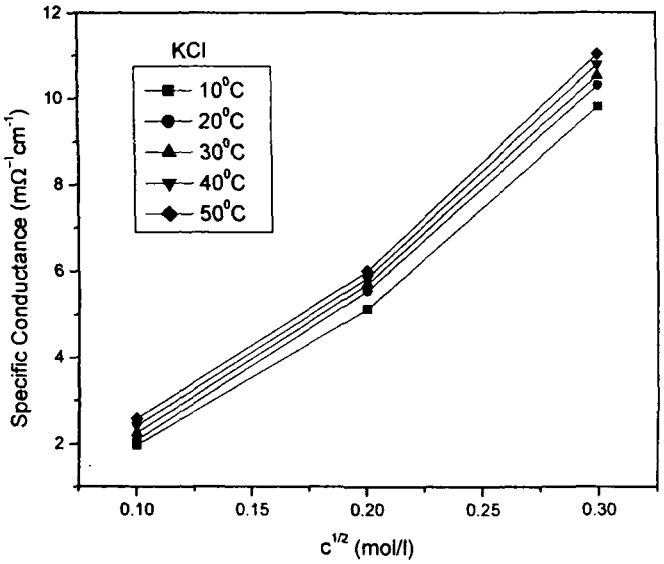

Figure 7 Plots of specific conductance ($m\Omega^{-1}cm^{-1}$) Vs square root of concentration for electrolytes at different temperature through Cobalt arsenate membrane

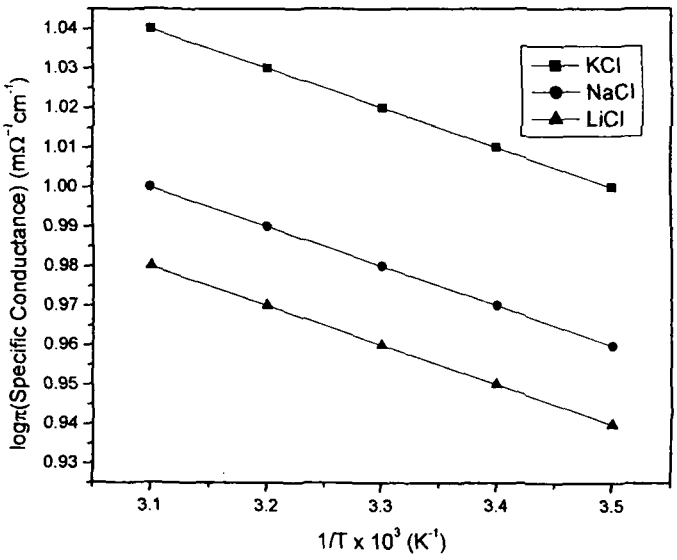

Figure 8 Arrhenius plots of specific conductance Vs 1/T 10^3 for 1:1 electrolytes through Cobalt arsenate membrane

Table 7 Calculated values of Activation Parameters for 1:1 electrolytes through Cobalt arsenate membrane

Electrolytes	Conc.(mol/l)	E_a (KJ/mole)	ΔH^*(KJ/mole)	ΔG^*(KJ/mole)	$-\Delta S^*(JK^{-1}mol^{-1})$
KCl	0.1	2.82	0.37	34.87	117.75
	0.01	5.77	3.32	39.28	122.73
NaCl	0.1	2.64	0.19	34.86	118.33
	0.01	5.70	3.25	39.27	122.92
LiCl	0.1	2.51	0.06	34.84	118.71
	0.01	5.47	3.02	39.26	123.69

Table 8 Relation between Crystallographic radius and activation energy of alkali chlorides

Ion	Crystallographic radii (Å)	Energy of activation (KJ/mole)
K^+	1.33	2.81
Na^+	0.93	2.64
Li^+	0.60	2.51

$$\Lambda = \left(\frac{RT}{Nh}\right) e^{-\left(\frac{\Delta H^*}{RT}\right)} e^{\left(\frac{\Delta S^*}{R}\right)} \qquad (15)$$

where Λ is the observed specific conductance, h the planck's constant, R the gas constant, N the Avogadro number, T the absolute temperature, ΔH^* the enthalpy of activation and ΔS^* the entropy of activation while the other terms have their usual meaning.

The enthalpy and entropy of activation are related to the free energy of activation, ΔG^*, by the Gibbs-Helmholtz equation

$$\Delta G^* = \Delta H^* - T\Delta S^* \qquad (16)$$

The enthalpy of activation is also related to the Arrhenius energy of activation, E_a, as

$$E_a = \Delta H^* + RT \qquad (17)$$

A plot of $\log\frac{\pi Nh}{RT}$ versus $\frac{1}{T}$ from experimental data, shown in figure 9, RT gives the value of ΔH^* /R and ΔS^*/R. ΔG^* and E_a were obtained by using equations (16) and (17). The values of various kinetic activation parameters E_a, ΔH^*, ΔG^* and ΔS^*derived for the diffusion of various electrolytes in membrane are given in table 7. The results indicate that the electrolyte permeation gives rise to a negative value of ΔS^*. Amongst the ions of the same valence the order of ΔS^* is as follows

$$K^+ > Na^+ > Li^+$$

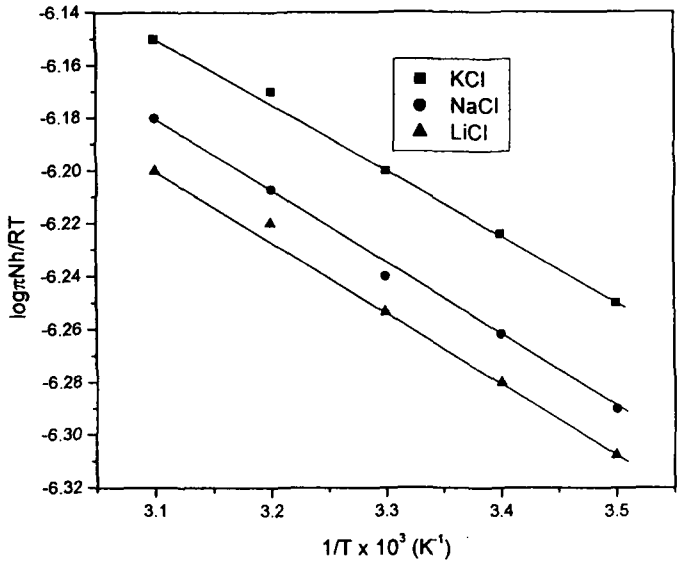

Figure 9 Plots of $\log\frac{\pi Nh}{RT}$ Vs 1/T 10^3 for 1:1 electrolytes through Cobalt arsenate membrane.

Thus, the negative values of ΔS^* indicated electrolyte diffusion with partial immobilization in the membrane, the relative partial immobility increasing with increase in the valence of ions constituting the electrolyte [44].

According to Eyring [43] , the values of ΔS^* indicate the mechanism of flow. the large positive ΔS^* is interpreted as reflecting bonds breaking, while low values indicate that permeation has taken place without bonds breaking. Negative ΔS^* values are considered to indicate either formation of a covalent bond between the permeating species and the membrane material or that the permeation through the membrane may not be the rate determining step.

Conclusions

The polystyrene based cobalt arsenate membrane was prepared and found that it was quite stable and did not show any dispersion in water and other electrolyte solutions. The theoretical values of membrane potential were obtained by using TMS equation at various concentrations and found to be closer to the experimental values. The transport properties of membrane are also controlled by ion distribution coefficients and the discrepancies in distribution coefficients with variation in the concentration of electrolytes is due to the prefential adsorption of some ions on the membrane surface. The membrane conductance bathed in different concentrations of various 1:1 electrolytes (KCl, NaCl and LiCl) and measured at several temperatures is reported. The binder polystyrene was selected because its cross-linked rigid framework provides an adequate adhesion to the cobalt arsenate, which accounts for the mechanical stability to the membrane.

Thus, in general the specific conductance of ions across the membrane varies almost linearly with concentration in the lower concentration range. The data suggest that the larger ions face more difficulties in crossing the membrane than the smaller ones. Hence, it can be explained that the magnitudes of E_a, $\Delta H^*$and ΔG^* must be higher for larger ions than the smaller ones. On the one hand, a high ΔS^* value associated with the high value of E_a for diffusion may suggest the existence of either a large zone of activation or loosening of more chain segments of the membrane. On the other hand, low value of ΔS^* implies either a small zone of activation or no loosening of the membrane structure upon permeation [44].

References

[1] A.A. Khan, Inamuddin, *Sensors and Actuators B* **120** (2006) 10

[2] A.A. Khan, Inamuddin, M.M. Alam, *React. Funct. Polymers* **63** (2005) 119.

[3] B. Pandit, U. Chudasma, *Bull. Mater. Sci.* **24** (2001) 265.

[4] H. Zhang, J.H. Pang, D. Wang, A. Li, X. Li, Z. Jiang, *J, Membr. Sci.* **264** (2005) 56.

[5] M.J. Shaw, P.N. Nesterenko, G.W. Dicinoski, P.R. Haddad, *J. Chromatogr. A* **997** (2003) 3.

[6] A. Yamauchi, A.M.E. Sayed, K. Mizuguchi, M. Kodama, Y. Sugita, *J. Membr. Sci.* **283** (2006) 301.

[7] N. Islam, N.A. Bulla, S. Islam, *Biochim. Biophys. Acta* **1667** (2004) 174.

[8] A. Tanioka, H. Matsumoto, R. Yamamota, *Sci. Technol. Adv. Mater.* **5** (2004) 461.

[9] C. Wu. S. Zhang, D. Yang, J. Wei, C. Yan, X. Jian, *J. Membr. Sci.* **279** (2006) 238.

[10] R.K. Nagarale, G.S. Gohil, V.K. Shahi, R. Rangarajan, *J. Colloid Interface Sci.* **287** (2005) 198.

[11] R.K. Nagarale, G.S. Gohil, V.K. Shahi, G.S. Trivedi, R. Rangarajan, *J. Colloid Interface Sci.* **277** (2004) 162.

[12] Y. Kobatake, T. Noriaki, Y. Toyoshima, H. Fujita, *J. Phys. Chem.* **69** (1965) 3981.

[13] S. Bouraneze, A. Szymczyk, P. Fievet, A. Vidonne, *J. Membr. Sci.* **290** (2007) 216.

[14] A. Nakajima, T. Miyasaka, K. Sakai, T. Tsukahara, *J. Membr. Sci.* **187** (2001) 129.

[15] F. Jabeen, Rafiuddin, *J. Sol. Gel Sci. Technol.* **44** (2007) 195.

[16] A. Canas, M.J. Ariza, J. Benavente, *J. Colloid Interface Sci.* **246** (2002) 150.

[17] N. Lakshminarayanaiah, Transport phenomena in membrane, Academic Press, New York, 1969.

[18] A.A. Khan, A. Khan, Inamuddin, *Talanta* **72** (2007) 699.

[19] ASTM D543-95, Standard Particles for evaluating the resistance of plastics to chemical reagents, 1998.

[20] U. Razdan, S.V. Joshi, V.J. Shah, *Current Science* **85 (6)** (2003) 761.

[21] S. Koter, P. Piotrowski, J. Kerrs, *J. Membr. Sci.* **153** (1999) 761.

[22] J. Liu, T. Xu, M. Gong, F. Yu, Y. Yu, *J. Membr. Sci.* **283** (2006) 190.

[23] V.S. Silva, B. Ruffmann, S. Vetter, A. Mendes, L.M. Madeira, S.P. Nunes. *Catalysis Today* **104** (2005) 205.

[24] J.O. Titiloye, I. Hussain, *J. Colloid Interface Sci.* **318** (2008) 50.

[25] M. Resina, J. Macanás, J.D. Gyves, M. Muňoz, *J. Membr. Sci.* **289** (2007) 150.

[26] J.G. Aleman, J.M. Dicker, *J. Membr. Sci.* **235** (2004) 1.

[27] F. Jabeen, Rafiuddin, *J. Appl. Polym. Sci.* **110** (2008) 3023.

[28] J. Schaep, C. Vandecasteele, *J. Membr. Sci.* **188** (2001) 129.

[29] J.H. Tay, J. Liu, D.D. Sun, *Water Research* **36** (2000) 585.

[30] H. Matsumoto, A. Tanioka, T.J. Murata, M. Higa, K. Horiuchi, *J. Phys. Chem. B* **102** (1998) 5011.

[31] T.J. Chou, A. Tanioka, *J. Colloid Interface Sci.* **212** (1999) 293.

[32] W. Bowen, A. Mohammad, N. Hilal, *J. Membr. Sci.* **126** (1997) 91.

[33] X. Wang, T. Suru, M. Togoh, S. Nakao, S. Kimura, *J. Chem. Eng. Jpn.* **28 (2)** (1995) 186.

[34] V.K. Shahi, G.S. Trivedi, S.K. Thampy, R. Rangarajan, *J. Colloid Interface Sci.* **262** (2003) 566.

[35] R.E. Kesting, Synthetic Polymeric Membrane, McGraw Hill Book Company, New Delhi, 1971.

[36] V. Subramanyan, N. Lakshminarayanaiah, *J. Phys. Chem.* **72** (1968) 4314.

[37] H. Sherry, J.A. Marinsky, Ion Exchange, Dekker, New York, 1968.

[38] S. Islam, B.N. Waris, *Thermochim. Acta* **424** (2004) 165.

[39] J.L. Lovenam, Structure and Function in Biological Membranes, Holden-Day, San Fransisco, 1964.

[40] J.F. Danielli, H. Daysin, The permeability of Natural Membranes, McMillan, New York, 1943.

[41] T. Iijima, T. Obara, M. Isshiki, T. Seki, K. Adachi, *J.Colloid and Interface Sci.* **63** (1978) 421.

[42] C.A. Kumins, T.K. Kwei, J.Crank, G.S. Park, Diffusion in Polymers Academic Press, New York, 1968.

[43] S. Glasston, K.J. Laider, H. Eyring, The Theory of Rate Processes McGraw-Hill, New York, 1941.

[44] K.E. Shuler, C.A. Dames, K.J. Laidler, *J. Chem. Phys.* **17** (1949) 860.

CONCLUSION

The polystyrene based nickel, titanium and cobalt arsenate membranes have been prepared by sol-gel method. Polystyrene is suitable binder because of its cross-linked rigid framework which provides an adequate adhesion to the membrane. SEM images have provided guidance in the preparation of well-ordered precipitates, composite pore structure, micro/macro porosity, homogeneity, thickness, surface texture and crack-free membranes. Potentials across three polystyrene based nickel, titanium and cobalt arsenate membranes using various 1:1 electrolytes have been measured. The data have been used to calculate transference number of ions, mobility, distribution coefficient, charge effectiveness, permselectivity and examine the validity of the recently developed equations for membrane potential based on the principles of irreversible thermodynamics. The surface charge model work as a tool to improve the performance of the membrane filtration process and selectivity of ion exchange. The good agreement between the theoretical and the experimental data for the uni-univaent potentials proved the applicability of the relationship derived for the system. The two limiting forms of Kobatake's equation gave identical values of θ for the membrane taken in this investigation. Thus, the order of fixed charge density for electrolytes used was found to be KCl> NaCl> LiCl. The values of mobility of the electrolytes in the membrane phase were found to be high at lower concentration for all the electrolytes. The distribution coefficient values were found to be diminished with the increasing electrolyte concentration. The charge

effectiveness q, values for electrolytes used in this study are in the order of KCl > NaCl > LiCl. It can be seen that permselectivity decreased with the increase in the concentration of the salt solution.

The conductance values have been found to increase with increase in concentrations as well as with temperature. The slope of the plots of specific conductance versus concentration exhibits a decrease in its values at relatively higher concentrations compared to those in extremely dilute solutions. The activation energies were found to depend on the size of penetrate species and it decreased with increase in the concentrations of the electrolyte solutions. The values of ΔS^* were found to be negative indicating the partial immobilization of ions within the membrane. The order of membrane selectivity was found to be $K^+ > Na^+ > Li^+$

The partial immobility of the ionic species has been attributed to it interaction with the membrane matrix of low fixed density.